

# ELECTRON AND NEUTRINO SCATTERING IN THE QUASIELASTIC REGIME II

Carlotta Giusti  
Università and INFN, Pavia

# INCLUSIVE QUASIELASTIC SCATTERING ( $e, e'$ )

- only scattered electron detected
- all final nuclear states are included
- in the QE region the main contribution is given by the interaction on single nucleons and direct one-nucleon emission

# INCLUSIVE SCATTERING : IMPULSE APPROXIMATION

- ✱ IA : c.s given by the sum of integrated direct one-nucleon emission over all the nucleons
- ✱ IPSM :  $\sum_n$  over all occupied states in the SM,

# INCLUSIVE SCATTERING: FSI

DWIA RDWIA sum of 1NKO where FSI are described by a complex OP with an imaginary absorptive part does not conserve the flux

PWIA RPWIA FSI neglected

REAL POTENTIAL

rOP rROP only the real part of the OP: conserves the flux but it is conceptually wrong

RMF RELATIVISTIC MEAN FIELD: same real energy-independent potential of bound states  
Orthogonalization, fulfills dispersion relations and maintains the continuity equation

GF RGF GREEN'S FUNCTION complex OP conserves the flux  
consistent description of FSI in exclusive and inclusive QE electron scattering

# FSI for the inclusive scattering : Green's Function Model

- the components of the inclusive response are expressed in terms of the Green's operator
- under suitable approximations can be written in terms of the s.p. optical model Green's function
- the explicit calculation of the s.p. Green's function can be avoided by its spectral representation that is based on a biorthogonal expansion in terms of the eigenfunctions of the non Herm optical potential  $V$  and  $V^+$
- matrix elements similar to DWIA
- scattering states eigenfunctions of  $V$  and  $V^+$  (absorption and gain of flux): the imaginary part redistributes the flux and the total flux is conserved
- consistent treatment of FSI in the exclusive and in the inclusive scattering

# NUCLEAR RESPONSE

$$\begin{aligned}
 W^{\mu\mu} &= \sum_f \langle \Psi_i | J^{\mu+} | \Psi_f \rangle \langle \Psi_f | J^\mu | \Psi_i \rangle \delta(\omega + E_i - E_f) \\
 &= \sum_f \langle \Psi_i | J^{\mu+} \delta(\omega + E_i - H) | \Psi_f \rangle \langle \Psi_f | J^\mu | \Psi_i \rangle \\
 &= \langle \Psi_i | J^{\mu+} \delta(\omega + E_i - H) J^\mu | \Psi_i \rangle \quad \frac{1}{x \pm i\epsilon} = \mathcal{P} \left( \frac{1}{x} \right) \mp i\pi\delta(x) \\
 &= \frac{1}{\pi} \text{Im} \langle \Psi_i | J^{\mu+} G^+(\omega + E_f) J^\mu | \Psi_i \rangle \quad \delta(E - H) = \frac{1}{2\pi i} [G^\dagger(E) - G(E)]
 \end{aligned}$$

$$G^+(\omega + E_f) = \frac{1}{\omega + E_i - H - i\epsilon}$$

## GREEN'S FUNCTION

H nuclear Hamiltonian

The diagonal components of the hadron tensor are expressed in terms of the Green function  $G^+$  the full A-body propagator. Only an approximate treatment reduces the problem to a tractable form

with suitable approximations the components of the nuclear response are written in terms of **the s.p. optical model Green's function**

$$W^{\mu\mu} = \frac{1}{\pi} \text{Im} \langle \Psi_i | J^{\mu+} G^+(\omega + E_f) J^\mu | \Psi_i \rangle$$

■ one-body current

$$J^\mu \simeq \sum_{k=1}^A j_k^\mu$$

■ non diagonal terms neglected (high enough q)  $j_k^{\mu+} G^+ j_l^\mu \quad k \neq l$

$$\begin{aligned} W^{\mu\mu} &\simeq \frac{1}{\pi} \sum_k \text{Im} \langle \Psi_i | j_k^{\mu+} G^+(E_f) j_k^\mu | \Psi_i \rangle \\ &= \frac{Z}{\pi} \text{Im} \langle \Psi_i | j_{1p}^{\mu+} G^+(E_f) j_{1p}^\mu | \Psi_i \rangle + \frac{N}{\pi} \text{Im} \langle \Psi_i | j_{1n}^{\mu+} G^+(E_f) j_{1n}^\mu | \Psi_i \rangle \end{aligned}$$

■  $j_1^\mu | \Psi_i \rangle \simeq \sum_n P_n j_1^\mu | \Psi_i \rangle \quad P_n = \int d\vec{r}_1 | \vec{r}_1 n \rangle \langle \vec{r}_1 n |$

$n$  discrete eigenstate of  $H_{A-1}$  or isolated resonance in the continuum

$$P_n + Q_n = 1 \quad Q_n^2 = Q_n \quad \sum_n P_n + P' = 1 \quad Q_n = \sum_{m \neq n} Q_m + P'$$

$$W^{\mu\mu} = \frac{A}{\pi} \text{Im} \sum_{n,m} \langle \Psi_i | j_1^{\mu+} P_n G^+(E_f) P_m j_1^\mu | \Psi_i \rangle$$

$$P_n G^+(E_f) P_m j_1^\mu | \Psi_i \rangle \simeq 0 \quad \text{if } n \neq m \quad \leftarrow$$

$$\begin{aligned} W^{\mu\mu} &\simeq \frac{A}{\pi} \text{Im} \sum_n \langle \Psi_i | j_1^{\mu+} \underbrace{P_n G^+(E_f) P_n}_{G_n^+(E_f)} j_1^\mu | \Psi_i \rangle \\ &= A \sum_n W_n^{\mu\mu} \end{aligned}$$

$$G^+ \text{ replaced by } \sum_n G_n^+ \quad \leftarrow$$

$G_n^+(E_f)$  is the s.p. Green's function related to the Feshbach optical model Hamiltonian  $\mathcal{H}_n^+$



$$(E - H) G(E) = 1$$

$$\underbrace{P_n + Q_n}_{P_n} \longrightarrow (E - P_n H P_n) P_n G(E) P_n - P_n H Q_n G(E) P_n = P_n$$

$$Q_n \longrightarrow (E - Q_n H Q_n) Q_n G(E) P_n - Q_n H Q_n G(E) P_n = P_n$$

$$\longrightarrow Q_n G(E) P_n = \frac{1}{E - Q_n H Q_n + i\eta} Q_n H P_n G(E) P_n$$

$$P_n G(E) P_n = G_n(E) = \frac{P_n}{E - \mathcal{H}_n^A(E) + i\eta} \quad G_n^+(E) = \frac{P_n}{E - \mathcal{H}_n^{A+}(E) - i\eta}$$

$$\mathcal{H}_n^A(E) = P_n H P_n + P_n H Q_n \frac{1}{E - Q_n H Q_n + i\eta} Q_n H P_n$$

is the OP A-body Hamiltonian which describes the elastic scattering of a nucleon by an (A-1)-system in the state  $n$

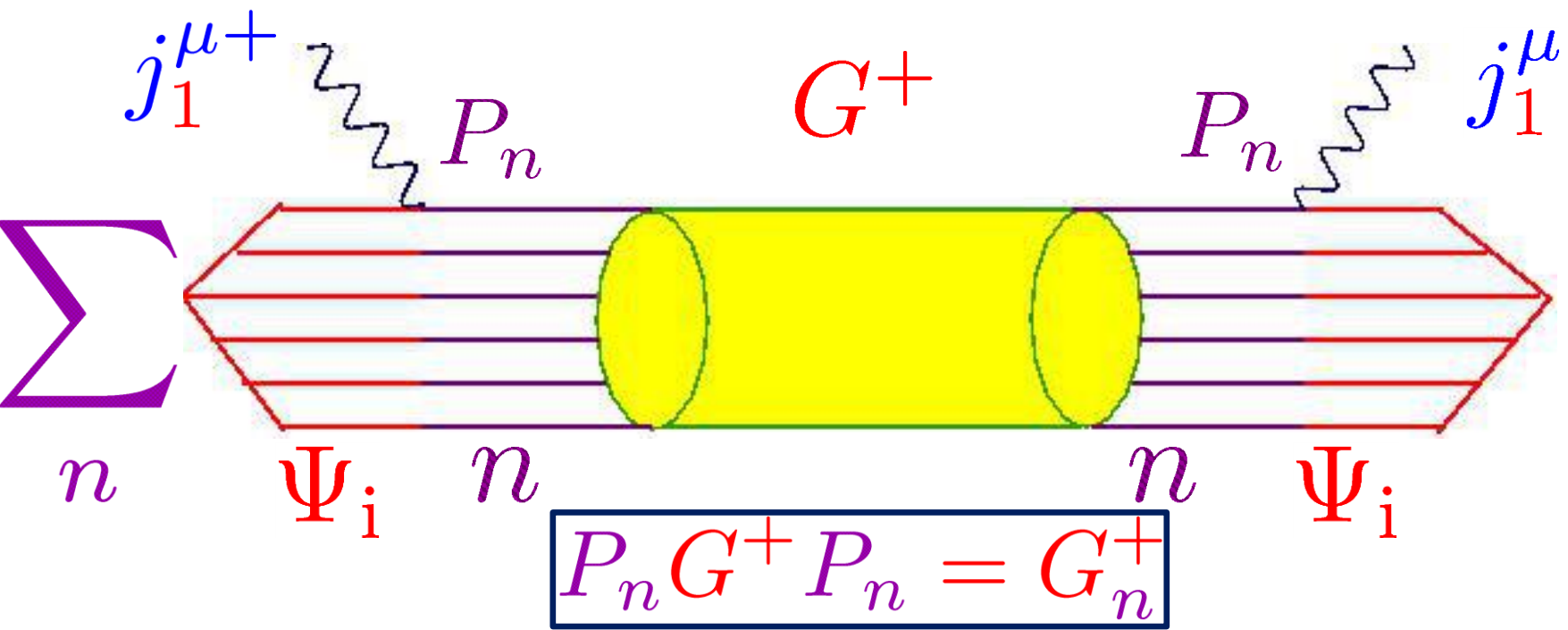
the matrix elements of  $G_n$  give the s.p. optical model Green's function

$$W^{\mu\mu} = \sum_n W_n^{\mu\mu} = \sum_i \overline{\sum_n} \frac{1}{\pi} \text{Im} \langle \Psi_i | \underbrace{j_1^{\mu+} P_n G^+(E_f) P_n j_1^\mu}_{G_n^+(E_f)} | \Psi_i \rangle$$

1.  $J^\mu$  1-body  $j_1^\mu$

2.  $j_1^\mu | \Psi_i \rangle \simeq \sum P_n j_1^\mu | \Psi_i \rangle \longrightarrow j_1^\mu$  produces only states and their combination  
 $P_n = \int d\vec{r}_1 | \vec{r}_1 n \rangle \langle \vec{r}_1 n |$   $| \vec{r}_1 n \rangle$

3.  $P_n G^+(E_f) P_m j_1^\mu | \Psi_i \rangle \simeq 0$  if  $n \neq m$   
 $P_n G^+(E_f) Q_n$



**ALL** final states are included in  $G^+$  which contains the total nuclear Hamiltonian  $H$

# Spectral decomposition of the nuclear response

The eigenfunctions of  $\mathcal{H}_n$  and  $\mathcal{H}_n^+$

$$\begin{aligned}\mathcal{H}_n^+(E_f) | \Phi_E^{(\mp)} \rangle &= E | \Phi_E^{(\mp)} \rangle \\ \mathcal{H}_n(E_f) | \tilde{\Phi}_E^{(\mp)} \rangle &= E | \tilde{\Phi}_E^{(\mp)} \rangle\end{aligned} \quad \forall n \quad E_f$$

form a biorthogonal system

$$\int dE | \Phi_E^{(\mp)} \rangle \langle \tilde{\Phi}_E^{(\mp)} | = \int dE | \tilde{\Phi}_E^{(\mp)} \rangle \langle \Phi_E^{(\mp)} | = 1 \quad \text{completeness}$$

$$\langle \tilde{\Phi}_E^{(\mp)} | \Phi_{E'}^{(\mp)} \rangle = \delta(E - E') \quad \text{orthogonality}$$

$$\begin{aligned}
W_n^{\mu\mu} &= \frac{1}{\pi} \text{Im} \langle \Psi_i | j_1^{\mu+} G_n^+(E_f) j_1^\mu | \Psi_i \rangle \\
&= \frac{1}{2\pi i} \langle \Psi_i | j_1^{\mu+} \left[ G_n^+(E_f - G_n(E_f)) \right] j_1^\mu | \Psi_i \rangle \\
&= \frac{1}{2\pi i} \int dE \left[ \langle \Psi_i | j_1^{\mu+} | \Phi_E^{(-)} \rangle \frac{1}{E_f - E - i\varepsilon} \langle \tilde{\Phi}_E^{(-)} | j_1^\mu | \Psi_i \rangle \right. \\
&\quad \left. - \langle \Psi_i | j_1^{\mu+} | \tilde{\Phi}_E^{(-)} \rangle \frac{1}{E_f - E + i\varepsilon} \langle \Phi_E^{(-)} | j_1^\mu | \Psi_i \rangle \right]
\end{aligned}$$

Spectral representation of  $G_n$  and  $G_n^+$

$$\frac{1}{x \pm i\varepsilon} = \mathcal{P} \left( \frac{1}{x} \right) \mp i\pi \delta(x)$$

$$\begin{aligned}
W_n^{\mu\mu} &= \frac{1}{\pi} \text{Im} \langle \Psi_i | j_1^{\mu+} G_n^+(E_f) j_1^\mu | \Psi_i \rangle \\
&= \frac{1}{2\pi i} \langle \Psi_i | j_1^{\mu+} \left[ G_n^+(E_f - G_n(E_f)) \right] j_1^\mu | \Psi_i \rangle \\
&= \frac{1}{2\pi i} \int dE \left[ \langle \Psi_i | j_1^{\mu+} | \Phi_E^{(-)} \rangle \frac{1}{E_f - E - i\varepsilon} \langle \tilde{\Phi}_E^{(-)} | j_1^\mu | \Psi_i \rangle \right. \\
&\quad \left. - \langle \Psi_i | j_1^{\mu+} | \tilde{\Phi}_E^{(-)} \rangle \frac{1}{E_f - E + i\varepsilon} \langle \Phi_E^{(-)} | j_1^\mu | \Psi_i \rangle \right]
\end{aligned}$$

Spectral representation of  $G_n$  and  $G_n^+$

$$\frac{1}{x \pm i\varepsilon} = \mathcal{P} \left( \frac{1}{x} \right) \mp i\pi\delta(x)$$

$$\begin{aligned}
W_n^{\mu\mu} &= \text{Re} \left[ \underbrace{\langle \Phi_{E_f}^{(-)} | j_1^\mu | \Psi_i \rangle \langle \tilde{\Phi}_{E_f}^{(-)} | j_1^\mu | \Psi_i \rangle^*}_{T_n^{\mu\mu}(E)} \right] \\
&- \frac{1}{\pi} \mathcal{P} \int \frac{dE}{E_f - E} \text{Im} \left[ \underbrace{\langle \Phi_{E_f}^{(-)} | j_1^\mu | \Psi_i \rangle \langle \tilde{\Phi}_{E_f}^{(-)} | j_1^\mu | \Psi_i \rangle^*}_{T_n^{\mu\mu}(E)} \right]
\end{aligned}$$

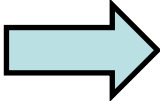
$$W^{\mu\mu} = \sum_n \left[ \text{Re} T_n^{\mu\mu}(E_f) - \frac{1}{\pi} \mathcal{P} \int \frac{dE}{E_f - E} \text{Im} T_n^{\mu\mu}(E_f) \right]$$

$$\langle \Phi_{E_f}^{(-)} | P_n j_1^\mu P_n | \Psi_i \rangle = \int d\vec{r} d\vec{r}_1 e^{i\vec{q}\cdot\vec{r}} \chi_{E,n}^{(-)*}(\vec{r}_1) j^\mu(\vec{r}_1, \vec{r}) \lambda_n^{1/2} \phi_n(\vec{r}_1)$$

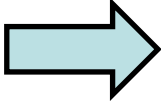
$$\langle \tilde{\Phi}_{E_f}^{(-)} | P_n j_1^\mu P_n | \Psi_i \rangle = \int d\vec{r} d\vec{r}_1 e^{i\vec{q}\cdot\vec{r}} \tilde{\chi}_{E,n}^{(-)*}(\vec{r}_1) j^\mu(\vec{r}_1, \vec{r}) \lambda_n^{1/2} \phi_n(\vec{r}_1)$$

The components of the inclusive response are written in terms of the same ingredients appearing in the **DWIA** approach of the **exclusive 1NKO**

The components of the inclusive response are written in terms of the same ingredients appearing in the **DWIA** approach of the **exclusive 1NKO**

$\chi^{(-)*}$   DW

$j^\mu$   1-body nuclear current

$\lambda^{1/2}\phi$   overlap



# INCLUSIVE SCATTERING

$$T_n^{\mu\mu}(E) = \lambda_n \int d\vec{r} d\vec{r}_1 e^{i\vec{q}\cdot\vec{r}} \chi_{E,n}^{(-)*}(\vec{r}_1) j^\mu(\vec{r}, \vec{r}_1) \phi_n(\vec{r}_1) \\ \times \left( \int d\vec{r}' d\vec{r}'_1 e^{i\vec{q}\cdot\vec{r}'} \tilde{\chi}_{E,n}^{(-)*}(\vec{r}'_1) j^\mu(\vec{r}', \vec{r}'_1) \phi_n(\vec{r}'_1) \right)^*$$

$\chi^{(-)}$   eigenstate of  $\mathcal{H}_n^+$   
absorption of flux

$\tilde{\chi}^{(-)}$   eigenstate of  $\mathcal{H}_n$   
gain of flux

The imaginary part of the optical potential is responsible for the redistribution of the strength in the different channels

# Interference between different channels

In the model

$$\langle \Psi_i | j^{\mu+} G^+(E_f) j^\mu | \Psi_i \rangle \simeq \sum_n \langle \Psi_i | j^{\mu+} G_n^+(E_f) j^\mu | \Psi_i \rangle$$

$$G^+(E) = \sum_n P_n G^+(E) (P_n + Q_n) = \sum_n (P_n + Q_n) G^+(E) P_n$$

If we set  $G^{+2}(E) \simeq \sum_n G_n^{+2}(E)$   $Q_n = \sum_{m \neq n} P_m + P'$

The exact relation  $G^{+2}(E) = -\frac{dG^+(E)}{dE}$  is not satisfied

$$\begin{aligned} -\frac{dG^+(E)}{dE} &\simeq -\sum_n \frac{dG_n^+(E)}{dE} = \sum_n G_n^+(E) (1 - \mathcal{H}_n^{+'}(E)) G_n^+(E) \\ &= \sum_n G_n^{+2}(E) - \sum_n G_n^+(E) \mathcal{V}_n^{+'}(E) G_n^+(E) \end{aligned}$$

When terms  $P_n G Q_n$  are neglected a discrepancy with the exact relation is obtained due to the energy depen. of the Feshbach OP that describes processes  $P_n H Q_n$

# Interference between different channels

In the model

$$\langle \Psi_i | j^{\mu+} G^+(E_f) j^\mu | \Psi_i \rangle \simeq \sum_n \langle \Psi_i | j^{\mu+} G_n^+(E_f) j^\mu | \Psi_i \rangle$$

$$G^+(E) = \sum_n P_n G^+(E) (P_n + \cancel{Q_n}) = \sum_n (P_n + \cancel{Q_n}) G^+(E) P_n$$

If we set  $G^{+2}(E) \simeq \sum_n G_n^{+2}(E)$   $Q_n = \sum_{m \neq n} P_m + P'$

The exact relation  $G^{+2}(E) = -\frac{dG^+(E)}{dE}$  is not satisfied

$$\begin{aligned} -\frac{dG^+(E)}{dE} &\simeq -\sum_n \frac{dG_n^+(E)}{dE} = \sum_n G_n^+(E) (1 - \mathcal{H}_n^{+'}(E)) G_n^+(E) \\ &= \sum_n G_n^{+2}(E) - \sum_n G_n^+(E) \mathcal{V}_n^{+'}(E) G_n^+(E) \end{aligned}$$

When terms  $P_n G Q_n$  are neglected a discrepancy with the exact relation is obtained due to the energy depen. of the Feshbach OP that describes processes  $P_n H Q_n$

When terms  $Q_n G P_n$  are neglected a discrepancy with the exact relation is obtained due to the energy dependence of the Feshbach OP that describes processes of the type  $P_n H Q_n$

The discrepancy can be eliminated and the approach improved

$$G(E) \simeq \sum_n \hat{G}_n(E)$$

$$\hat{G}_n(E) = \sqrt{1 - v'_n(E)} G_n(E) \sqrt{1 - v'_n(E)} \quad v''_n(E) \simeq 0$$

$$G^2(E) \simeq \sum_n \hat{G}_n^2(E) = \sum_n \sqrt{1 - v'_n(E)} G_n(E) (1 - v'_n(E)) G_n(E) \sqrt{1 - v'_n(E)}$$

When terms  $Q_n G P_n$  are neglected a discrepancy with the exact relation is obtained due to the energy dependence of the Feshbach OP that describes processes of the type  $P_n H Q_n$

The discrepancy can be eliminated and the approach improved

$$G(E) \simeq \sum_n \hat{G}_n(E)$$

$$\hat{G}_n(E) = \sqrt{1 - v'_n(E)} G_n(E) \sqrt{1 - v'_n(E)} \quad v''_n(E) \simeq 0$$

$$G^2(E) \simeq \sum_n \hat{G}_n^2(E) = \sum_n \sqrt{1 - v'_n(E)} G_n(E) (1 - v'_n(E)) G_n(E) \sqrt{1 - v'_n(E)}$$

operates in the same channel subspace and under the assumption of an almost linear energy dependence of the OP restores consistency with the exact relationship and includes most of the contributions of interference between different channels

When terms  $Q_n G P_n$  are neglected a discrepancy with the exact relation is obtained due to the energy dependence of the Feshbach OP that describes processes of the type  $P_n H Q_n$

The discrepancy can be eliminated and the approach improved

$$G(E) \simeq \sum_n \hat{G}_n(E)$$

$$\hat{G}_n(E) = \sqrt{1 - v'_n(E)} G_n(E) \sqrt{1 - v'_n(E)} \quad v''_n(E) \simeq 0$$

$$G^2(E) \simeq \sum_n \hat{G}_n^2(E) = \sum_n \sqrt{1 - v'_n(E)} G_n(E) (1 - v'_n(E)) G_n(E) \sqrt{1 - v'_n(E)}$$

$$-\frac{dG(E)}{dE} \simeq -\frac{d}{dE} \sum_n \hat{G}_n(E)$$

$$= \sum_n \sqrt{1 - v'_n(E)} G_n(E) (1 - v'_n(E)) G_n(E) \sqrt{1 - v'_n(E)}$$

$$\hat{G}_n(E) = \frac{P_n}{E - \hat{\mathcal{H}}_n + i\epsilon}$$

$$\hat{\mathcal{H}}_n = (1 - v'_n(E))^{-1/2} (\mathcal{H}_n(E) - E v'_n(E)) (1 - v'_n(E))^{-1/2}$$

is energy independent if  $v''_n(E) \simeq 0$

$$G_n(E) \Rightarrow \hat{G}_n(E) = \sqrt{1 - v'_n(E)} G_n(E) \sqrt{1 - v'_n(E)}$$

$$\mathcal{H}_n(E) \Rightarrow \hat{\mathcal{H}}_n = \sqrt{1 - v'_n(E)} (\mathcal{H}_n(E) - E v'_n(E)) \sqrt{1 - v'_n(E)}$$

$$\chi_E^{(-)} \Rightarrow \hat{\chi}_E^{(-)} = \sqrt{1 - v'_n(E)} \chi_E^{(-)}$$

$$\tilde{\chi}_E^{(-)} \Rightarrow \hat{\tilde{\chi}}_E^{(-)} = \sqrt{1 - v'_n(E)} \tilde{\chi}_E^{(-)}$$

The eigenfunctions of a non local energy independent potential can be written

$$\hat{\chi}_E^{(-)} = \sqrt{1 - v_{\mathbf{L}}^{*'}(E)} \chi_{\mathbf{L},E}^{(-)}$$

$$\hat{\tilde{\chi}}_E^{(-)} = \sqrt{1 - v'_{\mathbf{L}}(E)} \tilde{\chi}_{\mathbf{L},E}^{(-)}$$



The eigenfunctions of a non local energy independent potential can be written

$$\hat{\chi}_E^{(-)} = \sqrt{1 - v_L^{*'}(E)} \chi_{L,E}^{(-)}$$

$$\hat{\tilde{\chi}}_E^{(-)} = \sqrt{1 - v_L'(E)} \tilde{\chi}_{L,E}^{(-)}$$

eigenfunction of the local  
equivalent energy  
dependent potential

$$v_L^+(E) \quad v_L(E)$$

The eigenfunctions of a non local energy independent potential can be written

$$\hat{\chi}_E^{(-)} = \sqrt{1 - v_L^{*'}(E)} \chi_{L,E}^{(-)}$$

$$\hat{\tilde{\chi}}_E^{(-)} = \sqrt{1 - v_L'(E)} \tilde{\chi}_{L,E}^{(-)}$$

eigenfunction of the local  
equivalent energy  
dependent potential

$$v_L^+(E) v_L(E)$$



takes into account terms of interference between  
different channels and removes the whole energy  
dependence of  $v_L^+(E) v_L(E)$

# FSI for the inclusive scattering : Green's Function Model

$$W^{\mu\mu}(\omega, q) = \sum_n \left[ \mathbf{Re}T_n^{\mu\mu}(E_{\mathbf{f}} - \varepsilon_n, E_{\mathbf{f}} - \varepsilon_n) - \frac{1}{\pi} \mathcal{P} \int_M^\infty d\mathcal{E} \frac{1}{E_{\mathbf{f}} - \varepsilon_n - \mathcal{E}} \mathbf{Im}T_n^{\mu\mu}(\mathcal{E}, E_{\mathbf{f}} - \varepsilon_n) \right]$$

# FSI for the inclusive scattering : Green's Function Model

$$W^{\mu\mu}(\omega, q) = \sum_n \left[ \text{Re} \Gamma_n^{\mu\mu}(E_{\mathbf{f}} - \varepsilon_n, E_{\mathbf{f}} - \varepsilon_n) - \frac{1}{\pi} \mathcal{P} \int_M^\infty d\varepsilon \frac{1}{E_{\mathbf{f}} - \varepsilon_n - \varepsilon} \text{Im} \Gamma_n^{\mu\mu}(\varepsilon, E_{\mathbf{f}} - \varepsilon_n) \right]$$



$$T_n^{\mu\mu}(\varepsilon, E) = \lambda_n \langle \varphi_n | j^{\mu\dagger}(\mathbf{q}) \sqrt{1 - \mathcal{V}'(E)} | \tilde{\chi}_\varepsilon^{(-)}(E) \rangle \langle \chi_\varepsilon^{(-)}(E) | \sqrt{1 - \mathcal{V}'(E)} j^\mu(\mathbf{q}) | \varphi_n \rangle$$

# FSI for the inclusive scattering : Green's Function Model

$$W^{\mu\mu}(\omega, q) = \sum_n \left[ \text{Re} \Gamma_n^{\mu\mu}(E_{\mathbf{f}} - \varepsilon_n, E_{\mathbf{f}} - \varepsilon_n) - \frac{1}{\pi} \mathcal{P} \int_M^\infty d\varepsilon \frac{1}{E_{\mathbf{f}} - \varepsilon_n - \varepsilon} \text{Im} \Gamma_n^{\mu\mu}(\varepsilon, E_{\mathbf{f}} - \varepsilon_n) \right]$$



$$T_n^{\mu\mu}(\varepsilon, E) = \lambda_n \langle \varphi_n | j^{\mu\dagger}(\mathbf{q}) \sqrt{1 - \mathcal{V}'(E)} | \tilde{\chi}_\varepsilon^{(-)}(E) \rangle \langle \chi_\varepsilon^{(-)}(E) | \sqrt{1 - \mathcal{V}'(E)} j^\mu(\mathbf{q}) | \varphi_n \rangle$$

# FSI for the inclusive scattering : Green's Function Model

$$W^{\mu\mu}(\omega, q) = \sum_n \left[ \text{Re} \Gamma_n^{\mu\mu}(E_{\mathbf{f}} - \varepsilon_n, E_{\mathbf{f}} - \varepsilon_n) - \frac{1}{\pi} \mathcal{P} \int_M^\infty d\varepsilon \frac{1}{E_{\mathbf{f}} - \varepsilon_n - \varepsilon} \text{Im} \Gamma_n^{\mu\mu}(\varepsilon, E_{\mathbf{f}} - \varepsilon_n) \right]$$

$$T_n^{\mu\mu}(\mathcal{E}, E) = \lambda_n \langle \varphi_n | j^{\mu\dagger}(\mathbf{q}) \sqrt{1 - \mathcal{V}'(E)} | \tilde{\chi}_{\mathcal{E}}^{(-)}(E) \rangle \langle \chi_{\mathcal{E}}^{(-)}(E) | \sqrt{1 - \mathcal{V}'(E)} j^{\mu}(\mathbf{q}) | \varphi_n \rangle$$

interference between  
different channels

# FSI for the inclusive scattering : Green's Function Model

$$W^{\mu\mu}(\omega, q) = \sum_n \left[ \text{Re} \Gamma_n^{\mu\mu}(E_{\mathbf{f}} - \varepsilon_n, E_{\mathbf{f}} - \varepsilon_n) - \frac{1}{\pi} \mathcal{P} \int_M^\infty d\varepsilon \frac{1}{E_{\mathbf{f}} - \varepsilon_n - \varepsilon} \text{Im} \Gamma_n^{\mu\mu}(\varepsilon, E_{\mathbf{f}} - \varepsilon_n) \right]$$



$$T_n^{\mu\mu}(\varepsilon, E) = \lambda_n \langle \varphi_n | j^{\mu\dagger}(\mathbf{q}) \sqrt{1 - \mathcal{V}'(E)} | \tilde{\chi}_\varepsilon^{(-)}(E) \rangle \langle \chi_\varepsilon^{(-)}(E) | \sqrt{1 - \mathcal{V}'(E)} j^\mu(\mathbf{q}) | \varphi_n \rangle$$

# FSI for the inclusive scattering : Green's Function Model

$$W^{\mu\mu}(\omega, q) = \sum_n \left[ \text{Re} \Gamma_n^{\mu\mu}(E_{\mathbf{f}} - \varepsilon_n, E_{\mathbf{f}} - \varepsilon_n) - \frac{1}{\pi} \mathcal{P} \int_M^\infty d\varepsilon \frac{1}{E_{\mathbf{f}} - \varepsilon_n - \varepsilon} \text{Im} \Gamma_n^{\mu\mu}(\varepsilon, E_{\mathbf{f}} - \varepsilon_n) \right]$$



$$T_n^{\mu\mu}(\mathcal{E}, E) = \lambda_n \langle \varphi_n | j^{\mu\dagger}(\mathbf{q}) \sqrt{1 - \mathcal{V}'(E)} | \tilde{\chi}_\mathcal{E}^{(-)}(E) \rangle \langle \chi_\mathcal{E}^{(-)}(E) | \sqrt{1 - \mathcal{V}'(E)} j^\mu(\mathbf{q}) | \varphi_n \rangle$$

eigenfunctions of  $V$   
and  $V^+$



# FSI for the inclusive scattering : Green's Function Model

$$W^{\mu\mu}(\omega, q) = \sum_n \left[ \text{Re} \Gamma_n^{\mu\mu}(E_{\mathbf{f}} - \varepsilon_n, E_{\mathbf{f}} - \varepsilon_n) - \frac{1}{\pi} \mathcal{P} \int_M^\infty d\varepsilon \frac{1}{E_{\mathbf{f}} - \varepsilon_n - \varepsilon} \text{Im} \Gamma_n^{\mu\mu}(\varepsilon, E_{\mathbf{f}} - \varepsilon_n) \right]$$

$$T_n^{\mu\mu}(\mathcal{E}, E) = \lambda_n \langle \varphi_n | j^{\mu\dagger}(\mathbf{q}) \sqrt{1 - \mathcal{V}'(E)} | \tilde{\chi}_{\mathcal{E}}^{(-)}(E) \rangle \langle \chi_{\mathcal{E}}^{(-)}(E) | \sqrt{1 - \mathcal{V}'(E)} j^{\mu}(\mathbf{q}) | \varphi_n \rangle$$

loss of flux

# FSI for the inclusive scattering : Green's Function Model

$$W^{\mu\mu}(\omega, q) = \sum_n \left[ \text{Re} \Gamma_n^{\mu\mu}(E_{\mathbf{f}} - \varepsilon_n, E_{\mathbf{f}} - \varepsilon_n) - \frac{1}{\pi} \mathcal{P} \int_M^\infty d\varepsilon \frac{1}{E_{\mathbf{f}} - \varepsilon_n - \varepsilon} \text{Im} \Gamma_n^{\mu\mu}(\varepsilon, E_{\mathbf{f}} - \varepsilon_n) \right]$$

$$T_n^{\mu\mu}(\varepsilon, E) = \lambda_n \langle \varphi_n | j^{\mu\dagger}(\mathbf{q}) \sqrt{1 - \mathcal{V}'(E)} | \tilde{\chi}_\varepsilon^{(-)}(E) \rangle \langle \chi_\varepsilon^{(-)}(E) | \sqrt{1 - \mathcal{V}'(E)} j^\mu(\mathbf{q}) | \varphi_n \rangle$$

gain of flux

loss of flux

# FSI for the inclusive scattering : Green's Function Model

$$W^{\mu\mu}(\omega, q) = \sum_n \left[ \text{Re} \Gamma_n^{\mu\mu}(E_f - \varepsilon_n, E_f - \varepsilon_n) - \frac{1}{\pi} \mathcal{P} \int_M^\infty d\varepsilon \frac{1}{E_f - \varepsilon_n - \varepsilon} \text{Im} \Gamma_n^{\mu\mu}(\varepsilon, E_f - \varepsilon_n) \right]$$

$$T_n^{\mu\mu}(\mathcal{E}, E) = \lambda_n \langle \varphi_n | j^{\mu\dagger}(\mathbf{q}) \sqrt{1 - \mathcal{V}'(E)} | \tilde{\chi}_\mathcal{E}^{(-)}(E) \rangle \langle \chi_\mathcal{E}^{(-)}(E) | \sqrt{1 - \mathcal{V}'(E)} j^\mu(\mathbf{q}) | \varphi_n \rangle$$

gain of flux

loss of flux

Flux redistributed and conserved

The imaginary part of the optical potential is responsible for the redistribution of the flux among the different channels

# FSI for the inclusive scattering : Green's Function Model

$$W^{\mu\mu}(\omega, q) = \sum_n \left[ \text{Re} \Gamma_n^{\mu\mu}(E_f - \varepsilon_n, E_f - \varepsilon_n) - \frac{1}{\pi} \mathcal{P} \int_M^\infty d\varepsilon \frac{1}{E_f - \varepsilon_n - \varepsilon} \text{Im} \Gamma_n^{\mu\mu}(\varepsilon, E_f - \varepsilon_n) \right]$$

$$T_n^{\mu\mu}(\varepsilon, E) = \lambda_n \langle \varphi_n | j^{\mu\dagger}(\mathbf{q}) \sqrt{1 - \mathcal{V}'(E)} | \tilde{\chi}_\varepsilon^{(-)}(E) \rangle \langle \chi_\varepsilon^{(-)}(E) | \sqrt{1 - \mathcal{V}'(E)} j^\mu(\mathbf{q}) | \varphi_n \rangle$$

gain of flux

loss of flux

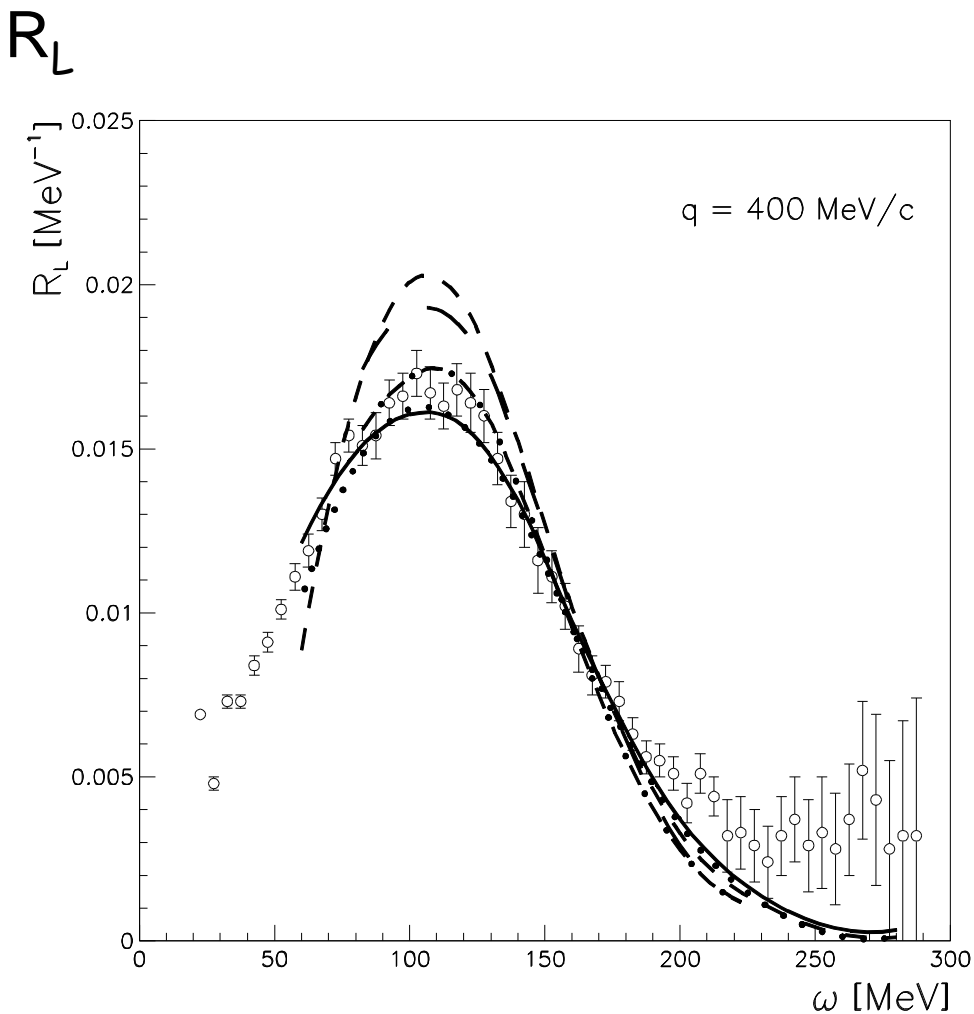
For a real optical potential  $V=V^*$  the second term vanishes and the nuclear response is given by the sum of all the integrated one-nucleon knockout processes (without absorption)

# CALCULATIONS

- phenomenological bound and scattering states: same ingredients in the inclusive and exclusive scattering
- FSI: phenomenological optical potential
- bound states: mean-field approach
- pure Shell Model description:  $\phi_n$  one-hole states in the target with a unitary spectral strength
- $\sum_n$  over all occupied states in the SM

$^{12}\text{C}(e, e')$

RGF - GF



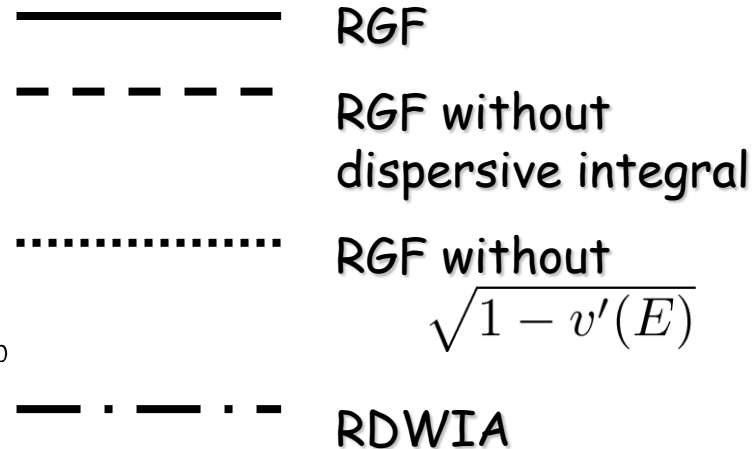
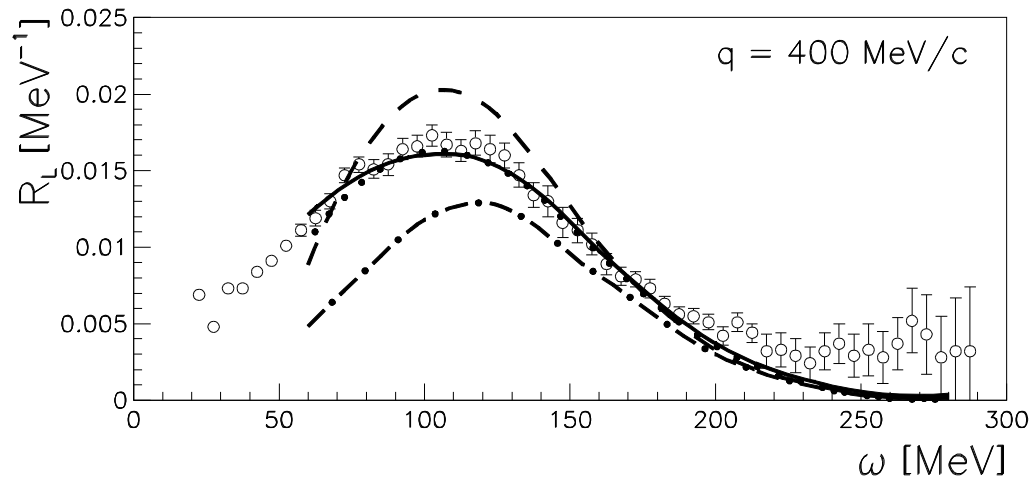
- RGF
- - - RGF without dispersive integral
- ⋯ RGF without  $\sqrt{1-v'(E)}$
- · - · GF
- - - GF without  $\sqrt{1-v'(E)}$

data from Saclay NPA 402 515 (1983)

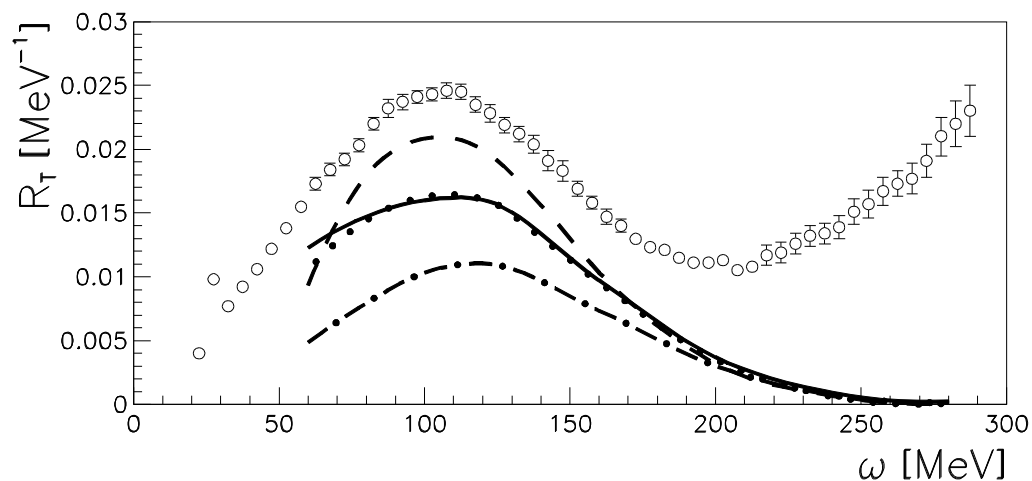
$^{12}\text{C}(e, e')$

RGF

$R_L$



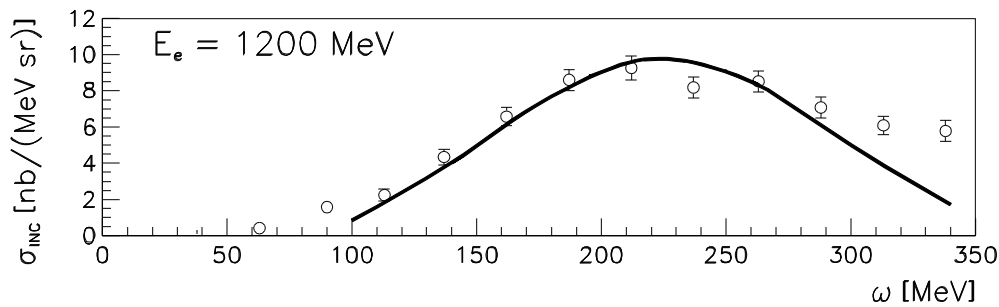
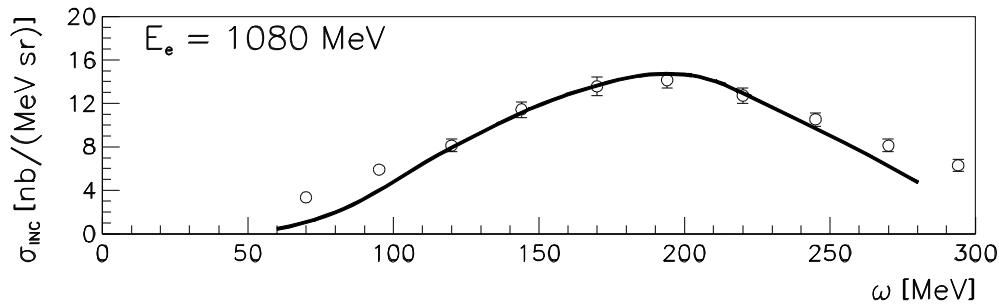
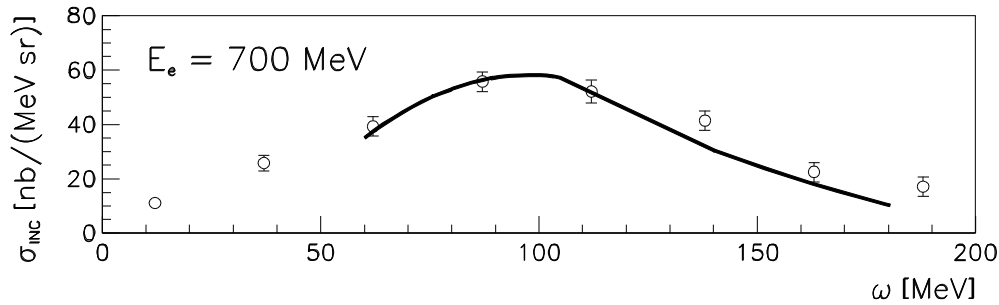
$R_T$



data from Saclay NPA 402 515 (1983)

$^{16}\text{O}(e, e')$

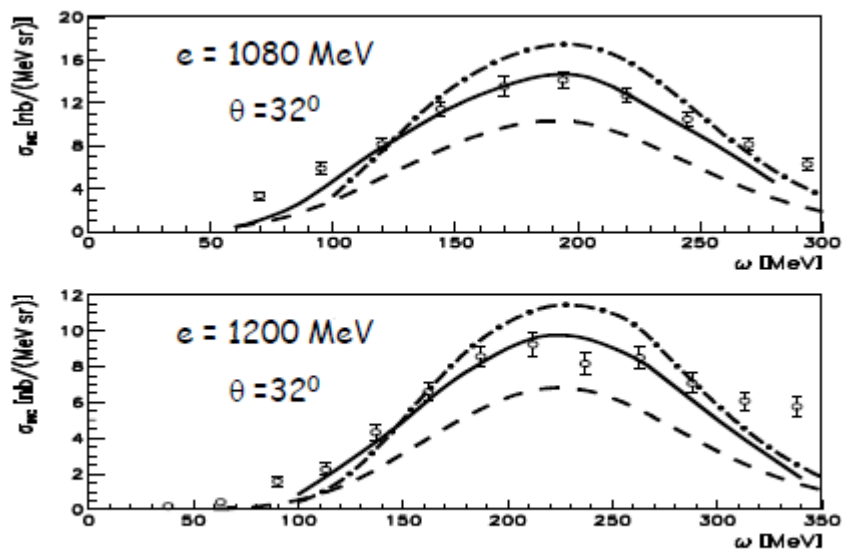
RGF



data from Frascati NPA 602 405 (1996)



# $^{16}\text{O}(e, e')$

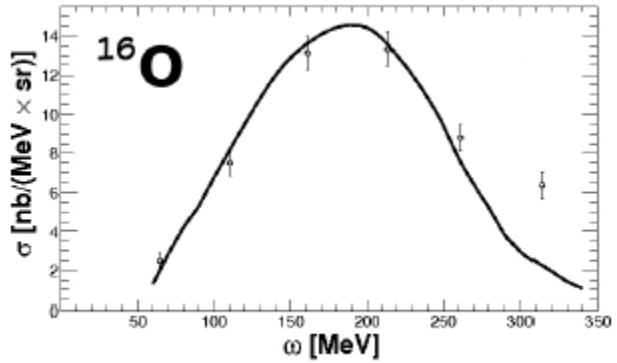


--- RPWIA  
— RGF  
- - - RDWIA

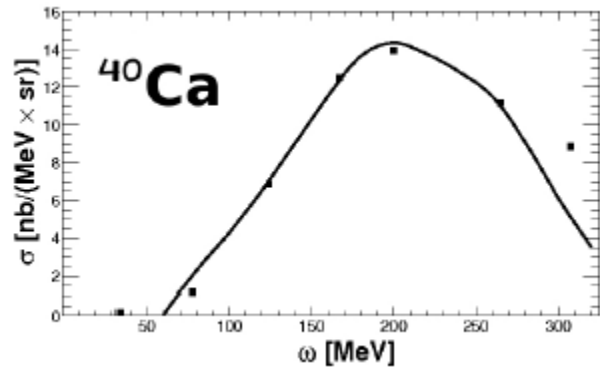
data from Frascati NPA 602 405 (1996)

$(e, e')$

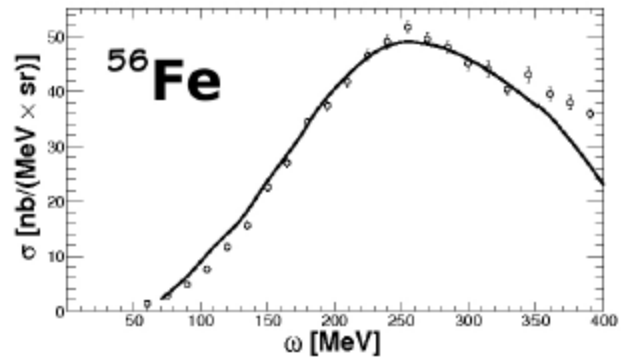
RGF



$$E_0 = 1080 \text{ MeV} \quad \vartheta = 32^\circ$$



$$E_0 = 841 \text{ MeV} \quad \vartheta = 45.5^\circ$$



$$E_0 = 2020 \text{ MeV} \quad \vartheta = 20^\circ$$

Different model: IA + Spectral function

# Different model: IA + spectral function

■ IA   $\sigma = \sum_N \sigma_{eN} \times \text{spectral function}$

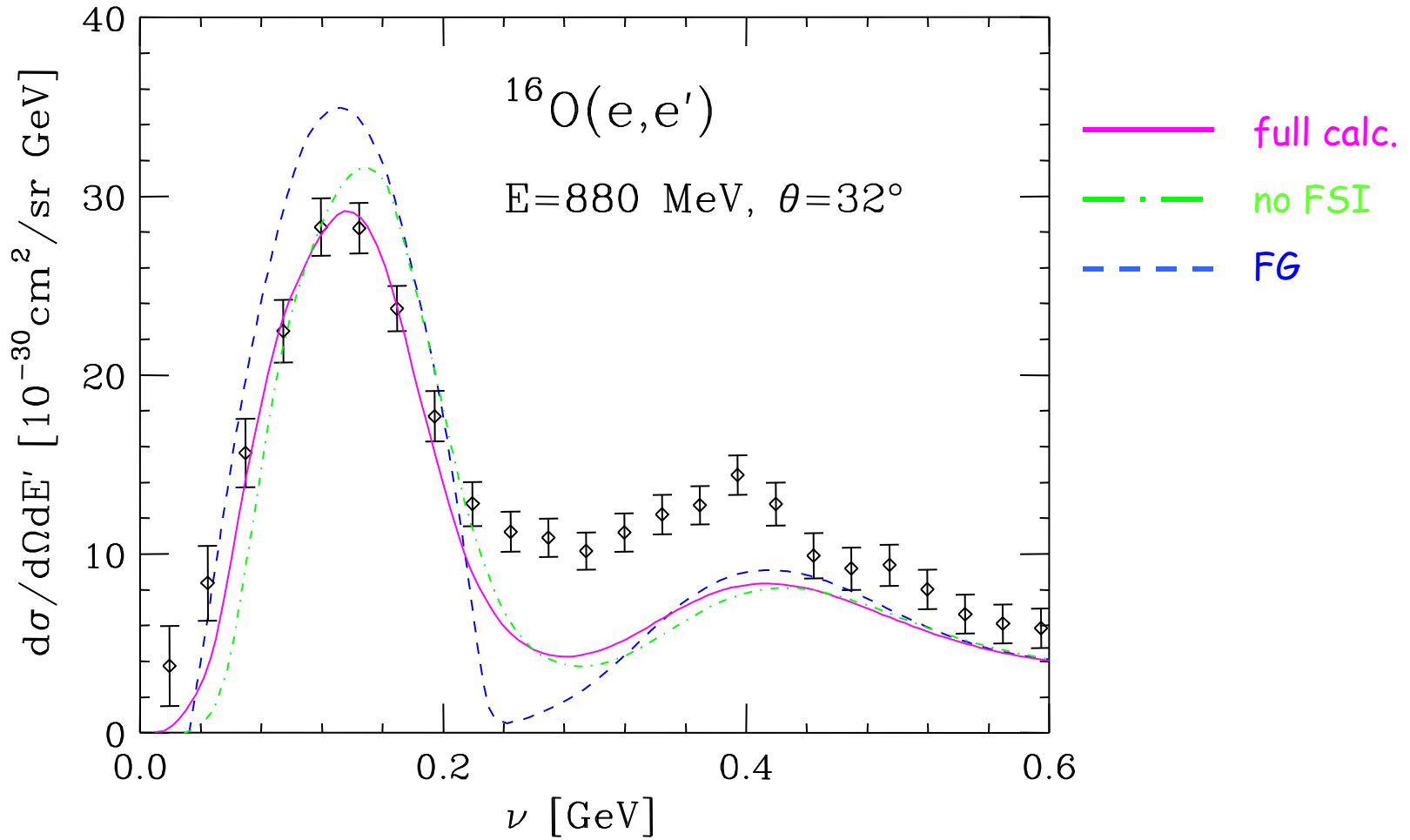
■ approach based on the nuclear many-body theory: the correlated spectral function of the target nucleus is obtained with a local density approximation in which nuclear matter results for a wide range of density values are combined with the exp information from (e,e'p) knockout reaction

■ statistical correlations: Pauli blocking included through a modification of the spectral function

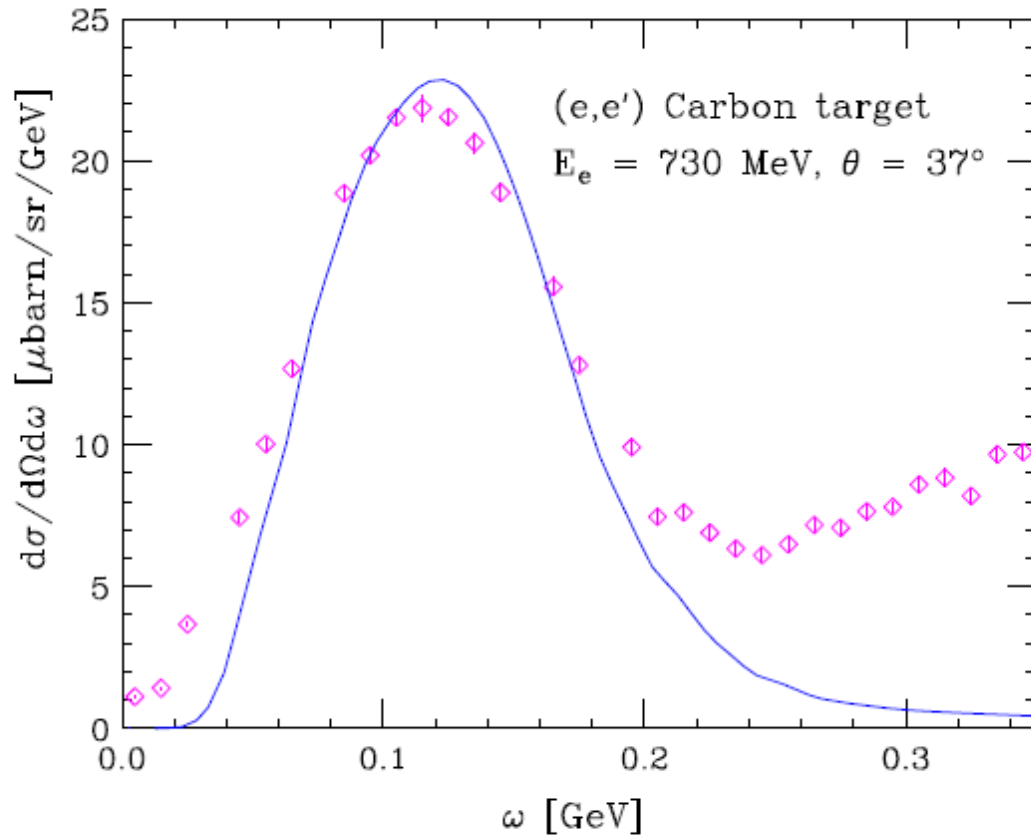
■ FSI: correlated Glauber approximation

- eikonal approximation: the struck nucleon moves along a straight trajectory with constant velocity
- frozen approximation: the spectator nucleons are seen by the struck nucleon as a collection of fixed scattering centers
- the propagator of the struck nucleon in the target factorized in terms of the free space propagator and of a part related to the nuclear transparency measured in (e,e'p)
- cross section in the convolution form

$$\frac{d\sigma}{d\Omega_{e'} d\nu} = \int d\nu' f_{\mathbf{q}}(\nu - \nu') \left( \frac{d\sigma}{d\Omega_{e'} d\nu'} \right)_{IA}$$



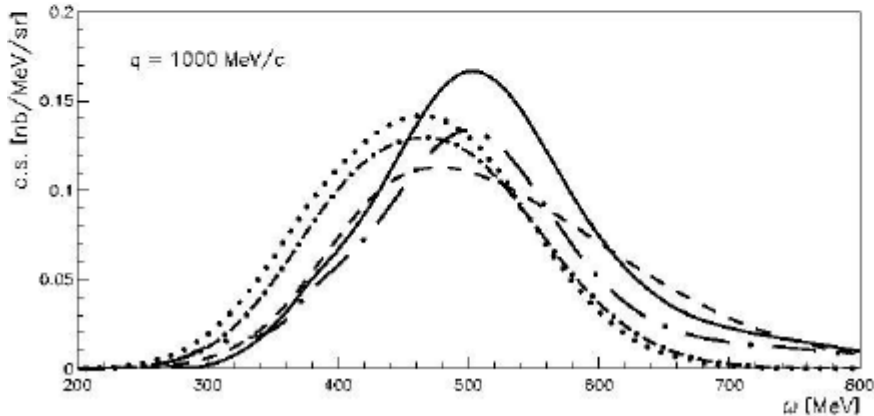
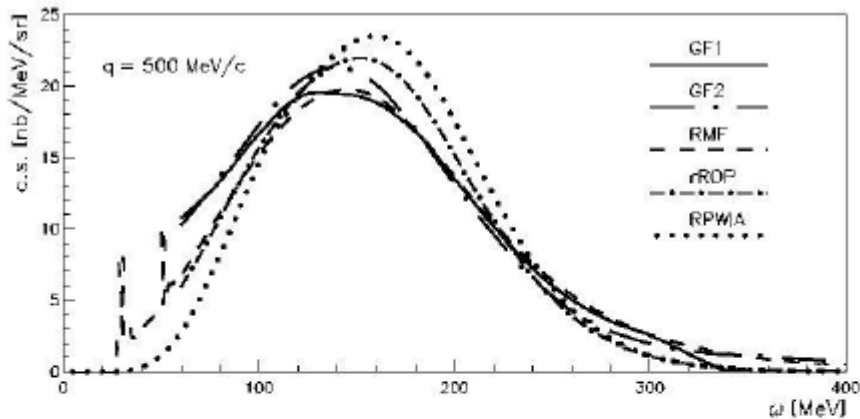
# $^{12}\text{C}(e, e')$



# $^{12}\text{C}(e, e')$

# comparison of relativistic models

$E_0 = 1 \text{ GeV}$



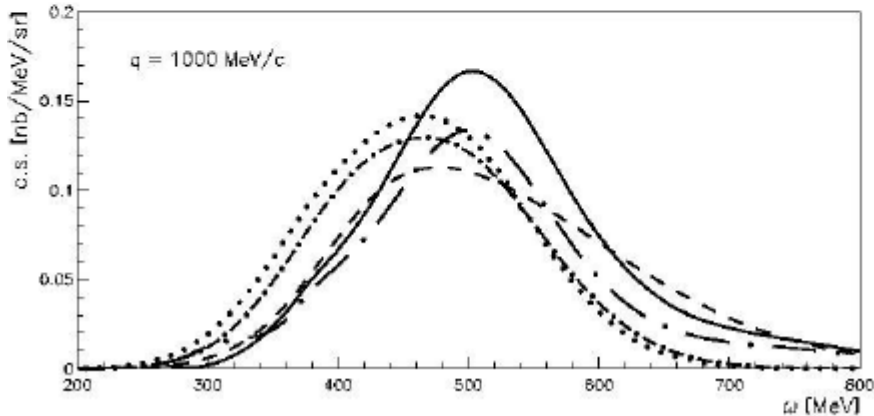
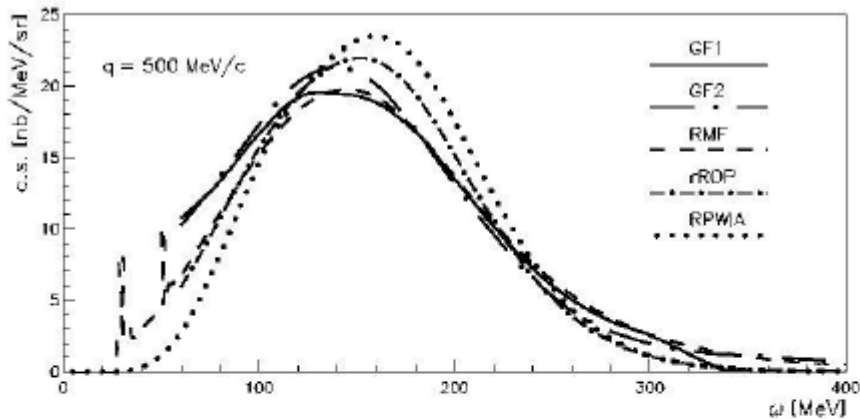
FSI

- RPWIA
- · - rROP
- RGF1
- · - RGF2
- - - RMF

# $^{12}\text{C}(e, e')$

# comparison of relativistic models

$E_0 = 1 \text{ GeV}$



FSI

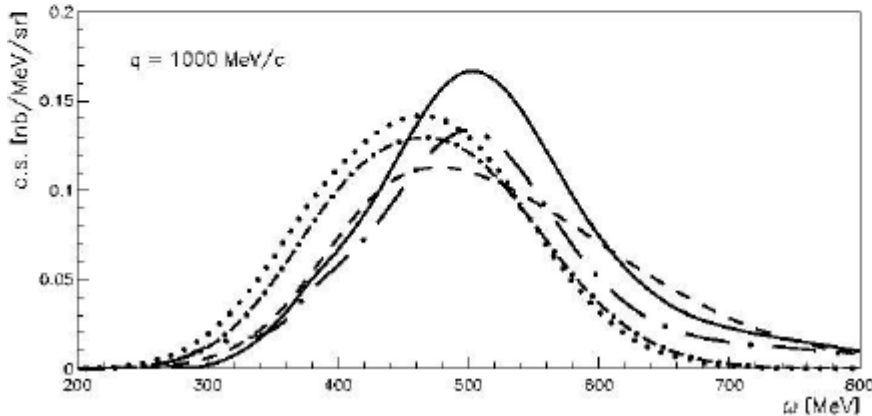
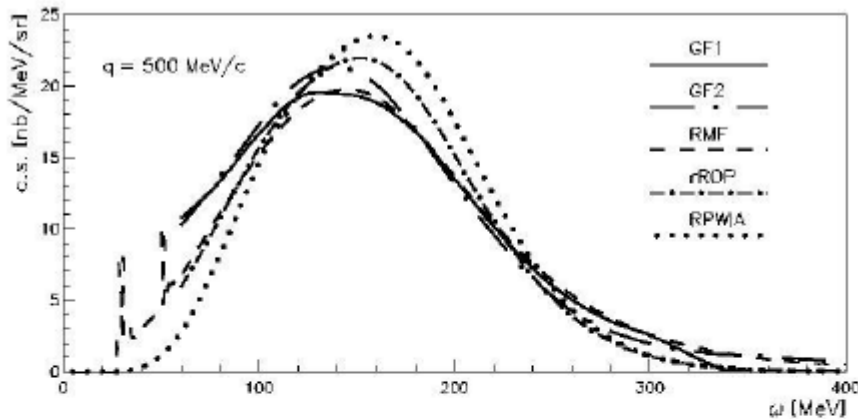
- RPWIA
- · - rROP
- RGF1 ←
- · - RGF2 ←
- - - RMF



# $^{12}\text{C}(e, e')$

# comparison of relativistic models

$E_0 = 1 \text{ GeV}$



## FSI

····· RPWIA

- · - rROP

— RGF1 ←

- · - RGF2 ←

- - - RMF

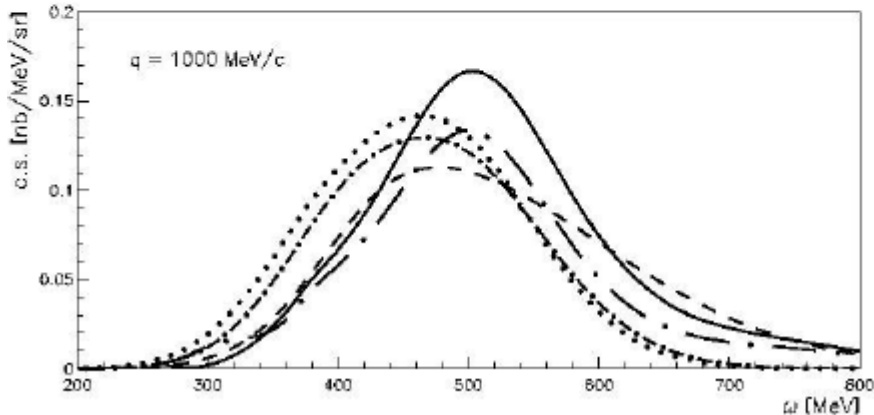
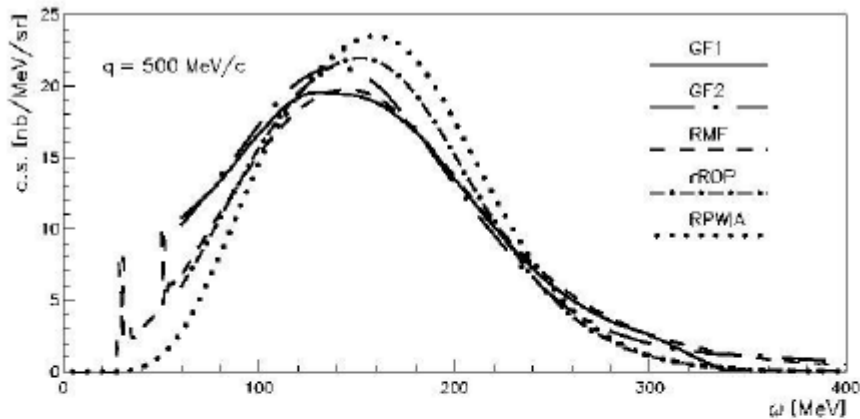
different  
parameterization of the  
optical potential: EDAD1

EDAD2

# $^{12}\text{C}(e, e')$

# comparison of relativistic models

$E_0 = 1 \text{ GeV}$



## FSI

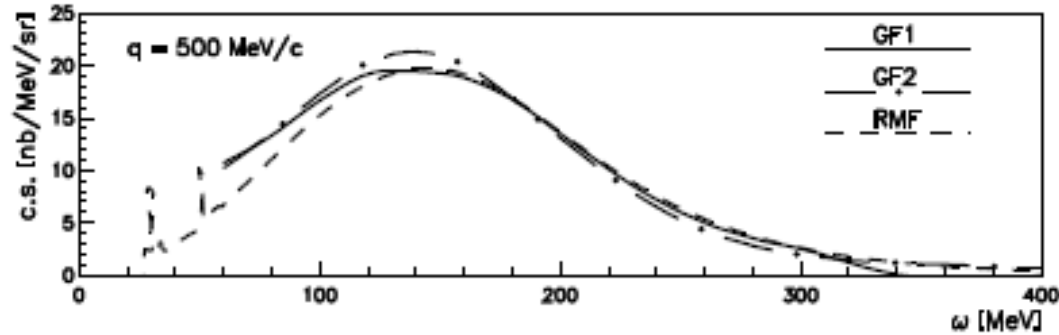
- RPWIA
- · - rROP
- RGF1 ←
- - - RGF2 ←
- - - RMF ←

# $^{12}\text{C}(e,e')$

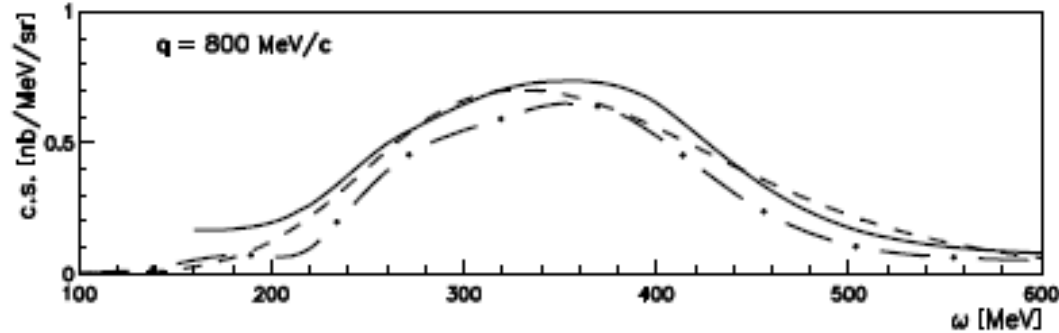
# comparison of relativistic models

**FSI**

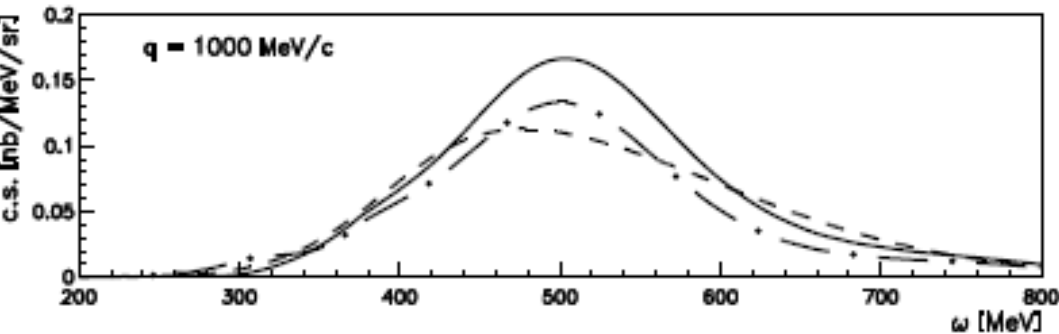
$q=500 \text{ MeV}/c$



$q=800 \text{ MeV}/c$



$q=1000 \text{ MeV}/c$



———— RGF1

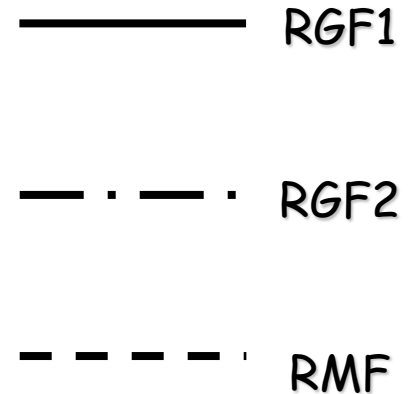
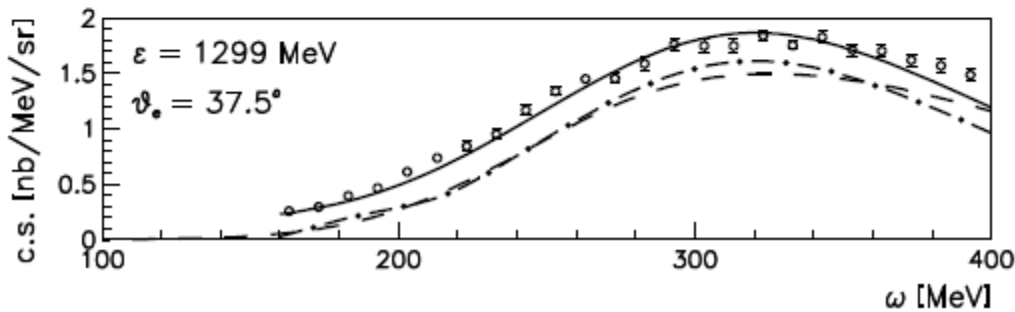
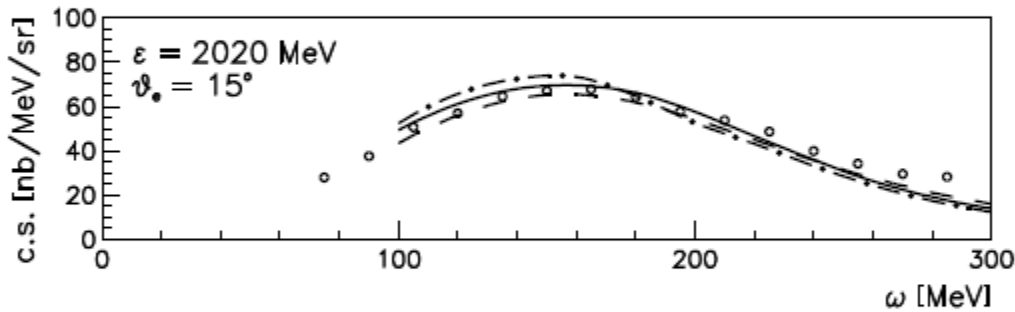
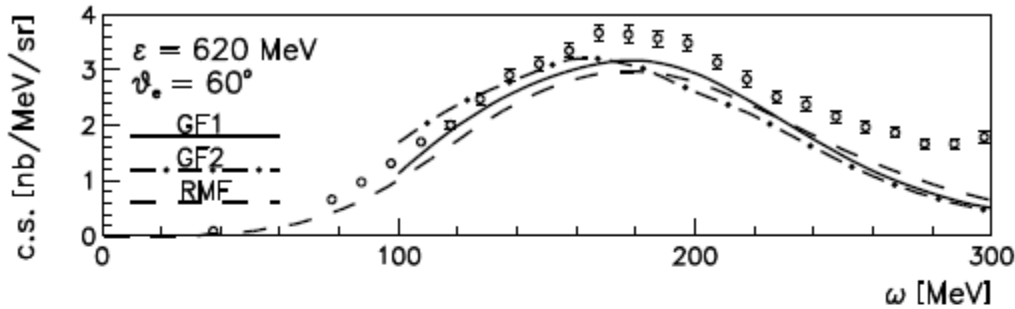
- · - · RGF2

- - - RMF

# $^{12}\text{C}(e, e')$

# comparison of relativistic models

FSI



# SCALING PROPERTIES

RGF



RMF

# SCALING FUNCTION

The analysis of  $(e,e')$  data has demonstrated the validity of scaling arguments

At sufficiently high  $q$  the scaling function  $f = \frac{d^2\sigma(q, \omega)/d\Omega dk'}{S^{s.n.}(q, \omega)}$

depends only upon one kinematical variable (scaling variable)

(SCALING OF I KIND)

is the same for all nuclei

(SCALING OF II KIND)

I+II

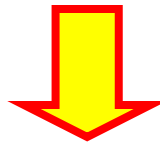
SUPERSCALING

In the QE region the scaling variable is obtained from the Relativistic Fermi Gas (RFG) where superscaling is exactly fulfilled

$$\psi_{\text{QE}} = \pm \sqrt{1/(2T_F) \left( q\sqrt{1 + 1/\tau} - \omega - 1 \right)}$$

+ (-) for  $\omega$  lower (higher) than the QEP, where  $\psi=0$

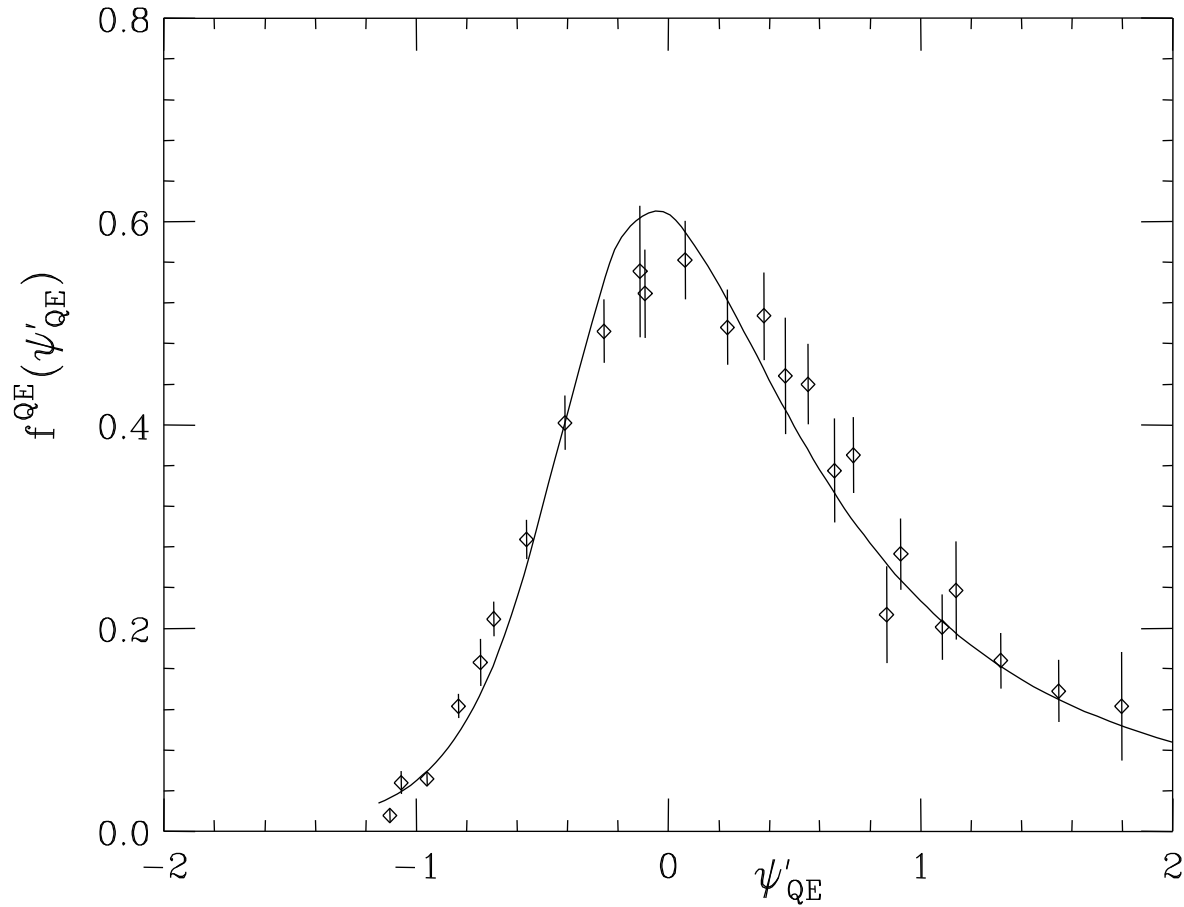
- Reasonable scaling of I kind at the left of QEP
- Excellent scaling of II kind in the same region
- Breaking of scaling particularly of I kind at the right of QEP (effects beyond IA)
- The longitudinal contribution superscales



$f^{\text{QE}}$

extracted from the data

# Experimental QE superscaling function



M.B. Barbaro, J.E. Amaro, J.A. Caballero, T.W. Donnelly, A. Molinari, and I. Sick,  
Nucl. Phys. Proc. Suppl 155 (2006) 257



# SCALING FUNCTION

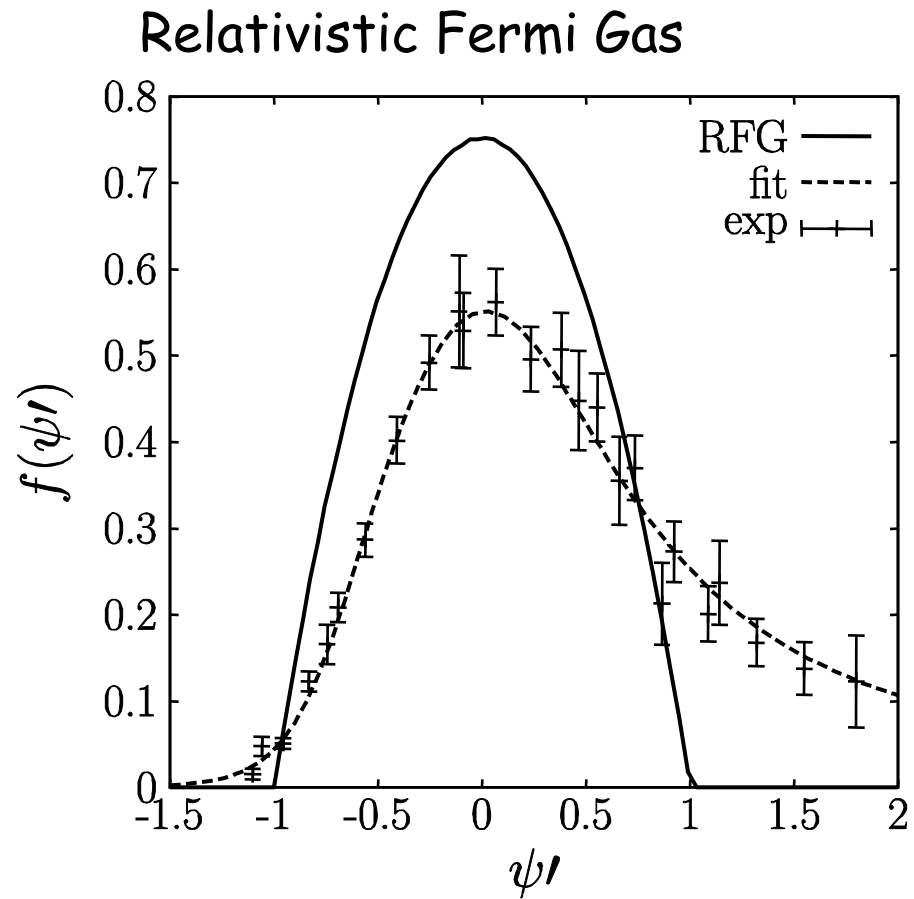
The properties of the experimental scaling function should be accounted for by microscopic calculations

The asymmetric shape of  $f^{QE}$  should be explained

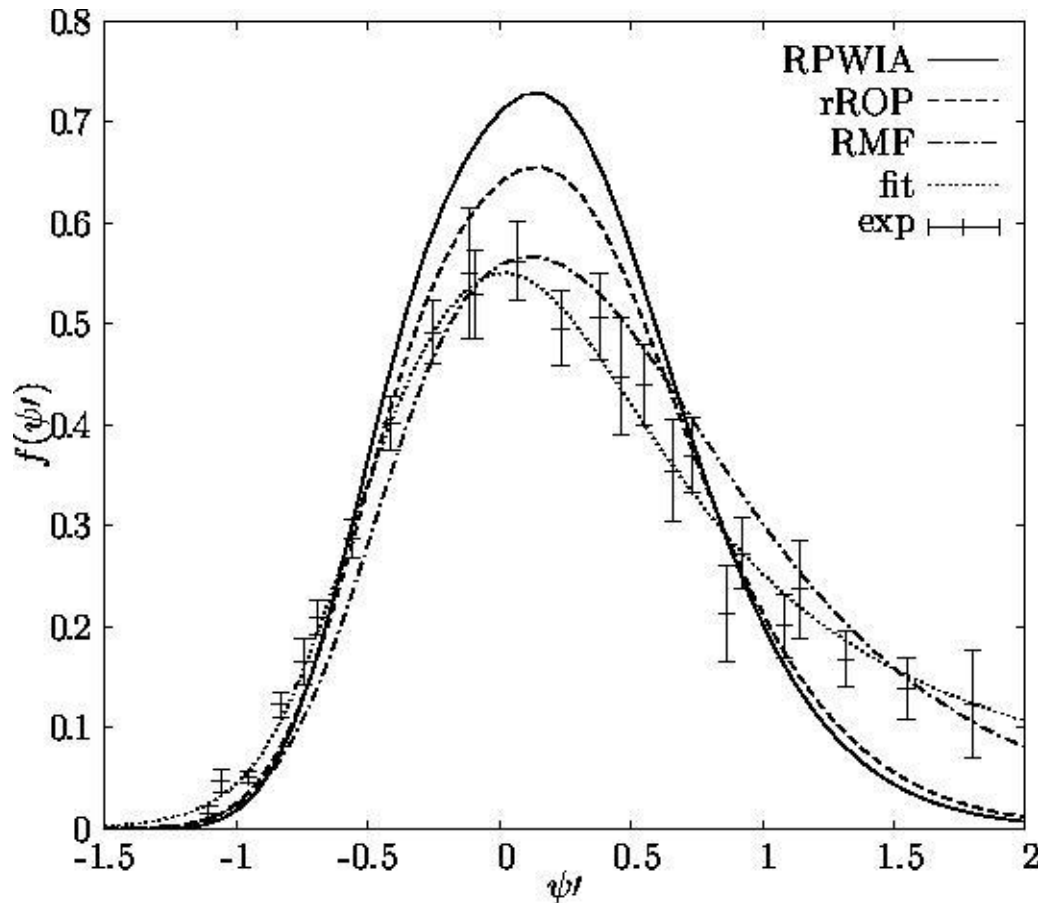
The scaling properties of different models can be verified

The associated scaling functions compared with the experimental  $f^{QE}$

# QE SUPERSCALING FUNCTION: RFG



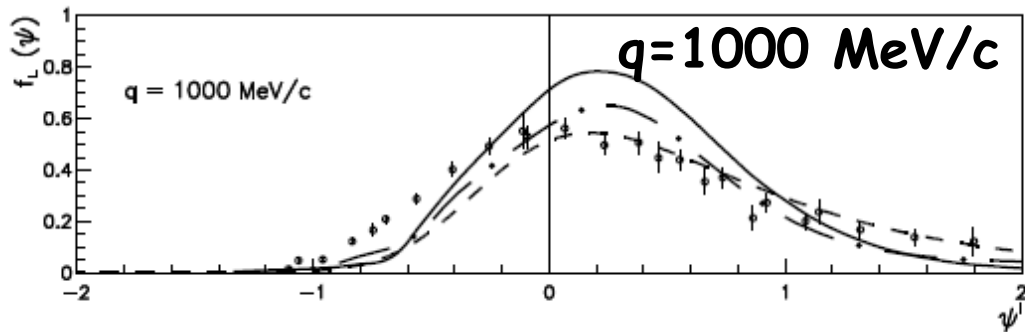
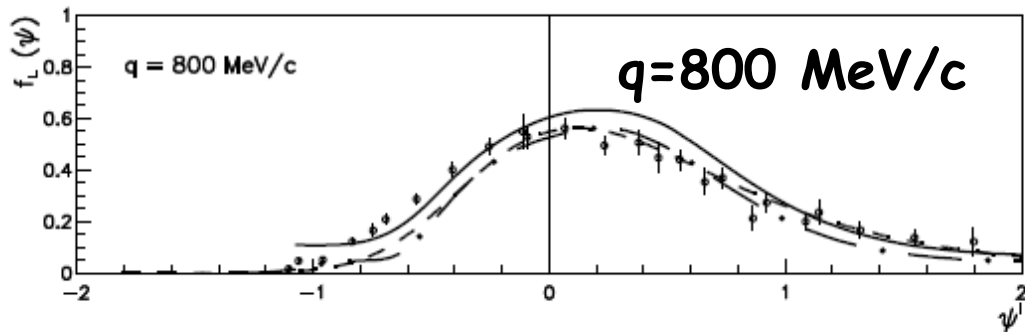
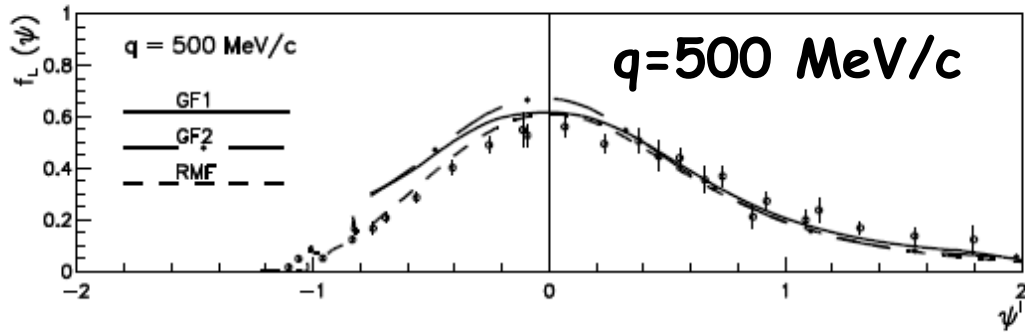
# QE SUPERSCALING FUNCTION: RPWIA, rROP, RMF



only RMF gives an asymmetric shape

J.A. Caballero J.E. Amaro, M.B. Barbaro, T.W. Donnelly, C. Maieron, and J.M. Udias  
PRL 95 (2005) 252502

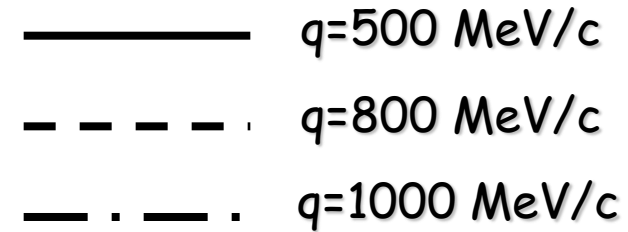
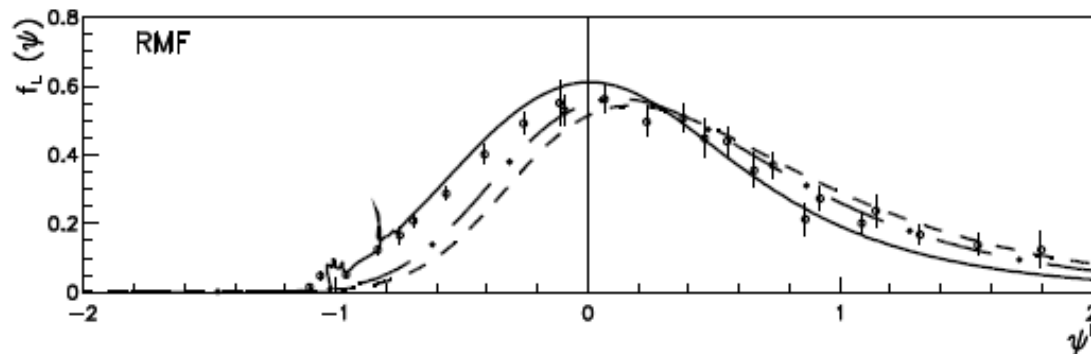
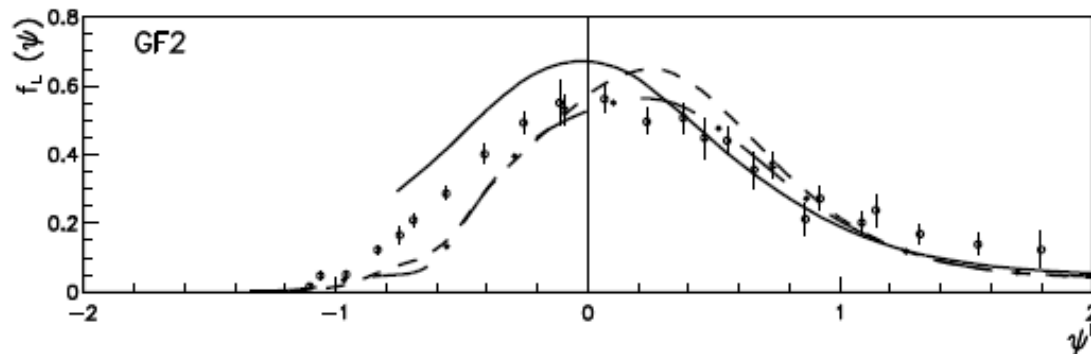
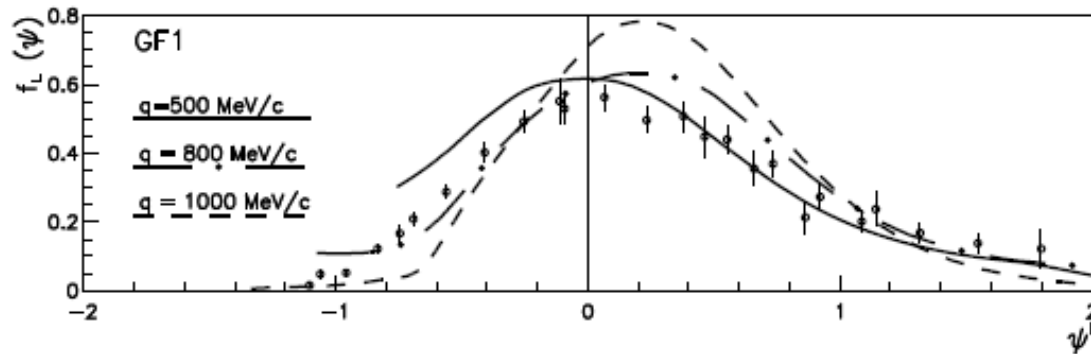
# QE SCALING FUNCTION: RGF, RMF



— RGF1  
- · - · RGF2  
- - - RMF

asymmetric shape

# Analysis first-kind scaling : RGF RMF



# DIFFERENT DESCRIPTIONS OF FSI

## RMF

real energy-independent MF reproduces nuclear saturation properties, purely nucleonic contribution, no information from scattering reactions explicitly incorporated



## RGF

complex energy-dependent phen. ROP fitted to elastic p-A scattering, incorporates information from scattering reactions

the imaginary part includes the overall effect of inelastic channels not included in other models based on the IA, (multinucleon, rescattering, non nucleonic).

Contributions of inelastic channels not included microscopically but recovered in the model by the Im part of the ROP, not univocally determined from elastic phenomenology

different ROP reproduce elastic p-A scatt. can give different predictions for non elastic observables

$\nu$ -nucleus scattering

# $\nu$ -nucleus scattering

- in electron scattering experiments the electron is a probe to investigate nuclear properties
- additional and complementary information on nuclear properties available from  $\nu$  scattering :  
excite nuclear modes inaccessible in electron scattering, information on hadronic weak current and strange nucleon form factors
- the aim of most  $\nu$  experiments is to investigate  $\nu$  properties



# $\nu$ -nucleus scattering

- $\nu$  properties not well known
- $\nu$  elusive particles, chargeless, almost massless and only weakly interacting, their presence can only be inferred detecting the particles they create when interacting with matter
- nuclei often used as  $\nu$  detectors providing relatively large cross sections
- a proper interpretation of data requires reliable calculations of  $\nu$ -nucleus cross sections where nuclear effects are taken into account and treated as accurately as possible

# $\nu$ -nucleus scattering

- its interest extends to different fields: astrophysics, cosmology, particle and nuclear physics
- useful tool to understand various astrophysical processes, to test the limits of the standard model, the properties of the weak interaction and to investigate nuclear structure
- in hadronic and nuclear physics gives information on the structure of the hadronic weak current and on the role of the strange quark contribution to the spin structure of the nucleon
- clean and accurate experimental information requires that nuclear effects are well under control
- nuclear effects: same models developed for electron scattering and tested in comparison with electron scattering data

QE electron and  $\nu$  nucleus  
scattering

## QE e-nucleus scattering

$$e + A \implies e' + N + (A - 1)$$

- both  $e'$  and  $N$  detected **one-nucleon knockout** ( $e, e'p$ )
- $(A-1)$  is a discrete eigenstate **exclusive** ( $e, e'p$ )
- only  $e'$  detected **inclusive** ( $e, e'$ )

## QE $\nu$ -nucleus scattering

$$\nu_l(\bar{\nu}_l) + A \implies \nu_l(\bar{\nu}_l) + N + (A - 1) \quad \text{NC}$$

$$\nu_l(\bar{\nu}_l) + A \implies l^-(l^+) + N + (A - 1) \quad \text{CC}$$

## QE e-nucleus scattering

$$e + A \implies e' + N + (A - 1)$$

- both  $e'$  and  $N$  detected **one-nucleon knockout** ( $e, e'p$ )
- $(A-1)$  is a discrete eigenstate **exclusive** ( $e, e'p$ )
- only  $e'$  detected **inclusive** ( $e, e'$ )

## QE $\nu$ -nucleus scattering

$$\nu_l(\bar{\nu}_l) + A \implies \nu_l(\bar{\nu}_l) + N + (A - 1) \quad \text{NC}$$

$$\nu_l(\bar{\nu}_l) + A \implies l^-(l^+) + N + (A - 1) \quad \text{CC}$$

- only  $N$  detected **semi-inclusive** NC and CC

## QE e-nucleus scattering

$$e + A \implies e' + N + (A - 1)$$

- both  $e'$  and  $N$  detected **one-nucleon knockout** ( $e, e'p$ )
- $(A-1)$  is a discrete eigenstate **exclusive** ( $e, e'p$ )
- only  $e'$  detected **inclusive** ( $e, e'$ )

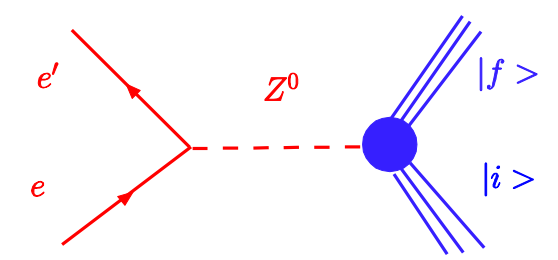
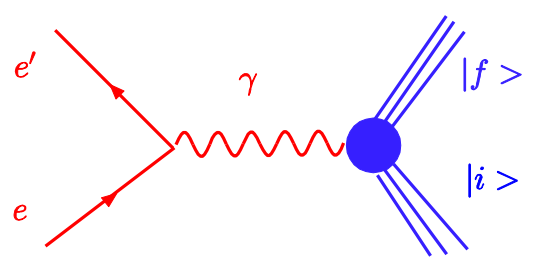
## QE $\nu$ -nucleus scattering

$$\nu_l(\bar{\nu}_l) + A \implies \nu_l(\bar{\nu}_l) + N + (A - 1) \quad \text{NC}$$

$$\nu_l(\bar{\nu}_l) + A \implies l^-(l^+) + N + (A - 1) \quad \text{CC}$$

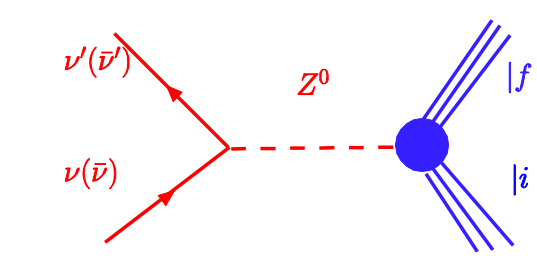
- only  $N$  detected **semi-inclusive** **NC** and **CC**
- only final lepton detected **inclusive** **CC**

# one-boson exchange

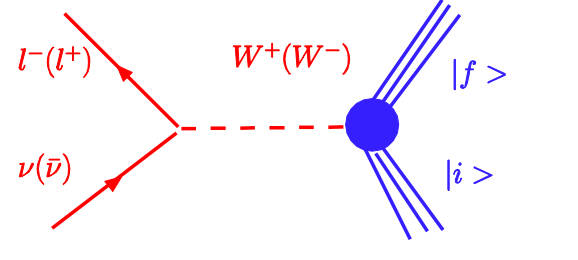


electron scattering

PVES



NC

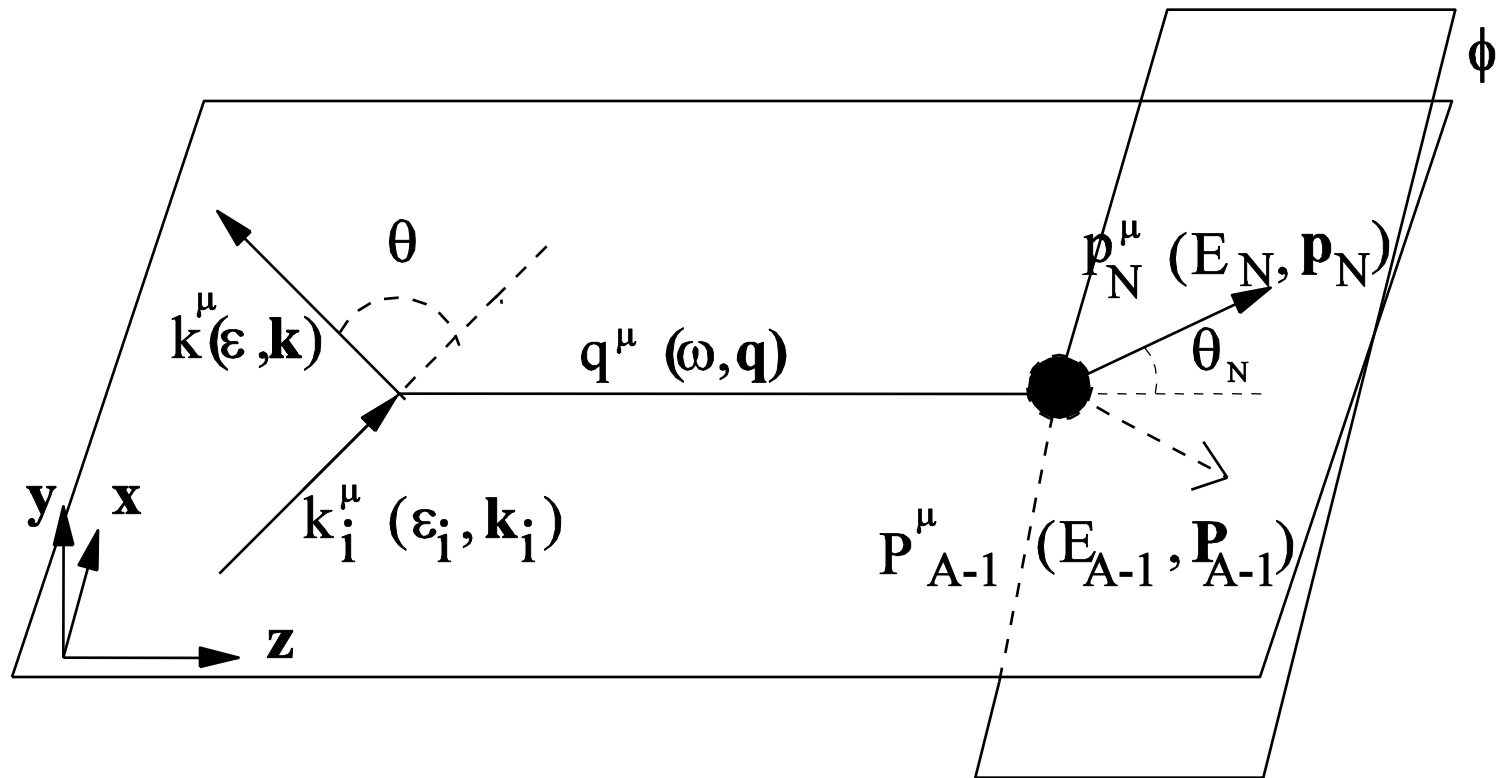


CC

neutrino scattering

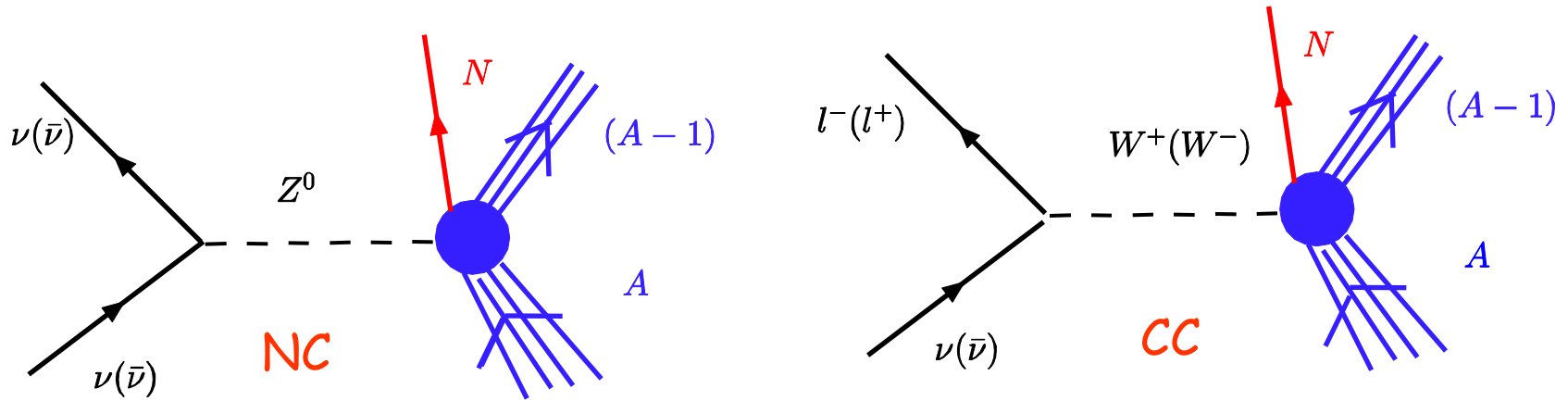
$$\sigma = K L^{\mu\nu} W_{\mu\nu}$$

# NC and CC QE scattering



$$y \parallel (k_i \times k)$$





$$\sigma = K L^{\mu\nu} W_{\mu\nu}$$

$$K = \frac{G_F^2}{2} 2\pi$$

$$G_F \simeq 1.16639 \times 10^{-11} \text{MeV}^{-2}$$

Fermi constant (NC)

$$K = \frac{G_F^2}{2} 2\pi \cos^2 \vartheta_C$$

$$\cos^2 \vartheta_C \simeq 0.9749$$

Cabibbo angle (CC)

Lepton tensor

$$L^{\mu\nu} = \frac{2}{\varepsilon_i \varepsilon} [l_S^{\mu\nu} \mp l_A^{\mu\nu}] \quad - \nu, + \bar{\nu}$$

$$l_S^{\mu\nu} = k_i^\mu k^\nu + k_i^\nu k^\mu - g^{\mu\nu} k_i \cdot k$$

$$l_A^{\mu\nu} = i \epsilon^{\mu\nu\alpha\beta} k_{i\alpha} k_\beta, \quad \epsilon_{0123} = -\epsilon^{0123} = 1$$

$$\frac{d\sigma}{d\varepsilon d\omega dT_N} = K \left[ v_0 R_{00} + v_{zz} R_{zz} - v_{0z} R_{0z} + v_T R_T \pm v_{xy} R_{xy} \right] \frac{|\mathbf{p}_N| E_N}{(2\pi)^3}$$

$$\frac{d\sigma}{d\varepsilon d\omega dT_N} = K \left[ v_0 R_{00} + v_{zz} R_{zz} - v_{0z} R_{0z} + v_T R_T \pm v_{xy} R_{xy} \right] \frac{|\mathbf{p}_N| E_N}{(2\pi)^3}$$

CC

NC

$$v_0 = 1 + \tilde{k} \cos \vartheta$$



$$v_0 = 2 \cos^2 \frac{\vartheta}{2} = \beta$$

$$v_{zz} = 1 + \tilde{k} \cos \vartheta - 2 \frac{\varepsilon_i |\mathbf{k}| \tilde{k}}{|\mathbf{q}|^2} \sin^2 \vartheta$$



$$v_{zz} = \frac{\omega^2}{|\mathbf{q}|^2} \beta$$

$$v_{0z} = \frac{\omega}{|\mathbf{q}|} \left( 1 + \tilde{k} \cos \vartheta \right) + \frac{m^2}{|\mathbf{q}| \varepsilon}$$



$$v_{0z} = \frac{\omega}{|\mathbf{q}|} \beta$$

$$v_T = 1 - \tilde{k} \cos \vartheta + \frac{\varepsilon_i |\mathbf{k}| \tilde{k}}{|\mathbf{q}|^2} \sin^2 \vartheta$$



$$v_T = \left( \tan^2 \frac{\vartheta}{2} + \frac{Q^2}{2|\mathbf{q}|^2} \right) \beta$$

$$v_{xy} = \frac{\varepsilon_i + \varepsilon}{|\mathbf{q}|} \left( 1 - \tilde{k} \cos \vartheta \right) - \frac{m^2}{|\mathbf{q}| \varepsilon}$$



$$v_{xy} = \tan \frac{\vartheta}{2} \left[ \tan^2 \frac{\vartheta}{2} + \frac{Q^2}{|\mathbf{q}|^2} \right]^{\frac{1}{2}} \beta$$

$m$



0

$$\tilde{k} = \frac{|\mathbf{k}|}{\varepsilon}$$



1

# response functions

$$R_{00} = W^{00}$$

$$R_{zz} = W^{zz}$$

$$R_{0z} = W^{0z} + W^{z0}$$

$$R_T = W^{xx} + W^{yy}$$

$$R_{xy} = i(W^{yx} - W^{xy})$$

$$W^{\mu\nu}(q, \omega) = \overline{\sum_{i,f}} \langle \Psi_f | \hat{J}^\mu(\mathbf{q}) | \Psi_i \rangle \langle \Psi_i | \hat{J}^{\nu\dagger}(\mathbf{q}) | \Psi_f \rangle \delta(E_i + \omega - E_f)$$

# response functions

$$R_{00} = W^{00}$$

$$R_{zz} = W^{zz}$$

$$R_{0z} = W^{0z} + W^{z0}$$

$$R_T = W^{xx} + W^{yy}$$

$$R_{xy} = i(W^{yx} - W^{xy})$$

$$W^{\mu\nu}(q, \omega) = \overline{\sum_{i,f}} \langle \Psi_f | \hat{J}^\mu(\mathbf{q}) | \Psi_i \rangle \langle \Psi_i | \hat{J}^{\nu\dagger}(\mathbf{q}) | \Psi_f \rangle \delta(E_i + \omega - E_f)$$

# One-body nuclear weak current

$$j^\mu = \left[ F_1^V(Q^2)\gamma^\mu + i\frac{\kappa}{2M}F_2^V(Q^2)\sigma^{\mu\nu}q_\nu - G_A(Q^2)\gamma^\mu\gamma^5 + F_P(Q^2)q^\mu\gamma^5 \right] \tau^\pm$$

CC

# One-body nuclear weak current

$$j^\mu = \left[ F_1^V(Q^2)\gamma^\mu + i\frac{\kappa}{2M}F_2^V(Q^2)\sigma^{\mu\nu}q_\nu - G_A(Q^2)\gamma^\mu\gamma^5 + F_P(Q^2)q^\mu\gamma^5 \right] \tau^\pm$$

CC

$$F_P = \frac{2MG_A}{m_\pi^2 + Q^2}$$

induced pseudoscalar form factor

# One-body nuclear weak current

$$j^\mu = \left[ F_1^V(Q^2)\gamma^\mu + i\frac{\kappa}{2M}F_2^V(Q^2)\sigma^{\mu\nu}q_\nu - G_A(Q^2)\gamma^\mu\gamma^5 + F_P(Q^2)q^\mu\gamma^5 \right] \tau^\pm$$

CC

$$F_P = \frac{2MG_A}{m_\pi^2 + Q^2}$$

induced pseudoscalar form factor

The axial form factor

$$G_A^{CC} = 1.26 \left( 1 + \frac{Q^2}{M_A^2} \right)^{-2}$$

CC

$$G_A^{p(n)NC} = \frac{1}{2} [ +(-)G_A^{CC} - G_A^s ]$$

NC

$$M_A = (1.03 \pm 0.02)\text{GeV}$$



# One-body nuclear weak current

$$j^\mu = \left[ F_1^V(Q^2)\gamma^\mu + i\frac{\kappa}{2M}F_2^V(Q^2)\sigma^{\mu\nu}q_\nu - G_A(Q^2)\gamma^\mu\gamma^5 + F_P(Q^2)q^\mu\gamma^5 \right] \tau^\pm$$

CC

$$F_P = \frac{2MG_A}{m_\pi^2 + Q^2}$$

induced pseudoscalar form factor

The axial form factor

$$G_A^{CC} = 1.26 \left( 1 + \frac{Q^2}{M_A^2} \right)^{-2}$$

CC

$$G_A^{p(n)NC} = \frac{1}{2} \left[ +(-)G_A^{CC} - \textcircled{G_A^s} \right]$$

NC

$$M_A = (1.03 \pm 0.02)\text{GeV}$$



possible strange-quark contribution

# One-body nuclear weak current

$$j^\mu = \left[ F_1^V(Q^2) \gamma^\mu + i \frac{\kappa}{2M} F_2^V(Q^2) \sigma^{\mu\nu} q_\nu - G_A(Q^2) \gamma^\mu \gamma^5 + F_P(Q^2) q^\mu \gamma^5 \right] \tau^\pm$$

The weak isovector Dirac and Pauli FF are related to the Dirac and Pauli elm FF by the CVC hypothesis

$$F_i^{V \text{ CC}} = F_i^p - F_i^n \quad \boxed{\text{CC}}$$

$$F_i^{Vp(n) \text{ NC}} = \left( \frac{1}{2} - 2 \sin^2 \theta_W \right) F_i^{p(n)} - \frac{1}{2} F_i^{n(p)} - \frac{1}{2} F_i^s \quad \boxed{\text{NC}}$$

$$\sin^2 \theta_W \simeq 0.23143$$

# One-body nuclear weak current

$$j^\mu = \left[ F_1^V(Q^2) \gamma^\mu + i \frac{\kappa}{2M} F_2^V(Q^2) \sigma^{\mu\nu} q_\nu - G_A(Q^2) \gamma^\mu \gamma^5 + F_P(Q^2) q^\mu \gamma^5 \right] \tau^\pm$$

The weak isovector Dirac and Pauli FF are related to the Dirac and Pauli elm FF by the CVC hypothesis

$$F_i^{V \text{ CC}} = F_i^p - F_i^n$$

$$F_i^{Vp(n) \text{ NC}} = \left( \frac{1}{2} - 2 \sin^2 \theta_W \right) F_i^{p(n)} - \frac{1}{2} F_i^{n(p)} - \frac{1}{2} F_i^s$$

CC

NC

$$\sin^2 \theta_W \simeq 0.23143$$

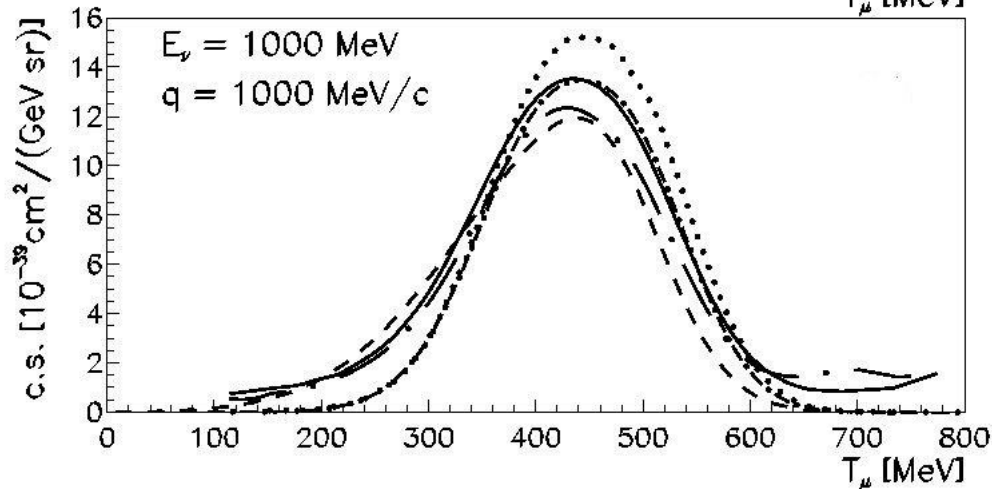
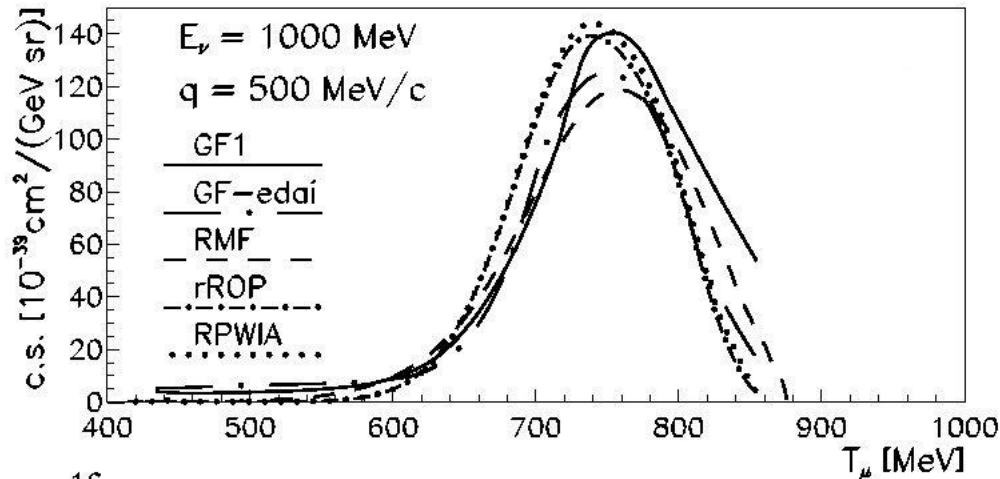


strange FF

$^{12}\text{C}(\nu_{\mu}, \mu^{-})$

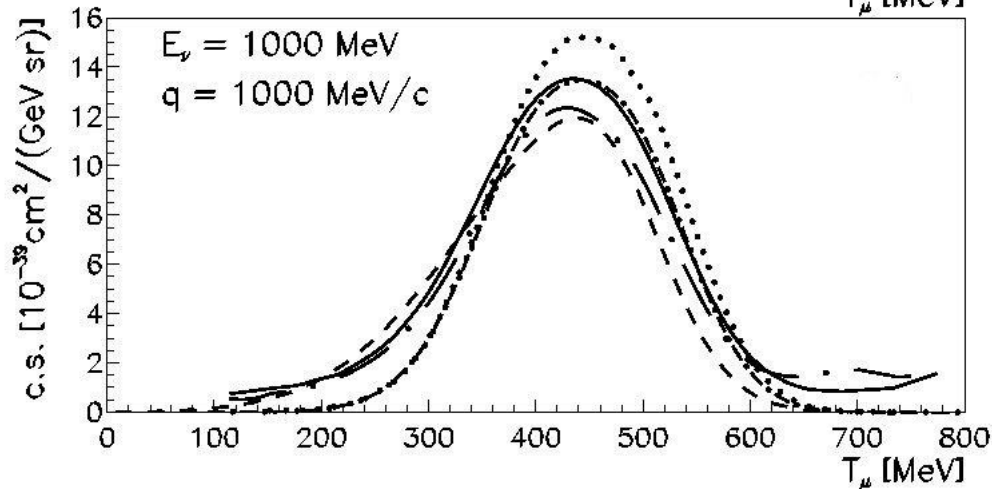
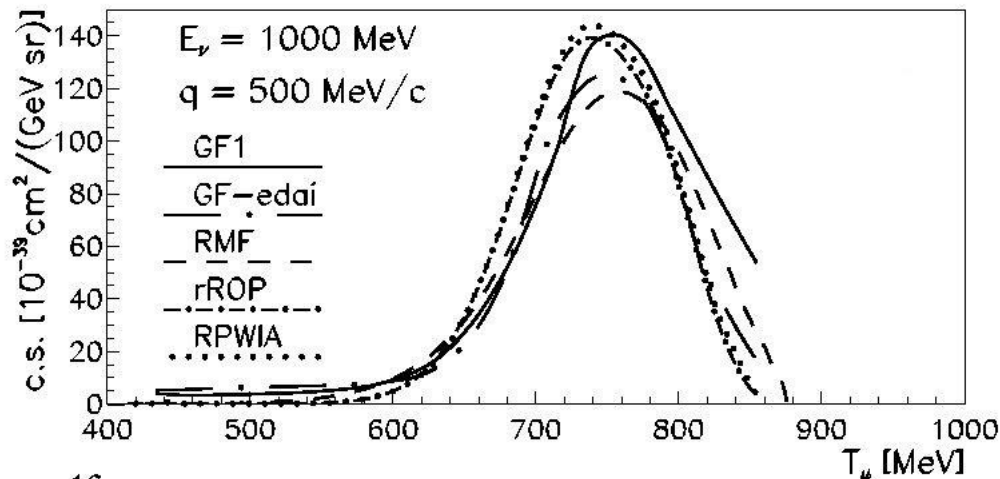
comparison of relativistic models

FSI



$^{12}\text{C}(\nu_{\mu}, \mu^{-})$

comparison of relativistic models



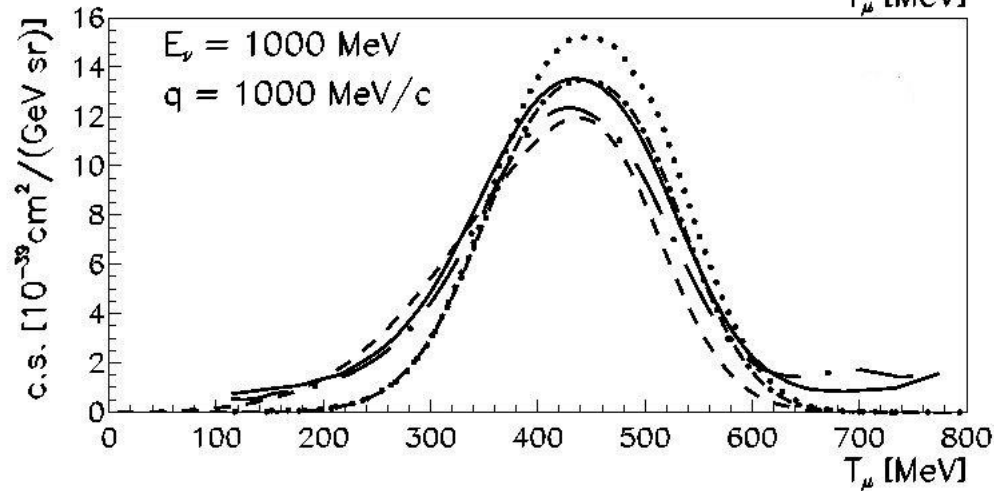
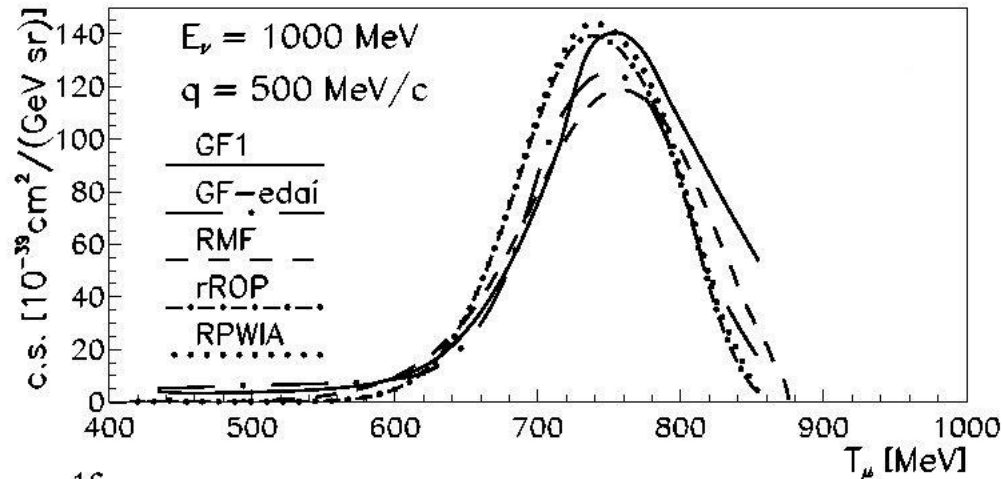
FSI

- ..... RPWIA
  - . - . - rROP
  - RGF1
  - . - . - RGF-EDAI
  - RMF
- 

EDAI A-independent for  $^{12}\text{C}$

$^{12}\text{C}(\nu_{\mu}, \mu^{-})$

comparison of relativistic models



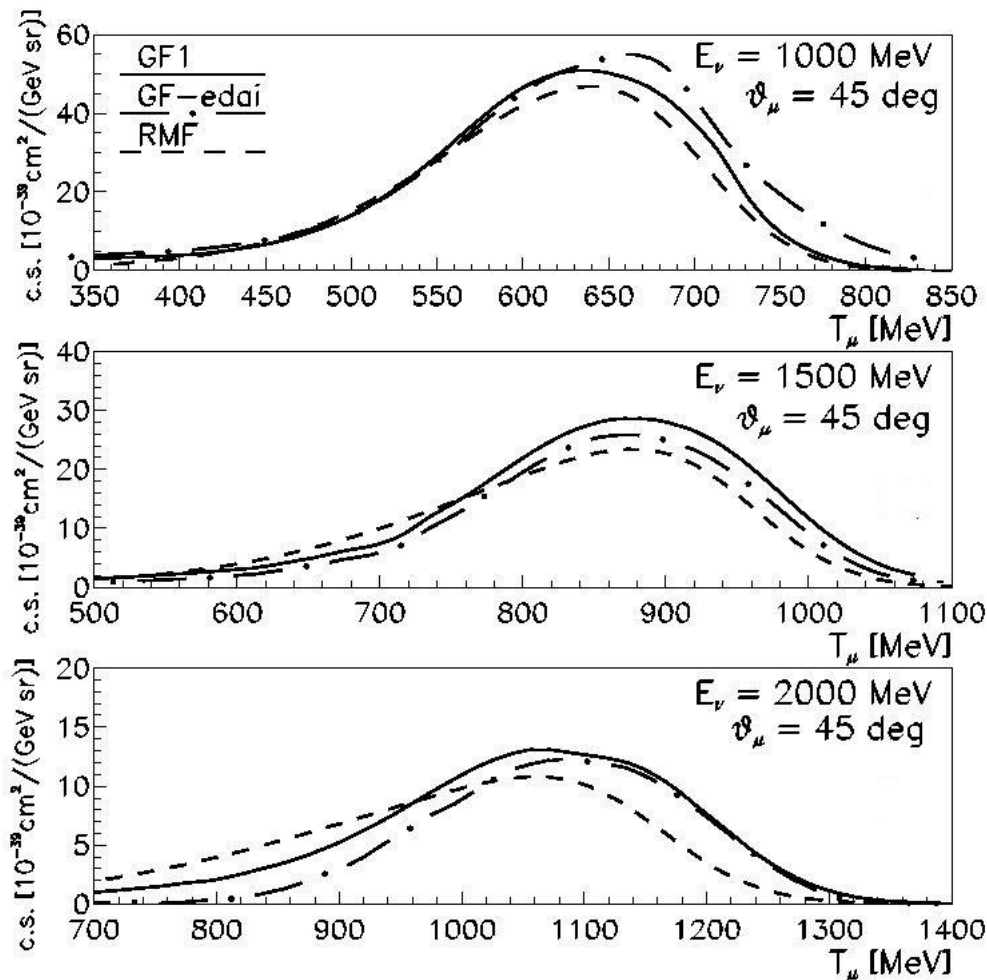
FSI



electron and neutrino scattering: different results

# $^{12}\text{C}(\nu_{\mu}, \mu^{-})$

## comparison of relativistic models

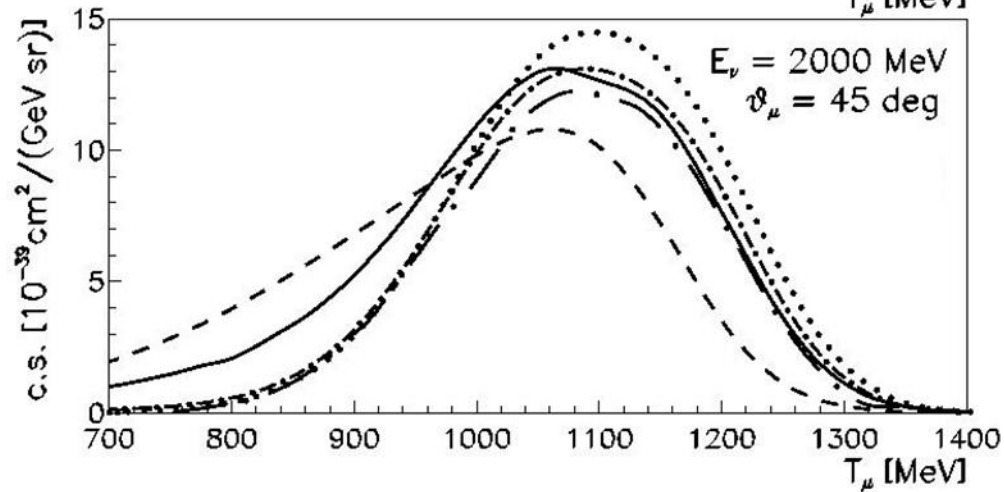
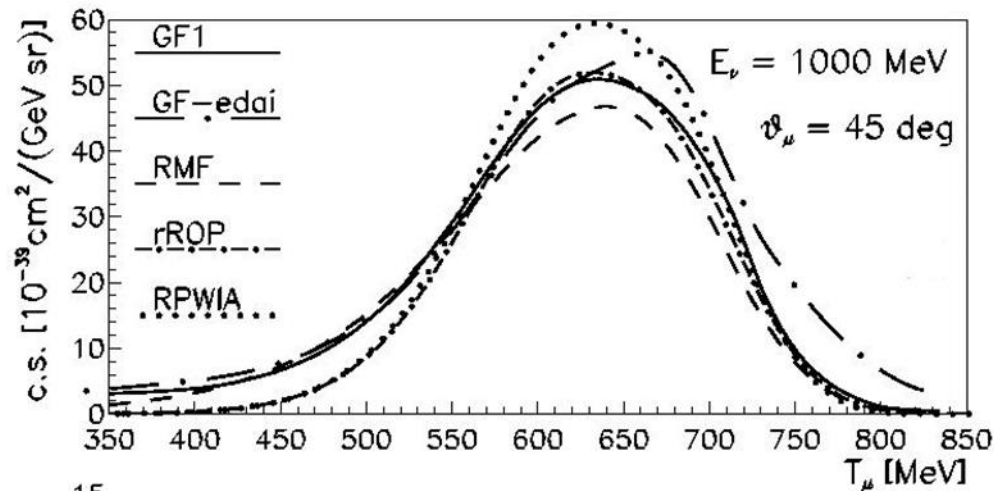


FSI



$$^{12}\text{C}(\nu_{\mu}, \mu^{-})$$

# comparison of relativistic models



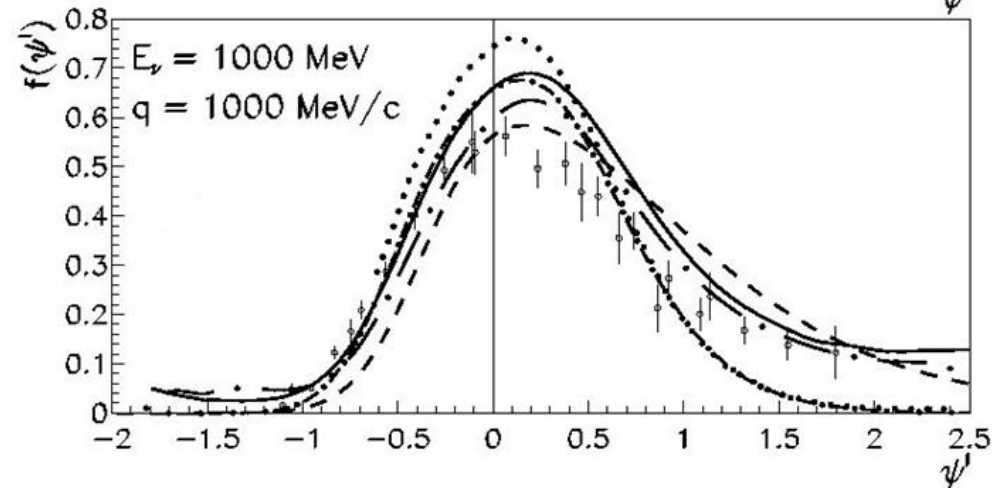
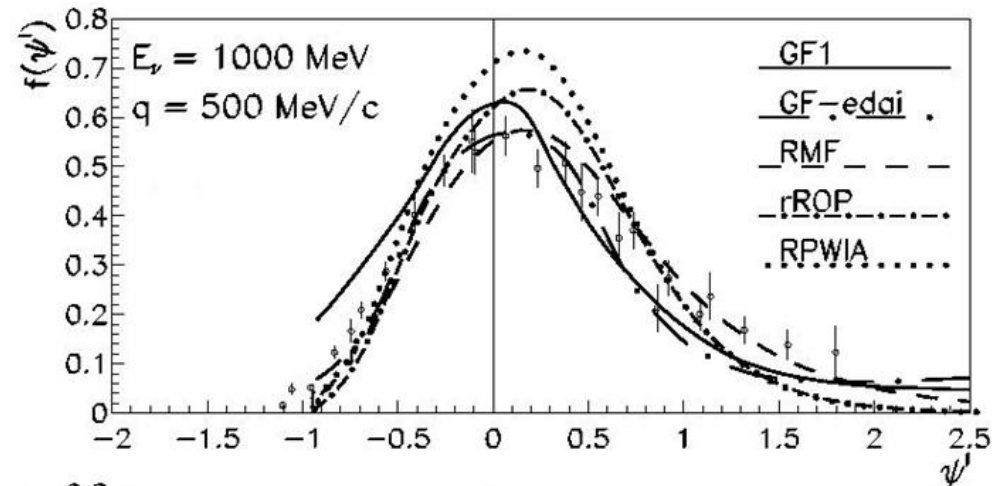
FSI



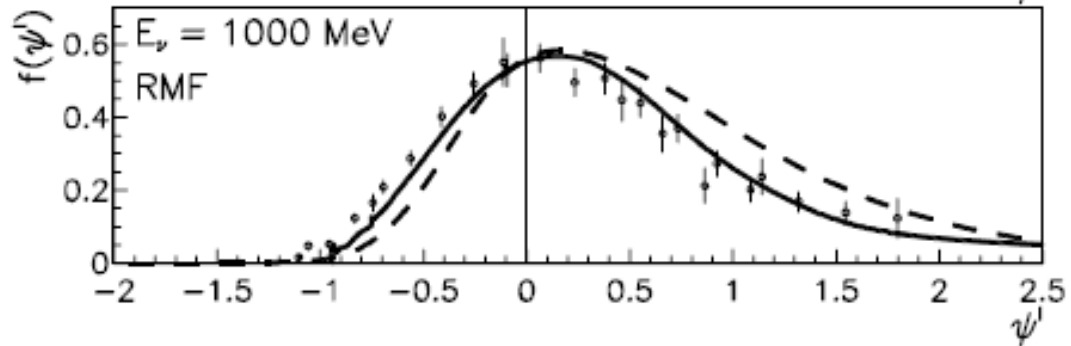
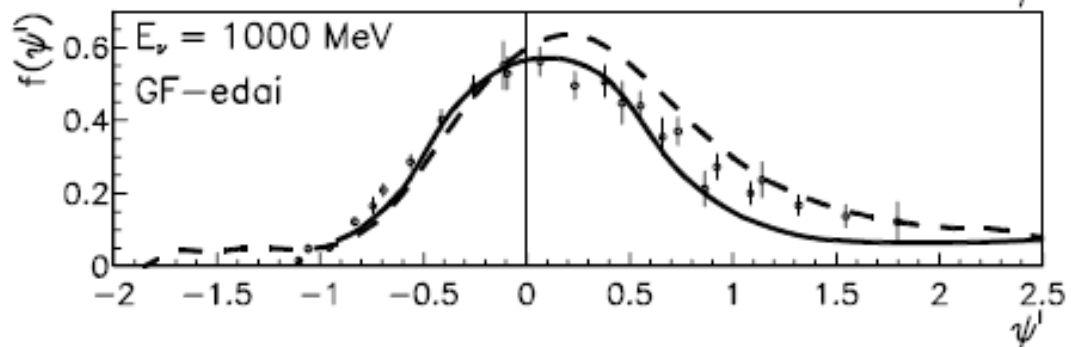
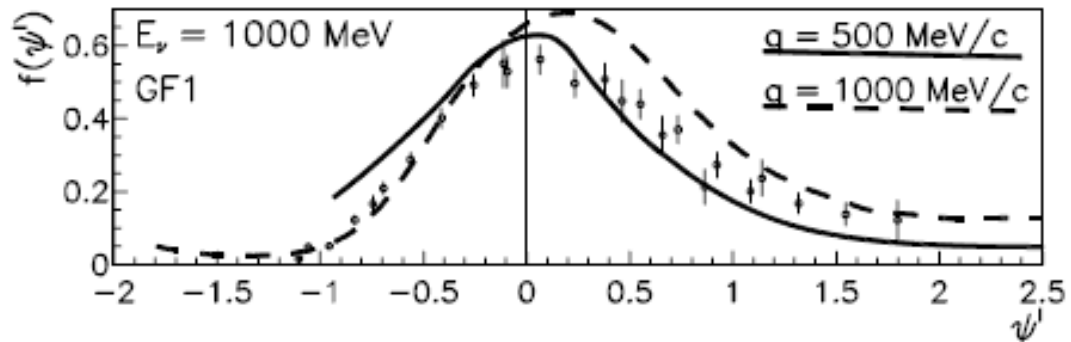


# QE SCALING FUNCTION: RGF, RMF

$$^{12}\text{C}(\nu_{\mu}, \mu^{-})$$



# Analysis first-kind scaling : RGF RMF



—  $q=500 \text{ MeV}/c$   
- - -  $q=1000 \text{ MeV}/c$

## COMPARISON RMF-RGF

RGF, RMF differences increase increasing  $q$

RGF sensitivity to the choice of the phenomenological ROP (imaginary part)

RGF gives larger cross sections than RMF

ROP includes contributions of inelastic channels

At higher  $q$  and energies ROP can include contributions from non-nucleonic d.o.f. (flux lost into inelastic  $\Delta$  excitation), which break scaling and should not be included in the QE longitudinal scaling function (purely nucleonic)

RMF better suited to describe the scaling function

RGF can give a better description of experimental c.s. which can include the inelastic channels

## COMPARISON RMF-RGF

Comparison RMF-RGF deeper understanding of nuclear effects (FSI) which may play a crucial role in the analysis of MiniBooNE CCQE data, which may receive important contributions from non-nucleonic excitations and multi-nucleon processes

# Comparison with MiniBooNe CCQE data

First Measurement of the Muon Neutrino Charged Current  
Quasielastic Double Differential Cross Section, PRD 81  
(2010) 092005

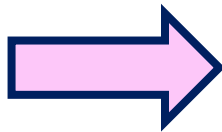


# Comparison with MiniBooNe CCQE data

First Measurement of the Muon Neutrino Charged Current Quasielastic Double Differential Cross Section, PRD 81 (2010) 092005

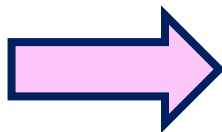


$$\frac{d^2\sigma}{dT_{\mu}d\cos\theta_{\mu}}$$



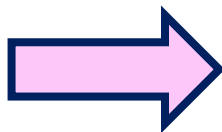
flux-averaged double differential cross section

$$\frac{d\sigma}{dQ_{QE}}$$



flux-integrated single differential cross section

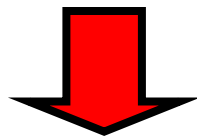
$$\sigma(E_{\nu})$$



flux-unfolded cross section

# Comparison with MiniBooNe CCQE data

First Measurement of the Muon Neutrino Charged Current Quasielastic Double Differential Cross Section, PRD 81 (2010) 092005



Measured cross sections larger than the predictions of the RFG model and of other more sophisticated models.

Unusually large values of the nucleon axial mass must be used to reproduce the data (about 30% larger)

# One-body CC nuclear weak current

$$j^\mu = \left[ F_1^V(Q^2)\gamma^\mu + i\frac{\kappa}{2M}F_2^V(Q^2)\sigma^{\mu\nu}q_\nu - G_A(Q^2)\gamma^\mu\gamma^5 + F_P(Q^2)q^\mu\gamma^5 \right] \tau^\pm$$

$$F_P = \frac{2MG_A}{m_\pi^2 + Q^2}$$

induced pseudoscalar form factor



# One-body CC nuclear weak current

$$j^\mu = \left[ F_1^V(Q^2)\gamma^\mu + i\frac{\kappa}{2M}F_2^V(Q^2)\sigma^{\mu\nu}q_\nu - \underbrace{G_A(Q^2)\gamma^\mu\gamma^5}_{\text{axial current}} + F_P(Q^2)q^\mu\gamma^5 \right] \tau^\pm$$

axial current

$$F_P = \frac{2MG_A}{m_\pi^2 + Q^2}$$

induced pseudoscalar form factor

# One-body CC nuclear weak current

$$j^\mu = \left[ F_1^V(Q^2)\gamma^\mu + i\frac{\kappa}{2M}F_2^V(Q^2)\sigma^{\mu\nu}q_\nu - \underbrace{G_A(Q^2)\gamma^\mu\gamma^5}_{\text{axial current}} + F_P(Q^2)q^\mu\gamma^5 \right] \tau^\pm$$

axial current

$$F_P = \frac{2MG_A}{m_\pi^2 + Q^2}$$

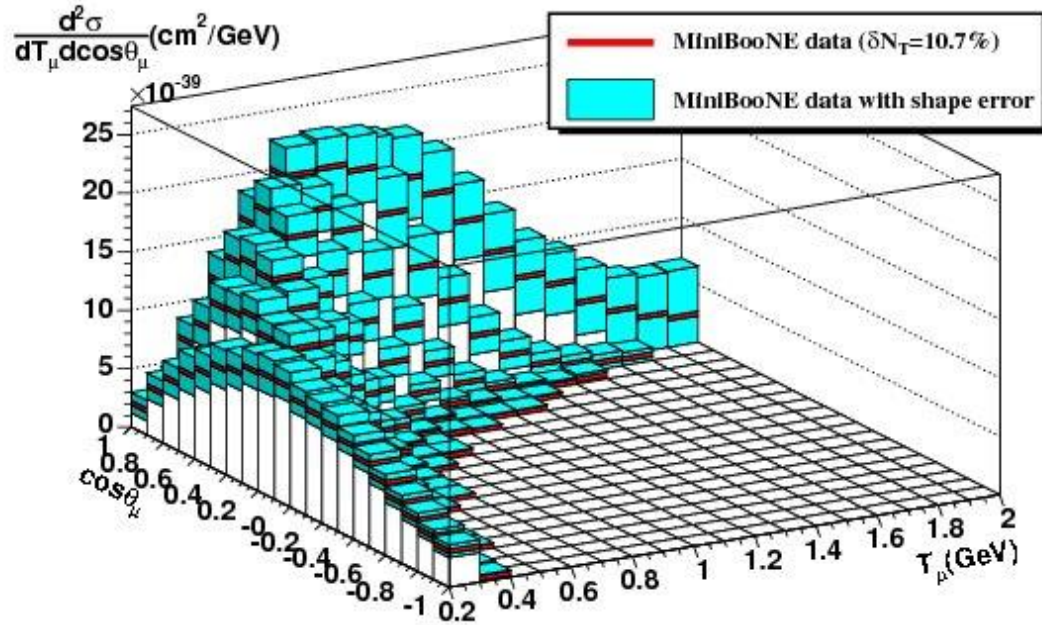
induced pseudoscalar form factor

$$G_A = 1.26 \left( 1 + \frac{Q^2}{M_A^2} \right)^{-2} \text{ axial form factor}$$

$$M_A = (1.03 \pm 0.02)\text{GeV}$$

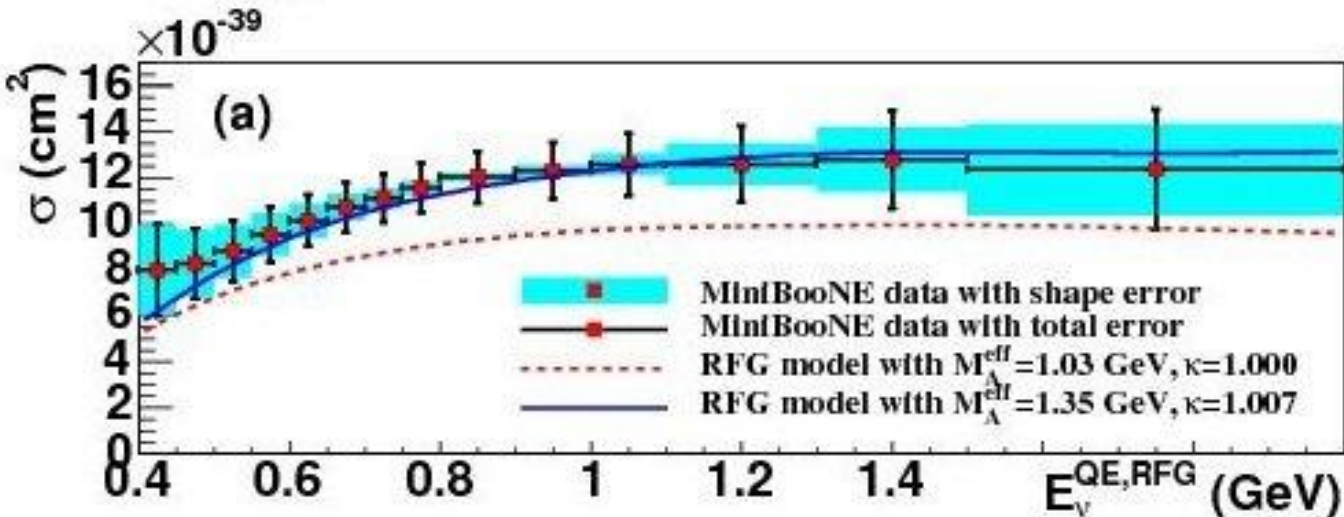
World average of measured values,  
mostly obtained from deuteron data

# MiniBooNe CCQE data



flux integrated double differential cross section

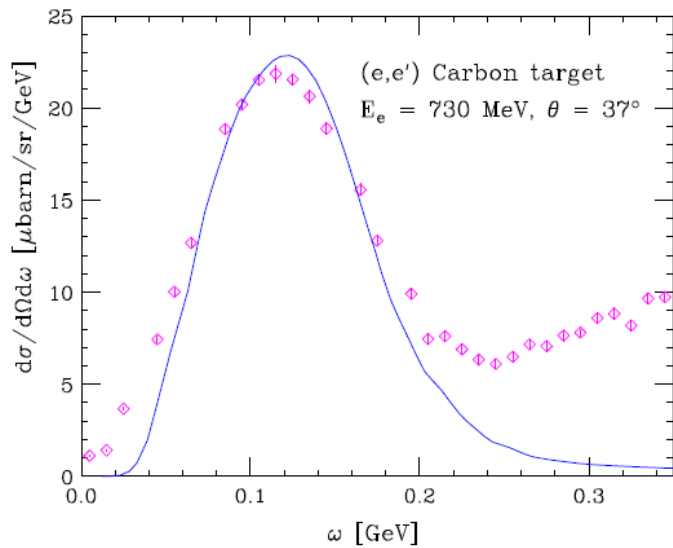
$$M_A = 1.35 \text{ GeV}$$



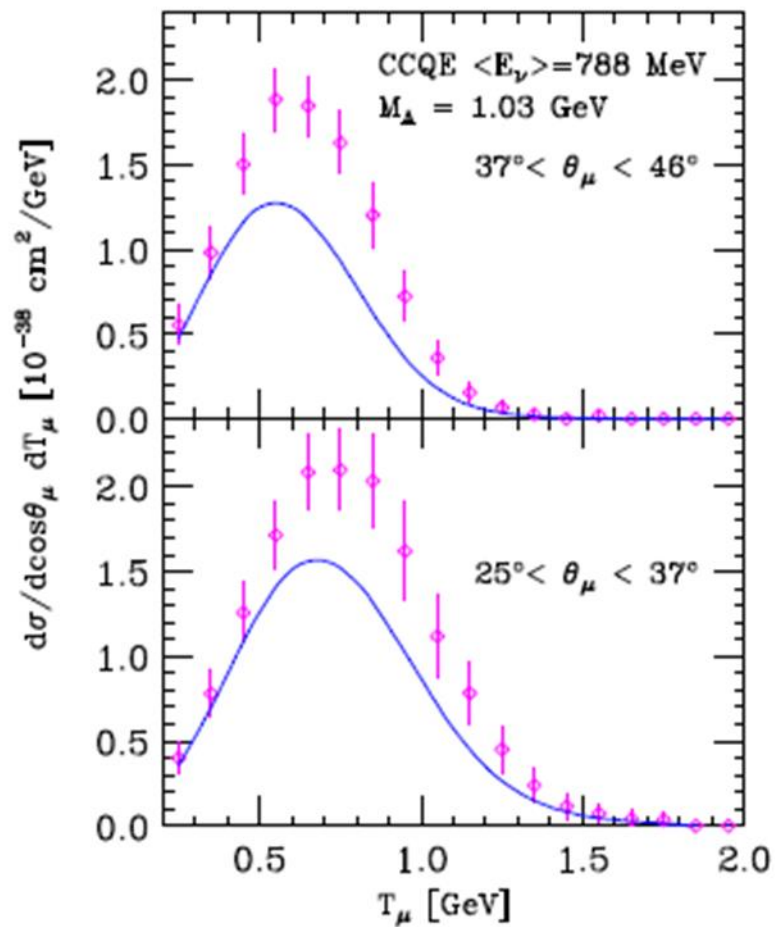
flux unfolded  $\nu_\mu$  CCQE cross section per neutron as a function of  $E_\nu$  compared with predictions of a RFG model

Models based on the IA with the standard value of the axial mass and including only 1NKO underestimate the CCQE MiniBooNE cross section

# $^{12}\text{C}(e, e')$



# $^{12}\text{C}(\nu_\mu, \mu^-)$



# Comparison with MiniBooNe CCQE data

A larger axial mass may be interpreted as an effective way to include medium effects not taken into account by the RFG model and by other models.

Before drawing conclusions all nuclear effects must be investigated

# Comparison with MiniBooNe CCQE data

A larger axial mass may be interpreted as an effective way to include medium effects not taken into account by the RFG model and by other models.

Before drawing conclusions all nuclear effects must be investigated

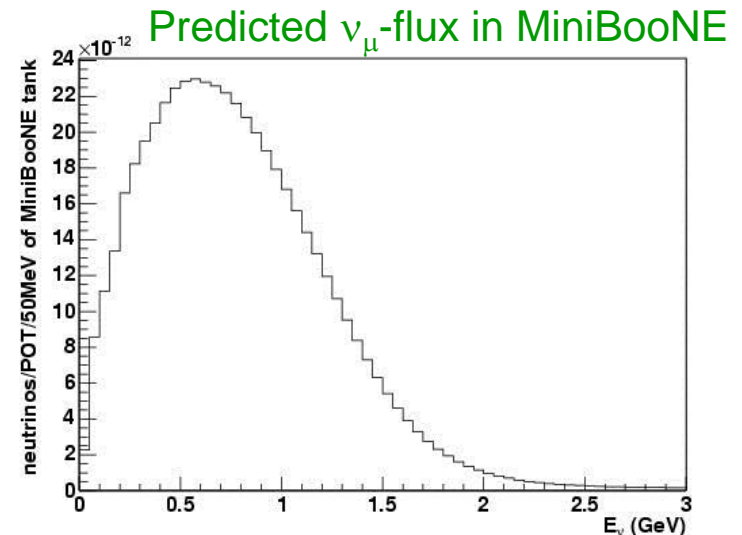
FSI

# Comparison with MiniBooNE CCQE data

CCQE double differential cross section  $\nu_\mu + {}^{12}\text{C} \longrightarrow \mu^- + X$

averaged over the MiniBooNE neutrino flux

$$\frac{d^2\sigma}{dT_\mu d\cos\theta} = \frac{1}{\Phi_{tot}} \int \left( \frac{d^2\sigma}{dT_\mu d\cos\theta} \right)_{E_\nu} \Phi(E_\nu) dE_\nu$$



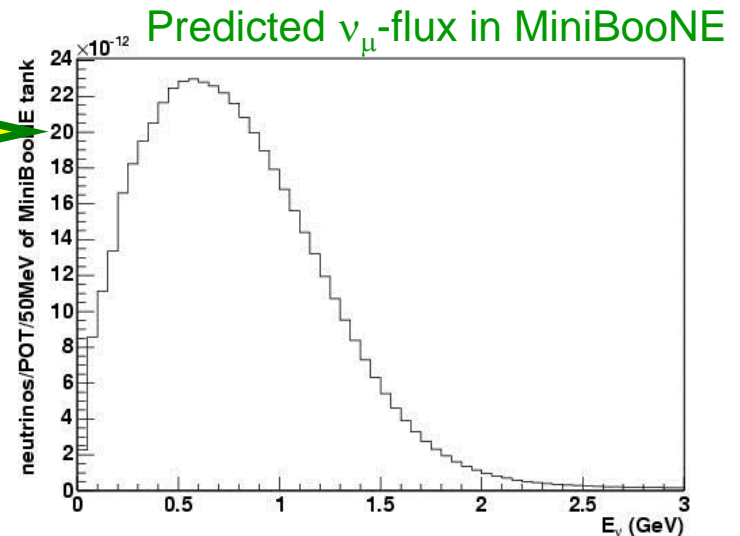


# Comparison with MiniBooNE CCQE data

CCQE double differential cross section  $\nu_\mu + {}^{12}\text{C} \longrightarrow \mu^- + X$

averaged over the MiniBooNE neutrino flux

$$\frac{d^2\sigma}{dT_\mu d\cos\theta} = \frac{1}{\Phi_{tot}} \int \left( \frac{d^2\sigma}{dT_\mu d\cos\theta} \right)_{E_\nu} \Phi(E_\nu) dE_\nu$$

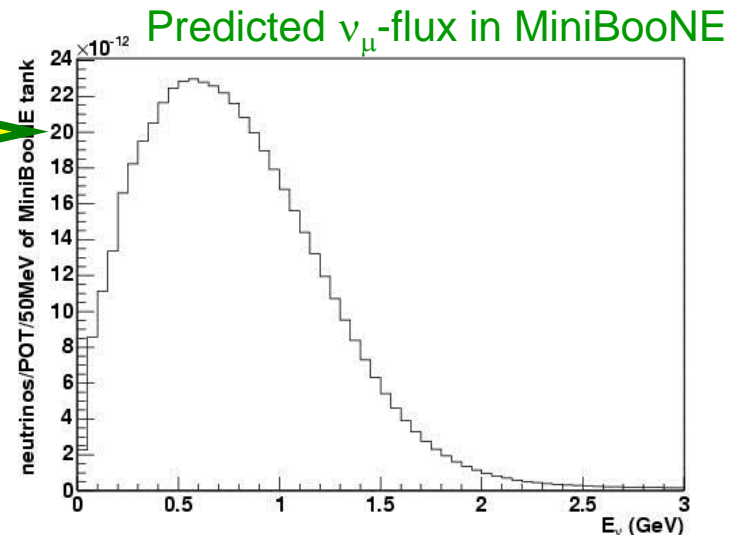


# Comparison with MiniBooNE CCQE data

CCQE double differential cross section  $\nu_\mu + {}^{12}\text{C} \longrightarrow \mu^- + X$

averaged over the MiniBooNE neutrino flux

$$\frac{d^2\sigma}{dT_\mu d\cos\theta} = \frac{1}{\Phi_{tot}} \int \left( \frac{d^2\sigma}{dT_\mu d\cos\theta} \right)_{E_\nu} \Phi(E_\nu) dE_\nu$$



data given in 0.1 GeV bins of  $T_\mu$  and 0.1 bins of  $\cos\theta_\mu$

# Differences between Electron and Neutrino Scattering

- **electron scattering :**

- beam energy known, cross section as a function of  $\omega$

- **neutrino scattering:**

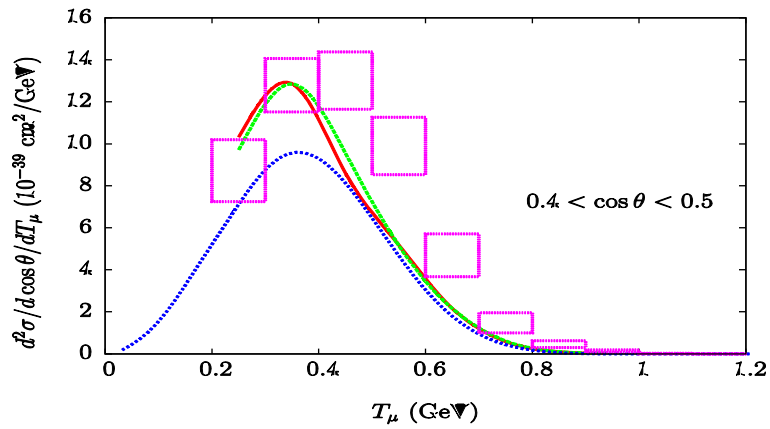
- axial current

- beam energy and  $\omega$  not known

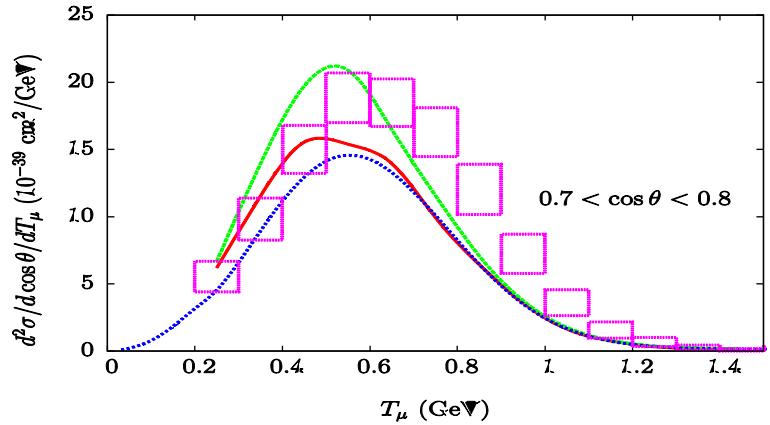
- calculations over the energy range relevant for the neutrino flux

the flux-average procedure can include contributions from different kinematic regions where the neutrino flux has significant strength, contributions other than 1-nucleon emission

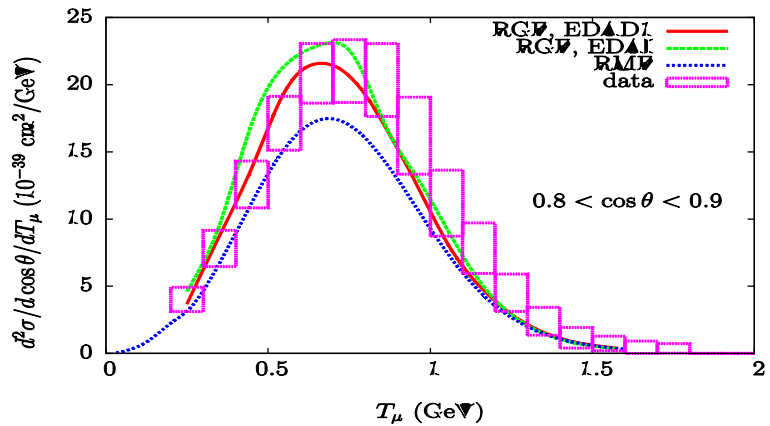
# Comparison with MiniBooNe CCQE data



$$0.4 < \cos \theta_{\mu} < 0.5$$



$$0.7 < \cos \theta_{\mu} < 0.8$$

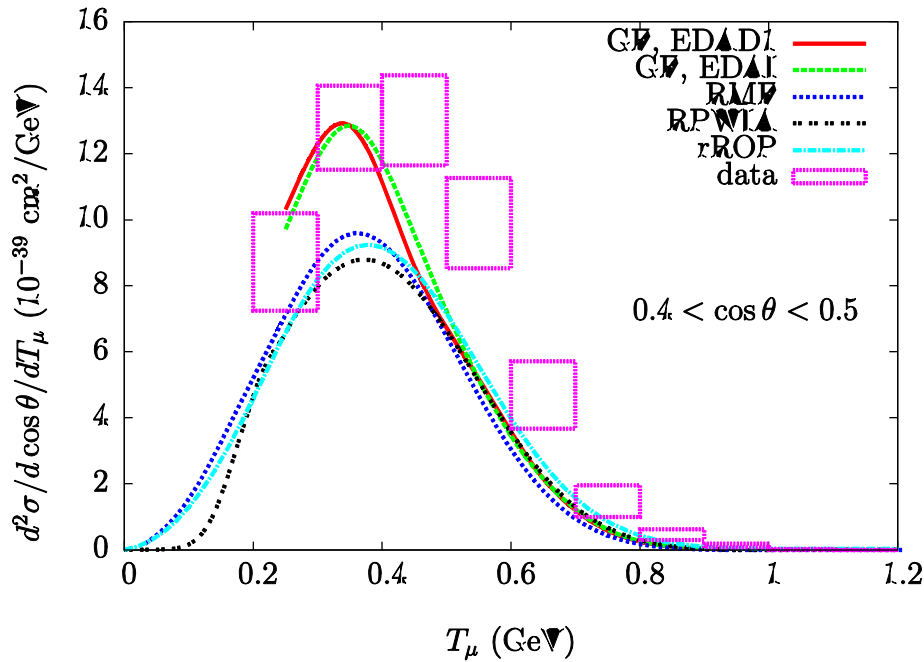


$$0.8 < \cos \theta_{\mu} < 0.9$$

- RGF-EDAI
- RGF-EDAD1
- RMF

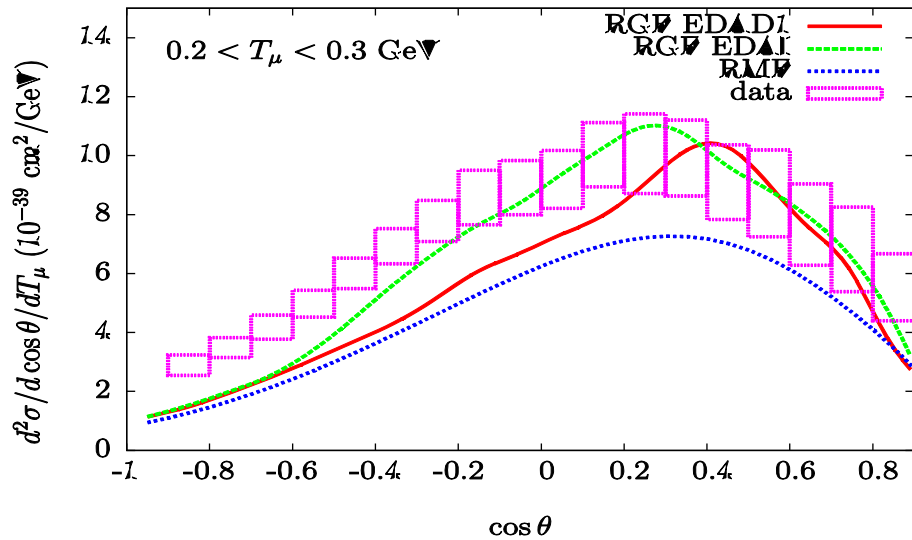
# Comparison with MiniBooNe CCQE data

$$0.4 < \cos\theta_\mu < 0.5$$



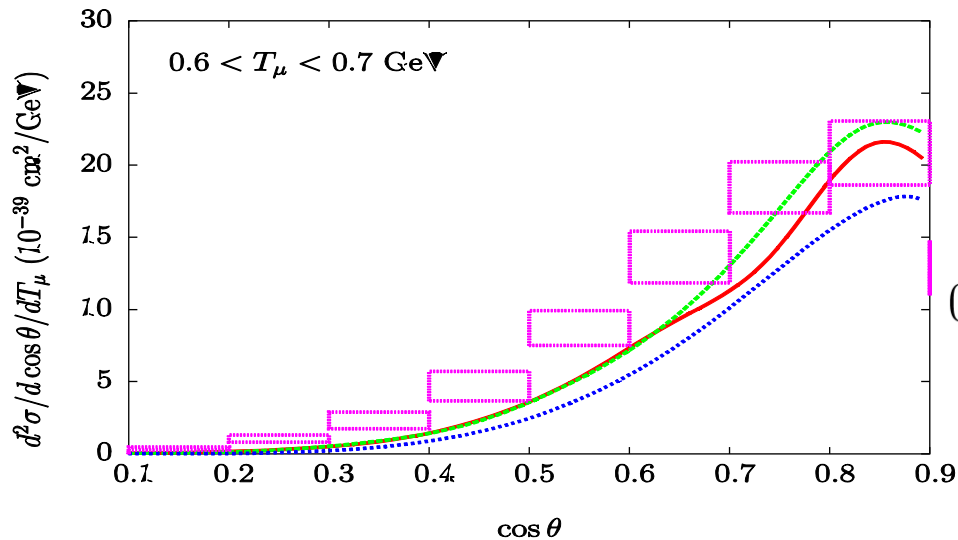
- RGF-EDAI
- RGF-EDAD1
- RMF
- RPWIA
- rROP

# Comparison with MiniBooNe CCQE data



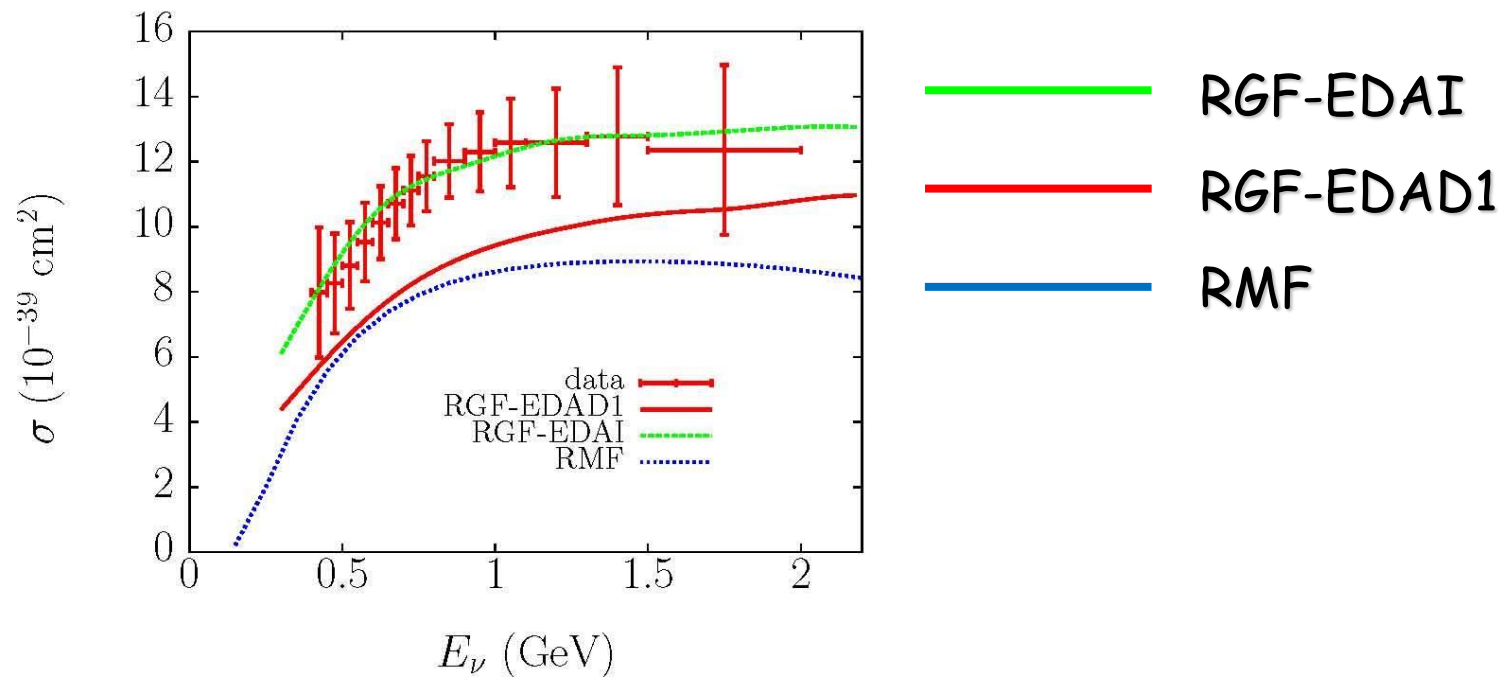
$0.2 < T_\mu < 0.3 \text{ GeV}$

- RGF-EDAI
- RGF-EDAD1
- RMF



$0.6 < T_\mu < 0.7 \text{ GeV}$

# Comparison with MiniBooNe CCQE data

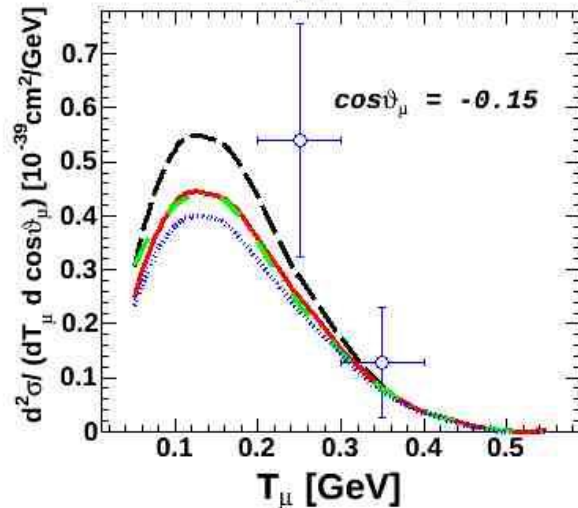
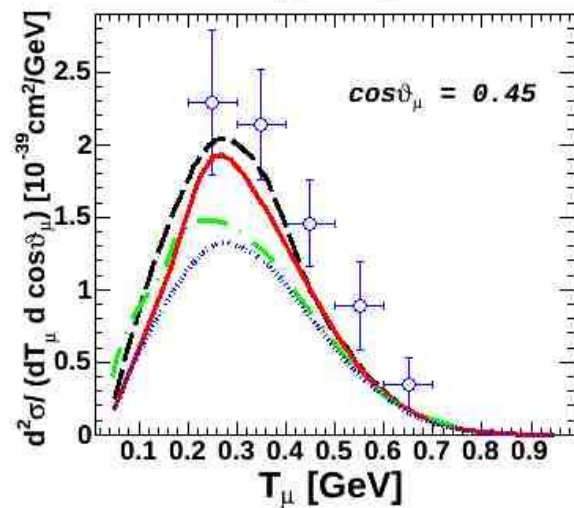
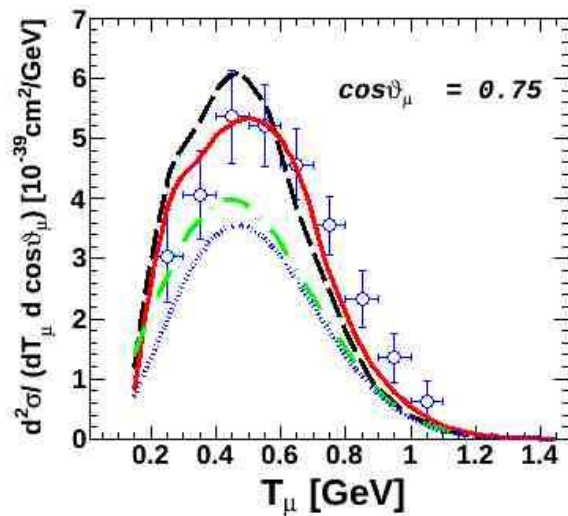
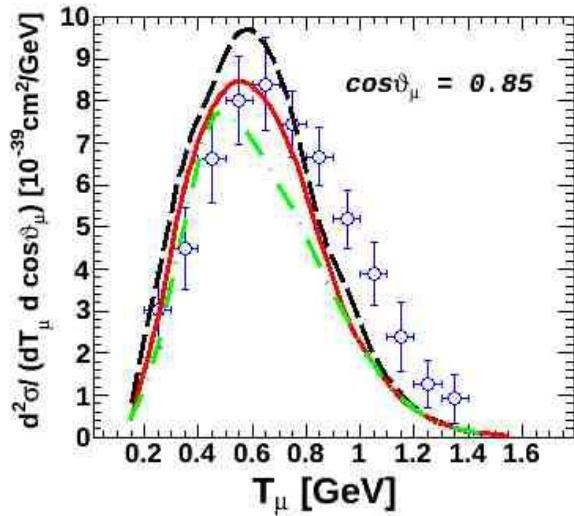


## CCQE antineutrino-nucleus scattering

- The MiniBooNE collaboration has measured CCQE  $\bar{\nu}$  events  
A.A. Aguilar-Arevalo et al. arXiv:1301.7067 [hep-ex]
- In the calculations vector-axial response constructive in neutrino scattering destructive in antineutrino scattering with respect to L and T responses
- $\bar{\nu}_\mu$  flux smaller and with lower average energy than  $\nu_\mu$  flux



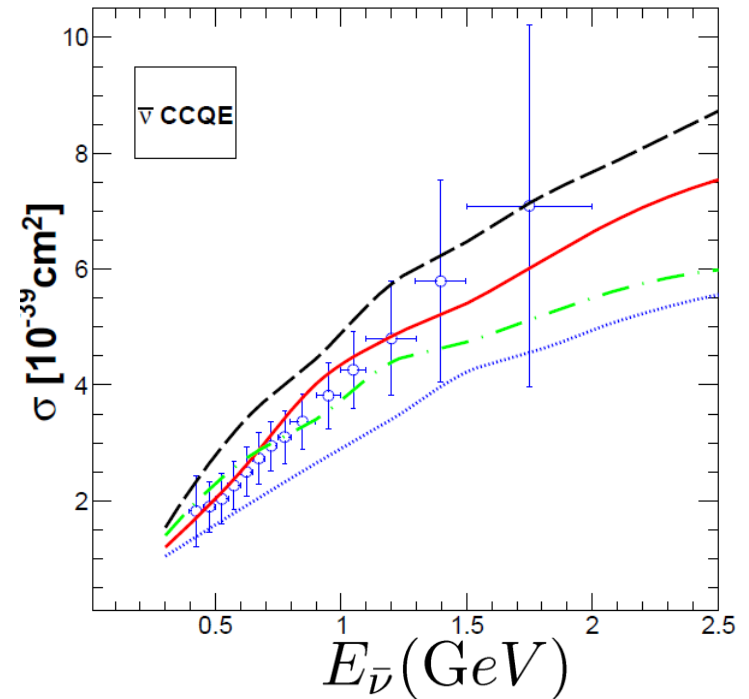
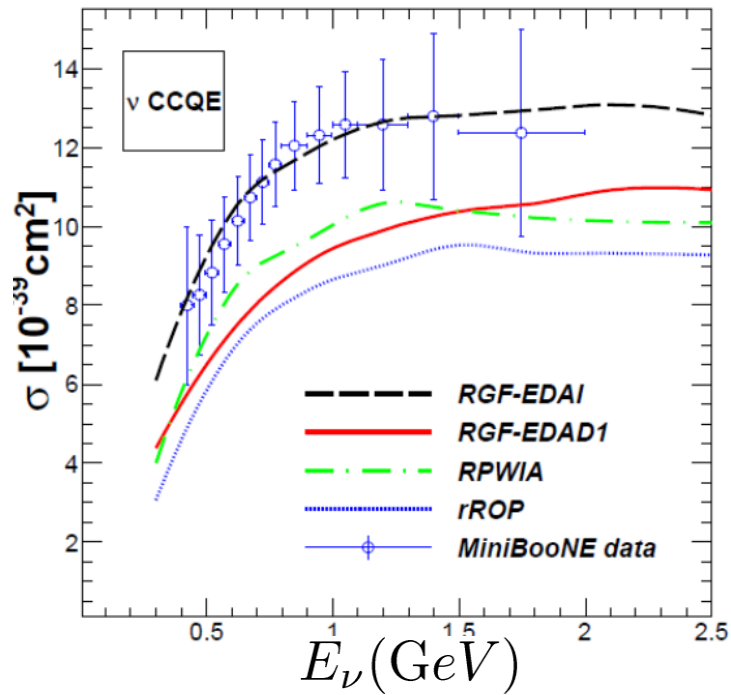
# CCQE antineutrino scattering



$$^{12}\text{C}(\bar{\nu}_\mu, \mu^+)$$

- RPWIA
- rROP
- RGF EDAI
- RGF-EDAD1

# Comparison CCQE neutrino-antineutrino scattering



# Comparison with MiniBooNE NCE data

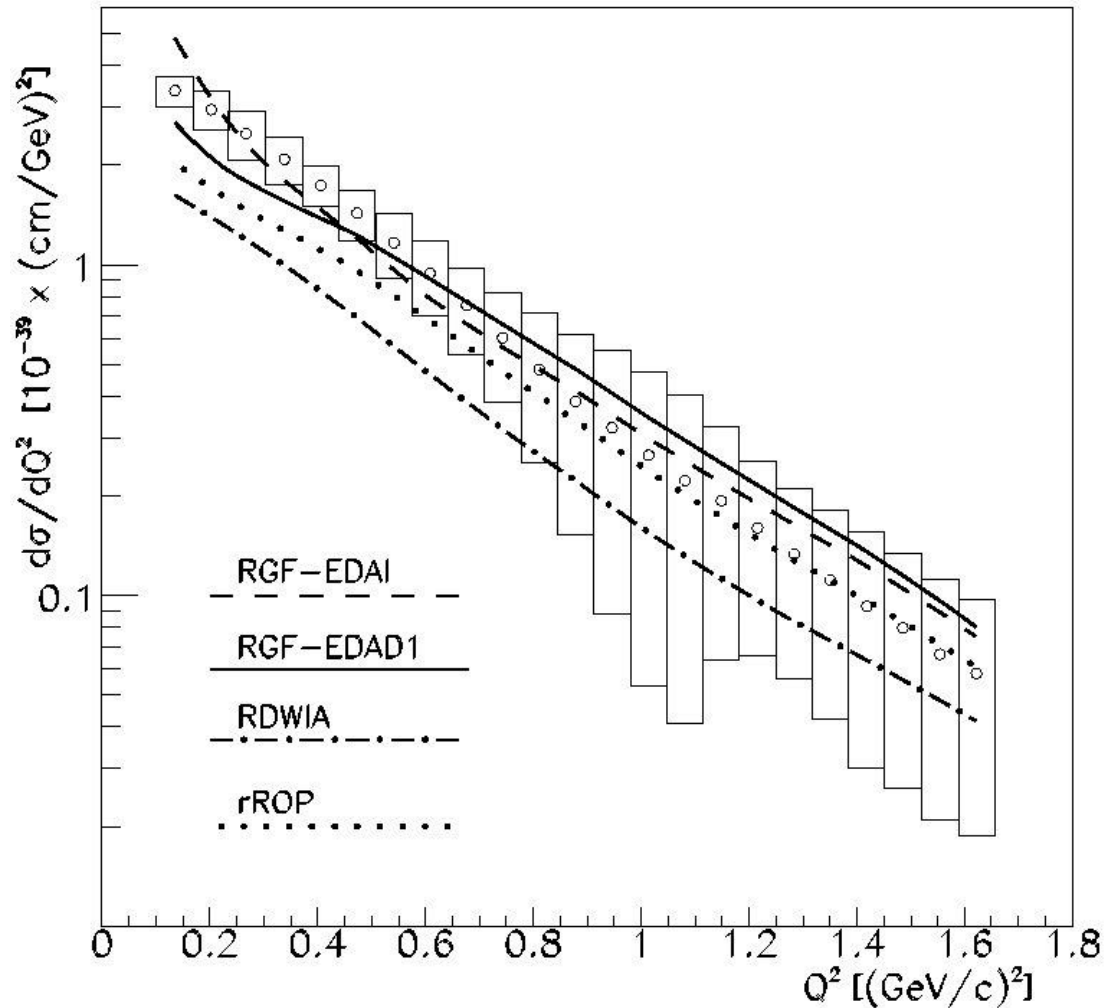
Measurement of the flux averaged neutral-current elastic (NCE) differential cross section on  $\text{CH}_2$  as a function of  $Q^2$   
PRD 82 092005 (2010)

The NCE cross section is presented as scattering from individual nucleons but consists of 3 different processes: neutrino scattering on free protons in H, bound protons and neutrons in C

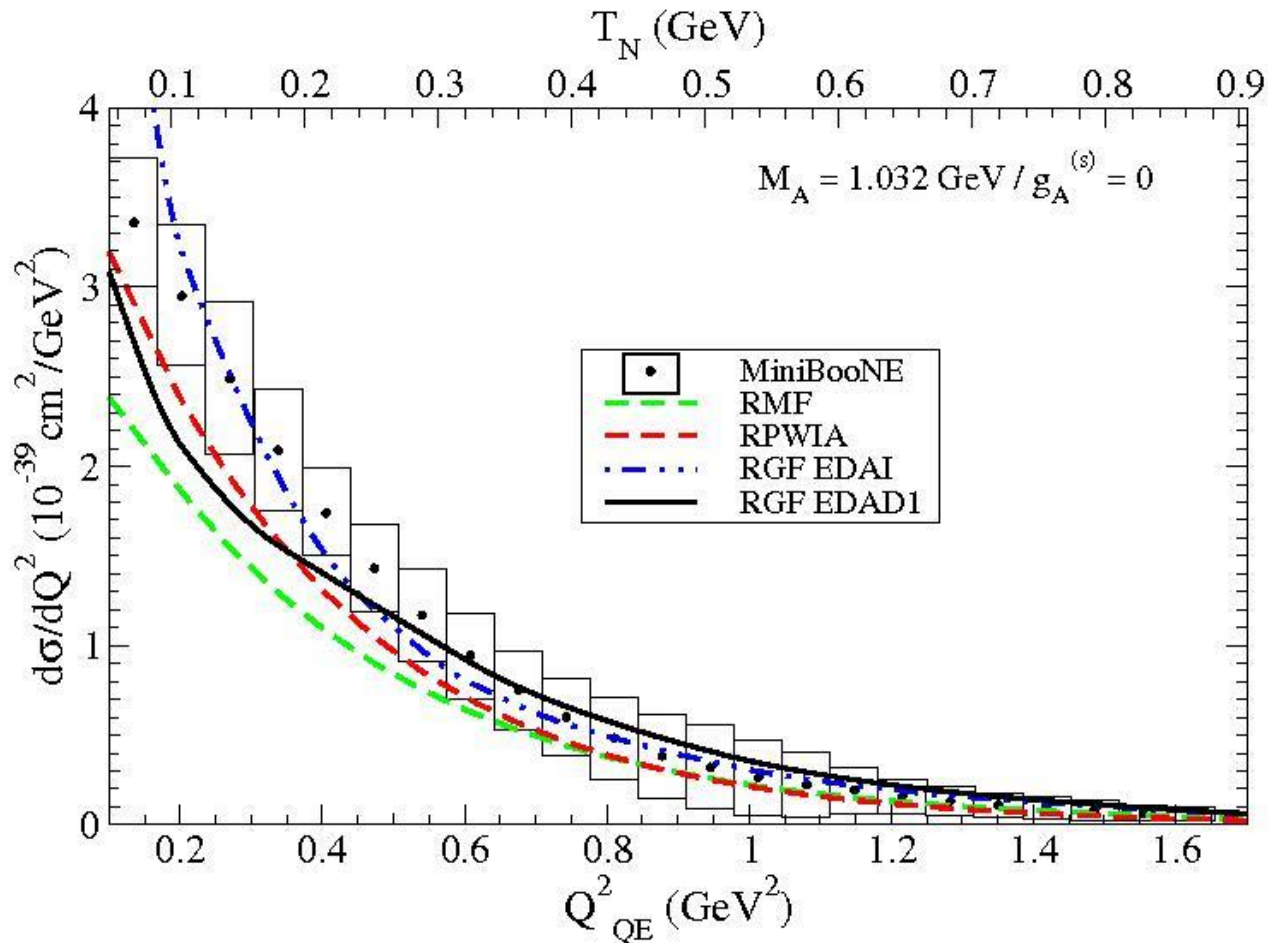
# NC $\nu$ -nucleus scattering

- only the outgoing nucleon is detected: semi-inclusive scattering
- FSI ?
- RDWIA : sum of all integrated exclusive 1NKO channels with absorptive imaginary part of the ROP. The imaginary part accounts for the flux lost in each channel towards other inelastic channels. Some of these reaction channels are not included in the experimental cross section when one nucleon is detected. For these channels RDWIA is correct, but there are channels excluded by the RDWIA and included in the experimental c.s.
- RGF recovers the flux lost to these channels but can include also contributions of channels not included in the semi-inclusive cross section
- we can expect RDWIA smaller and RGF larger than the experimental cross sections
- relevance of contributions neglected in RDWIA and added in RGF depends on kinematics

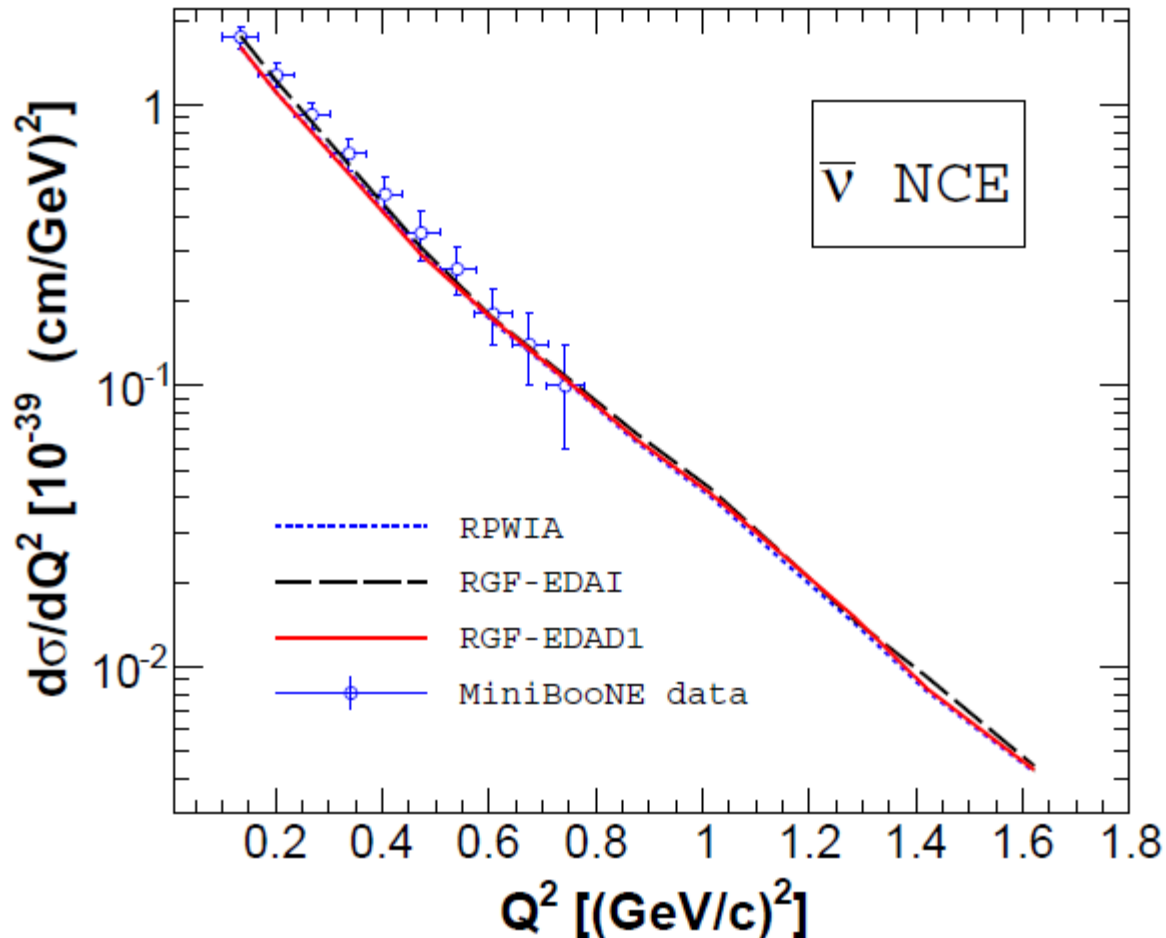
# Comparison with MiniBooNE NCE data



# Comparison with MiniBooNE NCE data



# Comparison with MiniBooNE NCE data



# QE $\nu$ -nucleus scattering

- models developed for QE electron-nucleus scattering applied to QE neutrino-nucleus scattering
- RGF description of FSI in the inclusive scattering
- RGF enhances the c.s. and gives results able to reproduce the MiniBooNE data with the standard value of  $M_A$
- enhancement due to the translation to the inclusive strength of the overall effect of inelastic channels (multi-nucleon, non-nucleonic rescattering...)
- inelastic contributions recovered in the RGF by the imaginary part of the ROP, not included explicitly in the model with a microscopic calculation, the role of different inelastic processes cannot be disentangled and we cannot attribute the enhancement to a particular effect
- other models including multi-nucleonic excitations reproduce the MiniBooNE data
- different models go in the same direction



## before drawing conclusions....

- more data needed, comparison of the results of different models helpful for a deeper understanding, careful evaluation of all nuclear effects is required
- reduce theoretical uncertainties
- RGF better determination of the phenomenological ROP which closely fulfills dispersion relations
- 2-body MEC not included in the model would require a new model (two-particle GF)
- everything should be done consistently in the model

# Strangeness in the nucleon

The net strangeness of the nucleon is 0

According to the quantum field theory in the cloud of a physical nucleon there must be pairs of strange particles

From the point of view of QCD the nucleon consists of u and d quarks and of a sea of  $q\bar{q}$  ( $u\bar{u}$ ,  $d\bar{d}$ ,  $s\bar{s}$ ) pairs produced by virtual gluons

How do the sea quarks, in particular strange quarks, contribute to the observed properties of the nucleon?

From the measurements by the EMC collaboration of the polarized structure function of the proton the one-nucleon matrix element of the axial strange current is comparable with those of the axial u and d current. Other experiments confirmed this result

# Strangeness in the nucleon

The one-nucleon matrix element of the axial quark current

$$\langle ps | \bar{q} \gamma^\alpha \gamma^5 q | ps \rangle = 2M s^\alpha g_A^q$$

$M$  nucleon mass,  $s^\alpha$  nucleon spin polarization vector

$g_A^q$  contribution of  $q\bar{q}$  to the spin of the nucleon

# Strangeness in the nucleon

The one-nucleon matrix element of the axial quark current

$$\langle ps | \bar{q} \gamma^\alpha \gamma^5 q | ps \rangle = 2M s^\alpha g_A^q$$

$M$  nucleon mass,  $s^\alpha$  nucleon spin polarization spin vector

$g_A^q$  contribution of  $q\bar{q}$  to the spin of the nucleon

First evidence that for strange quarks

$$g_A^s = G_A^s(Q^2 = 0) \neq 0$$

was obtained by the EMC exp measurement of deep inelastic scattering of polarized muons on polarized protons

This result triggered more experiments at CERN SLAC DESY and a lot of theoretical work

# Strangeness in the nucleon

The one-nucleon matrix element of the axial quark current

$$\langle ps | \bar{q} \gamma^\alpha \gamma^5 q | ps \rangle = 2M s^\alpha g_A^q$$

$M$  nucleon mass  $s^\alpha$  nucleon spin polarization spin vector

$g_A^q$  contribution of  $q\bar{q}$  to the spin of the nucleon

## Strange quarks

$$g_A^s = G_A^s(Q^2 = 0) \neq 0$$

(EMC and...)

different methods must be used to determine the matrix element of the strange current



## NC NEUTRINO SCATTERING

# One-body nuclear weak current

$$j^\mu = F_1^V(Q^2)\gamma^\mu + i\frac{\kappa}{2M}F_2^V(Q^2)\sigma^{\mu\nu}q_\nu - G_A(Q^2)\gamma^\mu\gamma^5$$

NC

$$F_i^{Vp(n) \text{ NC}} = \left(\frac{1}{2} - 2\sin^2\theta_W\right)F_i^{p(n)} - \frac{1}{2}F_i^{n(p)} - \frac{1}{2}F_i^s$$

$$G_A^{p(n) \text{ NC}} = \frac{1}{2} [ +(-)G_A^{\text{CC}} - G_A^{\text{s}} ]$$

# One-body nuclear weak current

$$j^\mu = F_1^V(Q^2)\gamma^\mu + i\frac{\kappa}{2M}F_2^V(Q^2)\sigma^{\mu\nu}q_\nu - G_A(Q^2)\gamma^\mu\gamma^5$$

NC

$$F_i^{Vp(n) \text{ NC}} = \left(\frac{1}{2} - 2\sin^2\theta_W\right) \left(F_i^{p(n)} - \frac{1}{2}F_i^{n(p)}\right) - \frac{1}{2}F_i^s$$

$$G_A^{p(n) \text{ NC}} = \frac{1}{2} [ +(-)G_A^{\text{CC}} - G_A^s ]$$



electromagnetic form factors  
electron scattering



# One-body nuclear weak current

$$j^\mu = F_1^V(Q^2)\gamma^\mu + i\frac{\kappa}{2M}F_2^V(Q^2)\sigma^{\mu\nu}q_\nu - G_A(Q^2)\gamma^\mu\gamma^5$$

NC

$$F_i^{Vp(n) \text{ NC}} = \left( \frac{1}{2} - 2\sin^2\theta_W \right) F_i^{p(n)} - \frac{1}{2}F_i^{n(p)} - \frac{1}{2}F_i^s$$

$$G_A^{p(n) \text{ NC}} = \frac{1}{2} [ +(-)G_A^{\text{CC}} - G_A^{\text{s}} ]$$

Weinberg angle  
NC processes



# One-body nuclear weak current

$$j^\mu = F_1^V(Q^2)\gamma^\mu + i\frac{\kappa}{2M}F_2^V(Q^2)\sigma^{\mu\nu}q_\nu - G_A(Q^2)\gamma^\mu\gamma^5$$

NC

$$F_i^{Vp(n) \text{ NC}} = \left(\frac{1}{2} - 2\sin^2\theta_W\right)F_i^{p(n)} - \frac{1}{2}F_i^{n(p)} - \frac{1}{2}F_i^s$$

$$G_A^{p(n) \text{ NC}} = \frac{1}{2} [ +(-) G_A^{\text{CC}} + G_A^s ]$$



axial form factor  
CC scattering



# One-body nuclear weak current

$$j^\mu = F_1^V(Q^2)\gamma^\mu + i\frac{\kappa}{2M}F_2^V(Q^2)\sigma^{\mu\nu}q_\nu - G_A(Q^2)\gamma^\mu\gamma^5$$

NC

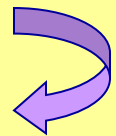
$$F_i^{Vp(n) \text{ NC}} = \left(\frac{1}{2} - 2\sin^2\theta_W\right)F_i^{p(n)} - \frac{1}{2}F_i^{n(p)} \left(\frac{1}{2}F_i^s\right)$$

$$G_A^{p(n) \text{ NC}} = \frac{1}{2} \left[ +(-)G_A^{\text{CC}} - \left(G_A^s\right) \right]$$

Strange form factors



NC  $\nu$  scattering + PV electron scattering



PVES electric and magnetic FF, NC axial FF

# Strange form factors

$$F_1^s(Q^2) = \frac{(\rho^s + \mu^s)\tau}{(1 + \tau)(1 + Q^2/M_V^2)^2} \quad F_2^s(Q^2) = \frac{(\mu^s - \tau\rho^s)}{(1 + \tau)(1 + Q^2/M_V^2)^2}$$
$$\tau = Q^2/(4M^2) \quad M_V = 0.843\text{GeV}$$

$$G_M^s = F_1^s - F_2^s = \mu^s \frac{1}{1 + Q^2/M_V^2} \quad G_E^s = F_1^s - \tau F_2^s = \rho^s \tau \frac{1}{1 + Q^2/M_V^2}$$

$$G_A^s = g_A^s \left(1 + \frac{Q^2}{M_A^2}\right)^{-2}$$

W.T Donnelly et al. NPA 541 (1992) 525

W. M Alberico et al. Phys. Rep 358 (2002) 227

$\mu^s \quad \rho^s \quad g_A^s$

# MiniBooNE NCE cross section

Does not depend on strangeness : the combined effects on proton and neutron events almost cancel

Sensitivity to the axial mass

Determination of strange form factors from NC cross sections difficult.

Theoretical uncertainties on the different approximations and ingredients of the models may be larger than the effects due to strange ff.

Precise c.s. measurements not easy due to difficulties in the determination of the absolute neutrino flux

Ratios of cross sections useful to determine strange form factors

# Ratios of cross sections

- difficulties due to the determination of  $\nu$  flux reduced because of the ratio
- contribution of nuclear effects strongly reduced because of the ratio
- form factors may contribute in a different way, e.g. with a different sign, in the numerator and in the denominator and strangeness effects can be emphasized in the ratio

# Ratios of cross sections

- $R^N(\nu/\bar{\nu}) = \frac{\sigma(\nu, \nu' N)}{\sigma(\bar{\nu}, \bar{\nu}' N)}$

difficult to deal with antineutrinos

- $R^\nu(p/n) = \frac{\sigma(\nu, \nu' p)}{\sigma(\nu, \nu' n)}$        $R^{\bar{\nu}}(p/n) = \frac{\sigma(\bar{\nu}, \bar{\nu}' p)}{\sigma(\bar{\nu}, \bar{\nu}' n)}$

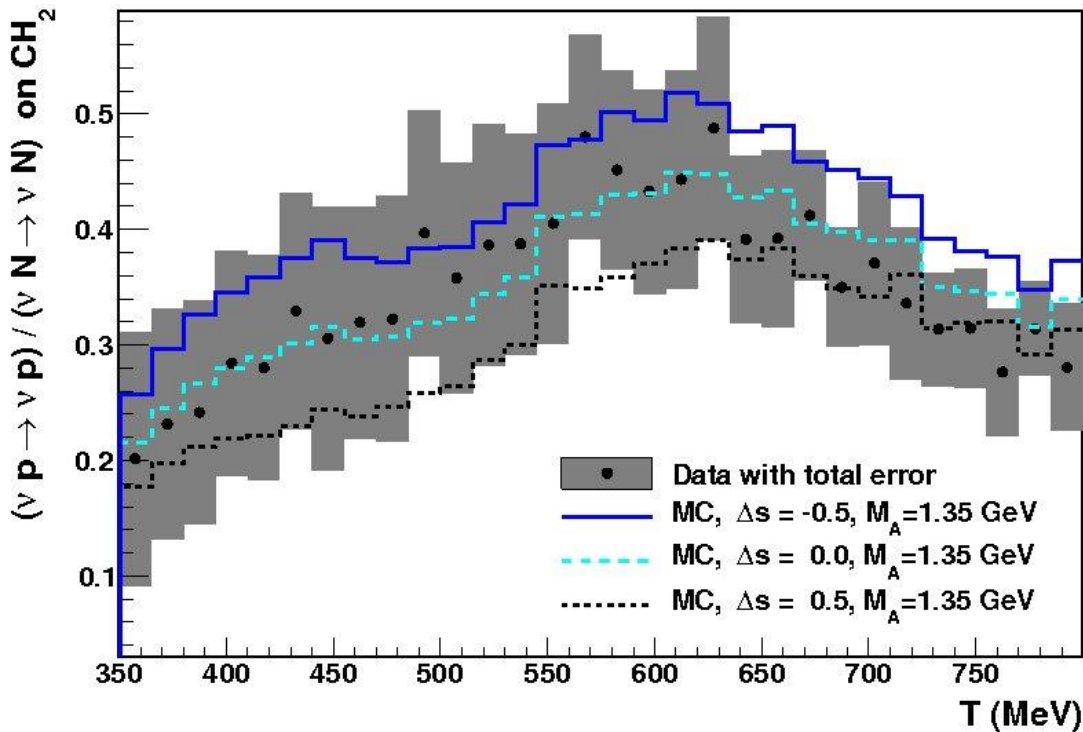
difficult to detect neutrons

- $R^p(\text{NC/CC}) = \frac{\sigma(\nu, \nu' p)}{\sigma(\nu, \mu^- p)}$        $R^n(\text{NC/CC}) = \frac{\sigma(\bar{\nu}, \bar{\nu}' n)}{\sigma(\bar{\nu}, \mu^+ n)}$

strangeness only in the numerator

# MiniBooNE measurement of $\Delta s$ ( $g_A^s$ )

$$\frac{\sigma(\nu, \nu' p)}{\sigma(\nu, \nu' N)}$$

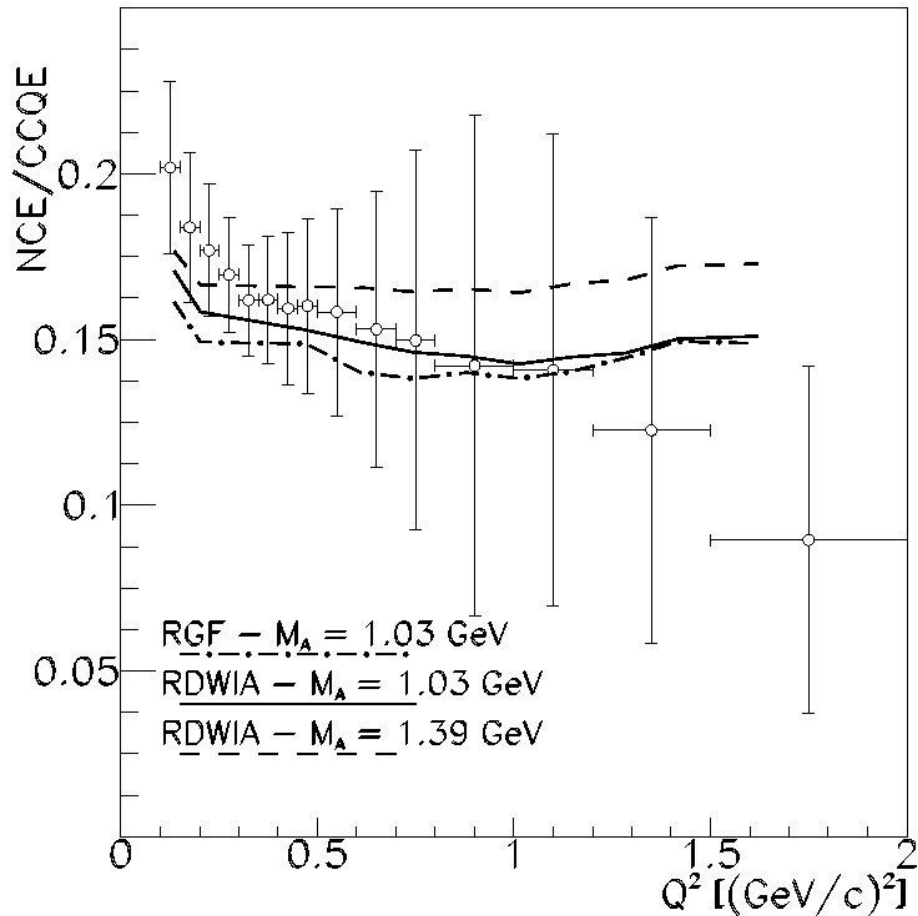


cannot isolate  $(\nu, \nu' n)$ ,  
only  $(\nu, \nu' p)$   
ratio as a function of  
the reconstructed  
nucleon kinetic energy  
errors large but first  
attempt to measure  
 $\Delta s$  using the ratio

$$\Delta s = 0.08 \pm 0.26$$



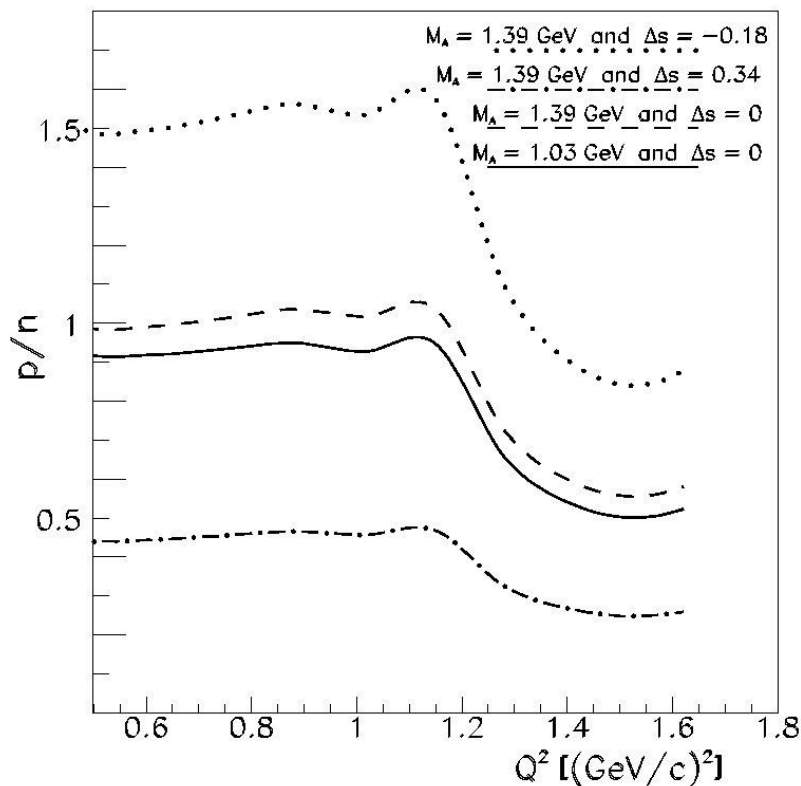
# MiniBooNE NCE/CCQE ratio



does not depend on FSI  
not useful to measure  $\Delta s$ :  
NCE c.s does not depend on  $\Delta s$   
depends on  $M_A$

$$\frac{\sigma(\nu, \nu' p)}{\sigma(\nu, \nu' n)}$$

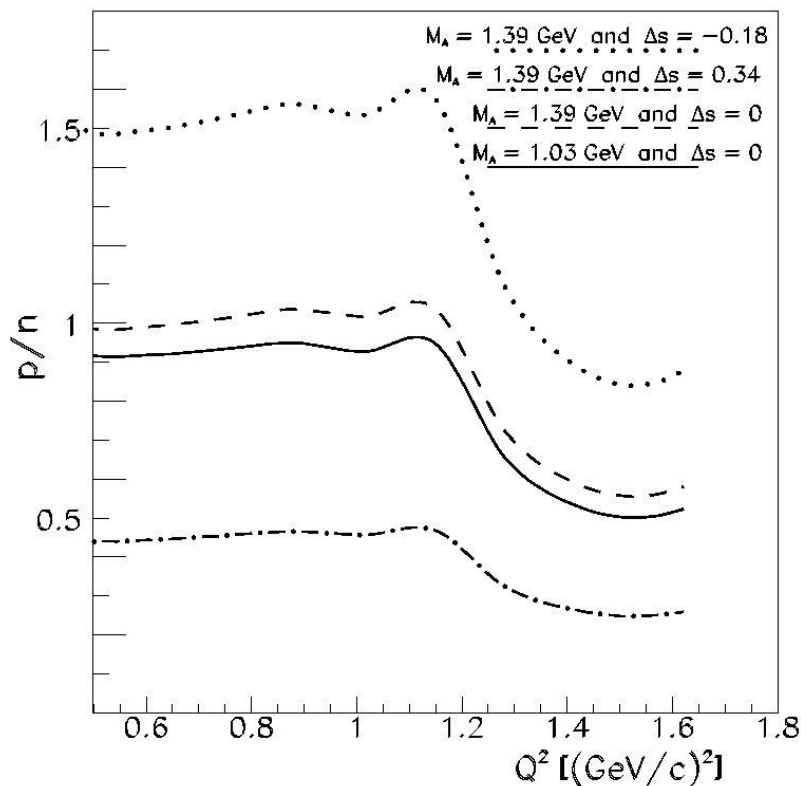
ratio of p/n MiniBooNE flux averaged c.s.



- $M_A = 1.03 \text{ GeV} \quad \Delta s = 0$
- - - - -  $M_A = 1.39 \text{ GeV} \quad \Delta s = 0$
- . - . -  $M_A = 1.39 \text{ GeV} \quad \Delta s = 0.34$
- .....  $M_A = 1.39 \text{ GeV} \quad \Delta s = -0.18$

$$\frac{\sigma(\nu, \nu' p)}{\sigma(\nu, \nu' n)}$$

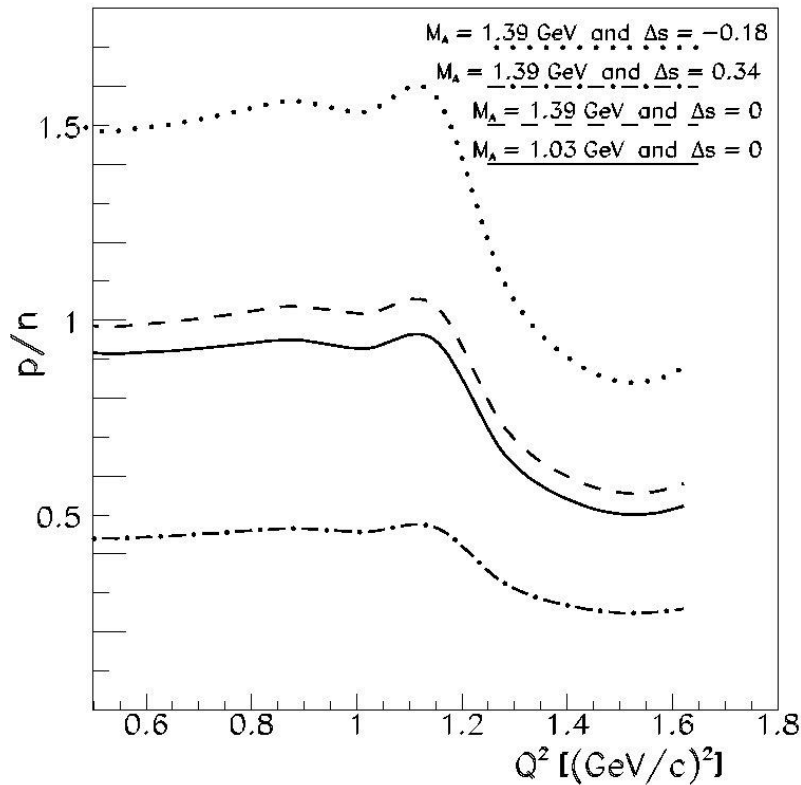
ratio of p/n MiniBooNE flux averaged c.s.



- $M_A = 1.03 \text{ GeV} \quad \Delta s = 0$
- - - - -  $M_A = 1.39 \text{ GeV} \quad \Delta s = 0$
- . - . -  $M_A = 1.39 \text{ GeV} \quad \Delta s = 0.34$
- .....  $M_A = 1.39 \text{ GeV} \quad \Delta s = -0.18$

$$\frac{\sigma(\nu, \nu' p)}{\sigma(\nu, \nu' n)}$$

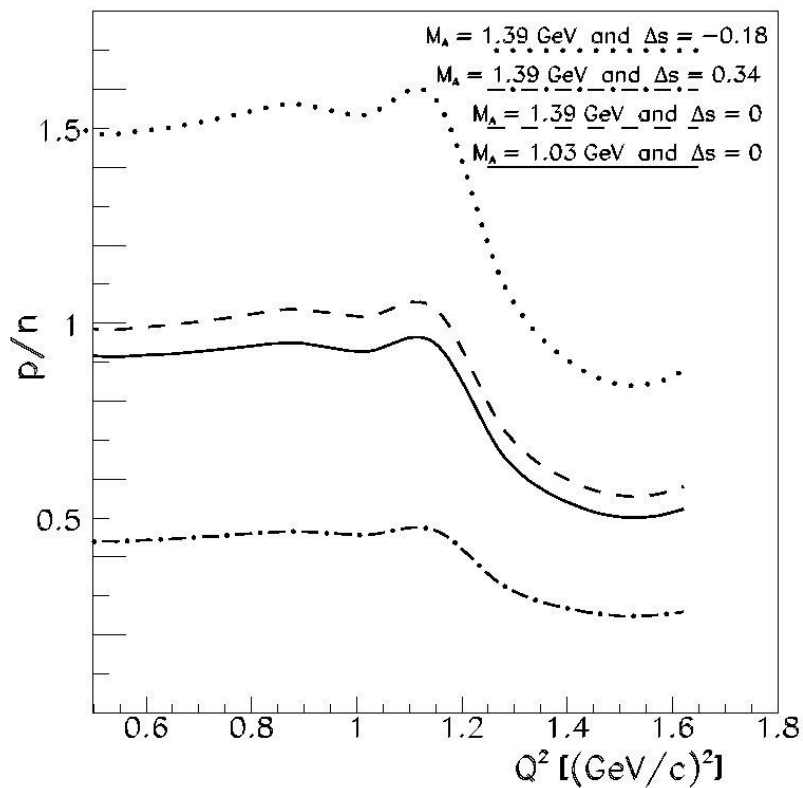
ratio of p/n MiniBooNE flux averaged c.s.



little dependence on  $M_A$   
 sensitivity to  $\Delta s$  as the  
 axial-vector strangeness  
 interferes with the isovector  
 contribution to the axial ff  
 with a different sign for  
 $(\nu, \nu' n)$  and  $(\nu, \nu' p)$

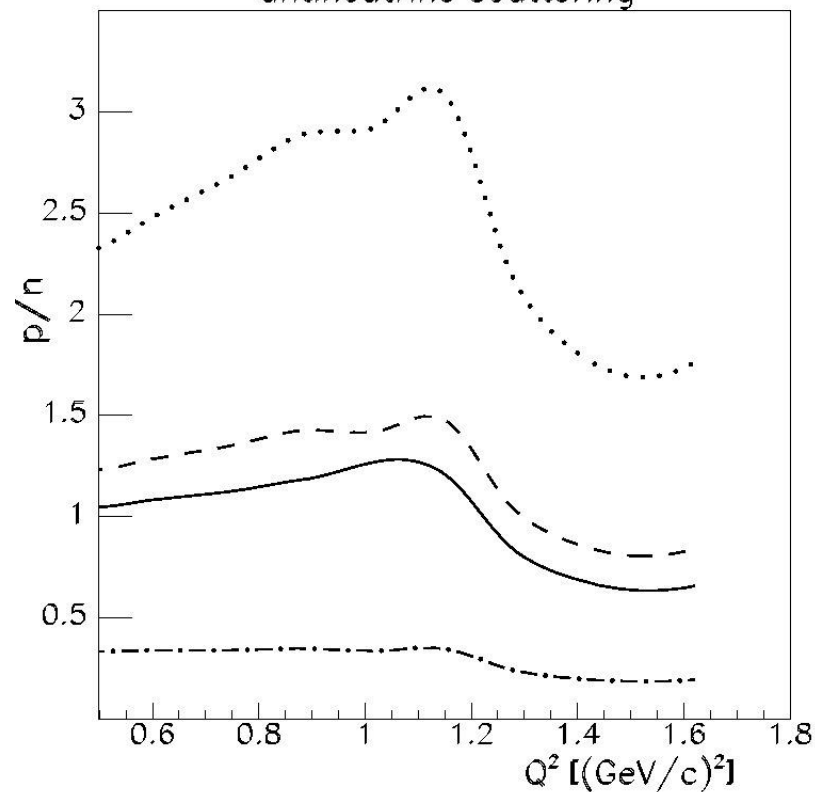
- $M_A = 1.03 \text{ GeV} \quad \Delta s = 0$
- - - - -  $M_A = 1.39 \text{ GeV} \quad \Delta s = 0$
- . - . -  $M_A = 1.39 \text{ GeV} \quad \Delta s = 0.34$
- .....  $M_A = 1.39 \text{ GeV} \quad \Delta s = -0.18$

$$\frac{\sigma(\nu, \nu' p)}{\sigma(\nu, \nu' n)}$$



$$\frac{\sigma(\bar{\nu}, \bar{\nu}' p)}{\sigma(\bar{\nu}, \bar{\nu}' n)}$$

antineutrino scattering



- $M_A = 1.03 \text{ GeV} \quad \Delta s = 0$
- - - - -  $M_A = 1.39 \text{ GeV} \quad \Delta s = 0$
- . - . -  $M_A = 1.39 \text{ GeV} \quad \Delta s = 0.34$
- .....  $M_A = 1.39 \text{ GeV} \quad \Delta s = -0.18$